COST-AWARE SECURE PROTOCOL DESIGN AND ANALYSIS

By

Di Tang

A DISSERTATION

Submitted
to Michigan State University
in partial fulfillment of the requirements
for the degree of

Electrical Engineering – Doctor of Philosophy

2015

ABSTRACT

COST-AWARE SECURE PROTOCOL DESIGN AND ANALYSIS

By

Di Tang

The recent technological progresses make sensor networks feasible to be widely used in both military and civilian applications. The nature of such networks makes energy consumption, communication delay and security the most essential issues for wireless sensor networks. However, these issues may be conflicting with each other. The existing works generally try to optimize one of these key issues without providing sufficient diversity and flexibility of various other requirements in protocol design. In this dissertation, we investigate the relationship and design trade-offs among these conflicting issues.

To deal with the lifetime optimization and security issues, we propose a novel secure and efficient Cost-Aware SEcure Routing (CASER) protocol to address them through two adjustable parameters: energy balance control (EBC) and security level to enforce energy balance and increase lifetime and determine the probabilistic distribution of random walking that provides routing security. We derive a tight numerical formula to quantitatively estimate the routing efficiency through the number of routing hops for a given routing security level. We also prove that CASER scheme can provide provable security under the quantitative security measurement criteria. Simulation results also show that the proposed CASER scheme can provide an excellent balance between routing efficiency and security while extending the network lifetime.

We then discover that the energy consumption is severely disproportional to the uniform energy deployment for the given network topology. To solve this problem, we propose an efficient non-uniform energy deployment strategy to optimize the network lifetime and increase the message delivery ratio under the same energy resource and security requirements. Our theoretical analysis and OPNET simulation results demonstrate that the updated CASER

protocol can provide an excellent trade-off between routing efficiency and energy consumption, while significantly extending the lifetime of the sensor networks in all scenarios. For the non-uniform energy deployment, our analysis shows that we can increase the lifetime and the total number of messages that can be delivered by more than four times under the same energy deployment, while achieving a high message delivery ratio and preventing routing traceback attacks.

In WSNs, congestion introduces not only buffer overflow, but also communication delay for forwarding messages from the source node to the sink. We propose a novel congestion-aware routing (CAR) scheme to reduce the end-to-end communication delay while increasing network throughput. CAR employs two routing strategies, shortest path routing strategy and congestion-aware strategy, to achieve a trade-off between energy efficiency and communication delay. The OPNET simulation results demonstrate that the proposed routing scheme can reduce the end-to-end communication delay by 50% while increasing the network throughput by more than two times in our settings.

People-centric urban sensing is envisioned as a novel urban sensing paradigm. Security, communication delay and delivery ratio are essential design issues in people-centric urban sensing networks. To address these three issues concurrently, we propose a novel delay-aware privacy preserving (DAPP) transmission scheme based on a combination of two-phase forwarding and secret sharing. The two-phase forwarding method detaches connection between the application data server and the source nodes, which renders it infeasible for the application data server to estimate source node identities. The underlying secret sharing scheme and dynamic pseudonym ensure confidentiality of the collected data and anonymity of participating users. DAPP provides a framework to achieve a design trade-off among security, communication delay and delivery ratio. The security analysis demonstrates that DAPP can preserve location privacy while defending against side information attacks. Theoretical analysis and simulation results show that our proposed algorithms can provide a flexible and diverse security design option for routing and data forwarding algorithm design.

Dedicated to my family

ACKNOWLEDGEMENTS

First of all, I would like to express my sincere gratitude to my advisor, Dr. Jian Ren, for his guidance, encouragement, and support in every stage of my graduate study. His knowledge, kindness, patience, passion, and vision affected me a lot and have provided me with lifetime benefits.

I am also grateful to my dissertation committee members, Professor Richard Enbody, Professor Subir Biswas, and Professor Wen Li, for their valuable comments and suggestions on the thesis draft, as well as for the experience as a student with these three outstanding teachers. I would also like to thank many faculty members of MSU who were the instructors for the courses I took. The course works have greatly enriched my knowledge and provided the background and foundations for my thesis research.

My PhD study could have never been completed without the help of my fellow graduate students at MSU. I would like to express my special thanks to the colleagues at our lab, Yun Li, Jian Li, Kai Zhou, Mohamed Afifi Ibrahim and Leron Lightfoot for their suggestions, helps, and all the happy and tough time we have been through. I also want to express my thanks to Dongliang Fang, Aimin Li, Meng Cai, Ying Liu, Jiayin Li, Qing Liu, Xiaochen Tang, Sara Kovensky Kalt, Brain Kalt, Lei Zhang, Xiaopeng Bi, Hanqing Li, Liangliang Li, Mingwu Gao and Qiong Huo, for their kind help during my staying at MSU, who enriched my study and life.

Finally, I would like to express my gratitude to my family. Their endless love and support always encourage me to deal with obstacles in every aspects of my life. In particular, I want to express my deepest gratitude to my dear wife, Lu Zhang, for her enduring love, encouragement, patience, and understanding.

TABLE OF CONTENTS

LIST OF TABLES

LIST OF FIGURES

LIST OF ALGORITHMS

KEY TO SYMBOLS AND ABBREVIATIONS

AP	Wireless Access Point
ACK	Acknowledgement
MAC	Medium Access Control
CASER	Cost-Aware Secure Routing
CSMA/CA	Carrier Sense Multiple Access with Collision Avoidance
CAR	Congestion-Aware Routing
DAPP	Delay-Aware Privacy Preserving Transmission Scheme
DIFS	Distributed Inter Frame Spacing
EBC	Energy Balance Control
iid	Independent and Identically Distributed
NSSI	Normalized Source-location Space Index
QoS	Quality of Service
RSIN	Routing to a Single Intermediate Node
RTS/CTS	Request-To-Send/Clear-To-Send Mechanism
SDI	Source-location Disclosure Index
SIFS	Short Inter Frame Spacing
SSI	Source-Location Space Index
WSN	Wireless Sensor Network

CHAPTER 1

INTRODUCTION

The recent technological advances make sensor networks technically and economically feasible to be widely used in both military and civilian applications, such as monitoring of ambient conditions related to the environment, precious species, critical infrastructures and traffic conditions. Energy efficiency, network lifetime, communication delay and delivery ratio are considered important metrics of performance measurement for wireless sensor networks, and have been extensively studied in [2–14]. Security is another key issue of protocol design, but yet less studied topic, partially due to the design trade-off between security and other performance issues. To address these design issues concurrently, we employ a cost-aware trade-off concept in designing routing algorithms for the traditional wireless sensor networks and for the emerging people-centric urban sensing networks. The proposed schemes are designed to provide flexible options for users to maximize the privacy protection based on the given performance requirements.

1.1 Source Location Privacy in Wireless Sensor Network

Traditional wireless sensor networks (WSNs) consist of a large number of untethered and unattended sensor nodes that are normally statically deployed for environment monitoring. These sensor nodes have very limited computational processing ability and storage capacity. They are powered by non-replenishable energy resources and equipped with a low-power radio to send and receive messages, which make energy efficiency and lifetime two major design metrics for WSNs protocol design.

In addition, WSNs rely on wireless communications, which is by nature a broadcast medium. It is more vulnerable to security attacks than its wired counterpart due to lack of a physical boundary. The low-power radio, limited processing ability and battery life make

security a very challenging issue. Computationally intensive cryptographic algorithms such as public-key cryptosystem, and large scale broadcasting-based protocols, may not be feasible for WSNs. Adversaries can even compromise some sensor nodes to obtain the cryptographic keys and reprogram compromised sensor nodes. These threats leave WSNs vulnerable to security attacks. Source location privacy is envisioned as one of the most essential security issues for WSNs. The exposure of source location may divulge the information of a sensing target, such as endangered species and critical military infrastructure. Adversaries equipped with sensitive radio receivers can easily monitor the transmission direction of any detected messages. They can further trace back to the source node hop by hop or deduce its location through traffic analysis when a static routing strategy is applied.

1.1.1 Routing Algorithm Design

In WSNs, sensor readings are usually transmitted to base stations hop by hop for further processing. Routing path is decided by a predesigned routing algorithm to ensure successful delivery of the collected data. Routing is a very challenging design issue in WSNs due to the inherent characteristics that distinguish WSNs from other wireless networks like ad-hoc networks or cellular networks. The relative large number of sensor nodes makes it impossible to build a global addressing table for each node. Due to the limited energy resources, routing algorithm should be designed with consideration of energy efficiency. In addition, burst events and static routing path may make the energy consumption unbalanced in a partial area. Then sensor nodes in the area will exhaust their energy which may decrease the network lifetime. Thus, a properly designed routing protocol should not only ensure high message delivery ratio and guarantee low energy consumption for packet delivery, but should also balance the energy consumption through entire sensor network, and thereby extend the sensor network lifetime.

In existing research, many routing protocols have been proposed to address the issues of energy efficiency, lifetime and latency. In these works, geographic routing has been widely

hailed as the most promising approach to generally scalable wireless routing. Geographic routing protocols utilize the geographic location information to route data packets hop-by-hop from the source to the destination [6,15]. The source chooses the immediate neighboring node to forward the message based on either the direction or the distance [2, 16–18]. The distance between the neighboring nodes can be estimated or acquired by signal strengths or using GPS equipment [19, 20]. The relative location information of neighbor nodes can be exchanged between neighboring nodes.

In [18], a geographic adaptive fidelity (GAF) routing scheme was proposed for sensor networks equipped with low power GPS receivers. In GAF, the network area is divided into fixed size virtual grids. In each grid, only one node is selected as the active node, while the others will sleep for a period to save energy. The sensor forwards the messages based on greedy geographic routing strategy.

A query based geographic and energy aware routing (GEAR) was proposed in [2]. In GEAR, the sink node disseminates requests with geographic attributes to a target region instead of using flooding. Each node forwards messages to its neighboring nodes based on the estimated cost and learning cost. The estimated cost considers both the distance to the destination and the remaining energy of sensor nodes. While the learning cost provides the updating information to deal with the local minimum problem.

While geographic routing algorithms have the advantages that each node only needs to maintain its neighboring information, and provide a higher efficiency and a better scalability for large scale WSNs, these algorithms may reach their local minimum, which can result in dead end or loops. To solve the local minimum problem, some variations of these basic routing algorithms were proposed in [6], including GEDIR, MFR and compass routing algorithm. The delivery ratio can be improved if each node is aware of its 2-hop neighbors. There are a few papers [3, 17, 21, 22] discussed combining greedy and face routing to solve the local minimum problem. The basic idea is to set the local topology of the network as a planar graph, and then the relay nodes try to forward messages along one or possibly a

sequence of adjacent faces toward the destination.

Lifetime is another area that has been extensively studied in WSNs. In [23], a routing scheme was proposed to find the sub-optimal path that can extend the lifetime of the WSNs instead of always selecting the lowest energy path. In the proposed scheme, multiple routing paths are set ahead by a reactive protocol such as AODV or directed diffusion. Then, the routing scheme will choose a path based on a probabilistic method according to the remaining energy. In [8], the authors assumed that the transmitter power level can be adjusted according to the distance between the transmitter and the receiver. Routing is formulated as a linear programming problem of neighboring node selection to maximize the network lifetime. Then [24] investigated the unbalanced energy consumption for uniformly deployed data-gathering sensor networks. In this paper, the network is divided into multiple corona zones and each node can perform data aggregation. A localized zone-based routing scheme was proposed to balance energy consumption among nodes within each corona. The authors in [9] formulated the integrated design of route selection, traffic load allocation, and sleep schedule to maximize the network lifetime. Based on the concept of opportunistic routing, [7] developed a routing metric to address both link reliability and node residual energy. The sensor node computes the optimal metric value in a localized area to achieve both reliability and lifetime maximization.

Although there have been many research papers deals with the lifetime of wireless sensor networks, only a few of them are related to energy aware geographic routing [2,4,15,25]. How to protect source location privacy remains a problem for geographic routing protocols. When the routing path remains unchanged for a period of time under static routing strategies, such as geographic based routing, exposure of routing information presents significant security threats to sensor networks. By acquisition of the location and routing information, the adversaries may be able to trace back to the source node easily.

1.1.2 Existing Solutions for Source Location Privacy in Wireless Sensor Networks

The nature of broadcast medium and limited resource makes WSNs more vulnerable to security attacks than its wired counterpart. Location privacy is one of most important security issues. Due to lack of a physical boundary and protection, it is possible for the adversaries to identify the message source or even identify the source location, even if strong data encryption is utilized. In particular, in the wireless sensor domain, anybody with an appropriate wireless receiver can monitor and intercept the sensor network communications. The adversaries may use expensive radio transceivers, powerful workstations and interact with the network from a distance since they are not restricted to using sensor network hardware. It is possible for the adversaries to perform jamming attacks and routing traceback attacks. To solve this problem, several schemes have been proposed to provide source location privacy through secure routing protocol design [1, 26–28].

The authors of [29] proposed to achieve source location privacy through trust mechanisms built in WSNs and neighboring nodes categorization. However, it requires a long delay to build the trust reputation infrastructure. Two schemes based on pseudonyms and cryptographic methods were proposed in [30]. These schemes demand huge memory storage and computational resources, which are not practical due to characteristics of WSNs and the serious open security concerns under traceback attacks.

In [31], source location privacy is provided through broadcasting that mixes valid messages with dummy messages. The main idea is that each node needs to transmit messages consistently. Whenever there is no valid message to transmit, the node transmits dummy messages. The transmission of dummy messages not only consumes significant amount of sensor energy, but also increases the network collisions and decreases the packet delivery ratio. Therefore, these schemes are not quite suitable for large scale wireless sensor networks.

Dynamic routing strategies based protocols are proposed to make it infeasible for adversaries to locate source nodes through traffic monitoring and analysis. In this way, source

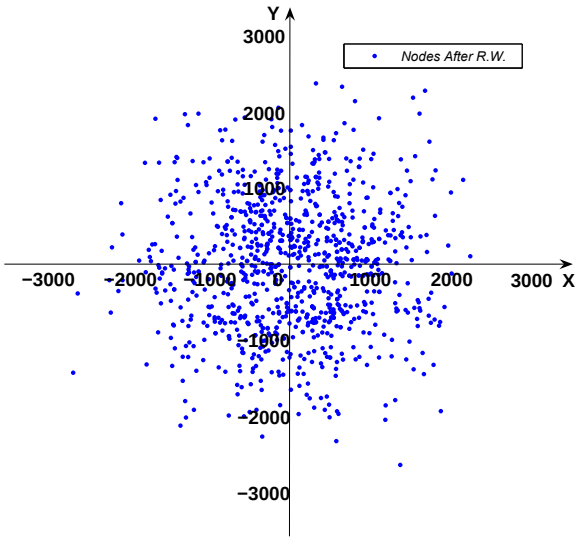

Figure 1.1 Nodes distribution through random routing

location privacy can be achieved. Existing works generally employ the idea that route messages to a node/nodes away from the message source based on random walking or direct walking. Directly application of random walking may introduce significant energy consumption without achieving good security requirement. Both theoretical and practical results demonstrate that if the message is routed randomly for h hops, then the messages will be largely distributed within $h/5$ hops away from the source node. As shown in Figure 1.1, the source node is located at $(0, 0)$ and $h = 50$. The transmission range is 250 meters at most for one hop. The statistic results show that the average hop distance between the source and the randomly selected nodes is only 4.2 hops. To solve this, the authors employ direct walking in phantom routing protocol [26]. Phantom routing involves two phases: a random walking phase and a subsequent flooding/single path routing phase. Each message is routed from the actual source to a phantom source along a designed directed walking through either sector-based approach or hop-based approach. The direction/sector information is stored in the header of the message. Then every forwarder on the random walking path forwards this message to a random neighbor based on the direction/sector determined by the source node. In this way, the phantom source can be away from the actual source. Unfortunately, once

the message is captured on the random walking path, the adversaries are able to get the direction/sector information stored in the header of the message. Therefore, exposure of the direction decreases the complexity for adversaries to trace back to the actual message source in the magnitude of 2^h. However, none of these schemes have considered energy balance and provided quantitative source location information leakage and security analysis.

In [1, 28], we developed a two-phase routing algorithm to provide both content confidentiality and source location privacy. The message source randomly selects an intermediate node in the sensor domain, then the intermediate node transmits the message to a network mixing ring which mix the messages from different directions among the ring. The message will be forwarded from the node in the ring domain based on probabilistic way. Then, in [32], we firstly developed criteria to quantitatively measure source location information leakage and security of routing-based schemes through source location disclosure index (SDI) and source location space index (SSI).

These schemes are generally designed to protect source location privacy without providing diversity and flexibility in protocol design. In fact, routing based schemes can preserve source node location privacy at the cost of additional energy consumption. The dynamic routing path selection may introduce unbalanced energy consumption in partial network, which may decrease the network lifetime significantly. Therefore, a proper designed secure routing algorithm should not only preserve source location privacy, but also consider energy efficiency and network lifetime.

1.1.3 Summary of Major Limitations

To the best of our knowledge, none of these schemes have considered privacy from a cost-aware perspective.

- The public-key encryption based algorithms are not suitable for WSNs due to the computation complexity.

- Broadcasting and dummy messages based schemes introduce significant amount energy consumption and collisions.
- Existing routing based algorithms may leak the direction information by capturing messages.
- Security is the only metric to measure performance of existing works.
- None of existing works address the quantitative relationship between the energy efficiency and security.
- Existing works fail to balance the energy consumption and extend lifetime of the network.

1.2 Congestion in Wireless Sensor Networks

Wireless sensor networks are designed to collect information and transmit sensed data to one or more sink nodes. The information of the sensed data is critical for real-time processing and decision-making in both military and civilian applications, such as monitoring the forest fire and target locating. For these applications, end-to-end communication delay is one of the most significant design issues for wireless sensor networks.

In WSNs, congestion not only increases the packet end-to-end communication delay, but also decreases the packet delivery ratio, network throughput and energy efficiency. In traditional networks, the existing works on congestion mainly focus on traffic control in both end-to-end and hop-by-hop communications. These algorithms are mainly applied to the transport layer or the Medium Access Control (MAC) layer. They are designed to avoid congestion by limiting the transmission rate or reducing traffic in the network. However, the aforementioned strategies are unsuitable for event-driven WSNs for the following two reasons. First, reducing the source traffic may affect the validity of decision-making. For example, forest rangers cannot locate the real fire source since the traffic of real source node is

limited. Second, the traffic control strategies have a negative impact on real-time processing. As an example, ecological observers cannot obtain the accurate number of pandas since the traffic control algorithm postpones the transmission of critical sensor nodes to reduce the congestion in the MAC layer. The delayed information from the partial region may affect the correctness of real-time processing. How to reduce end-to-end communication delay remains one of the most important design issues for congestion control algorithms.

1.2.1 Existing Solutions for Congestion Mitigation

Congestion control is a critical design issue in WSNs. In [10], the authors classified congestion into two categories. One is defined as node-level congestion caused by buffer overflow. And the other one is defined as link-level congestion caused by distributed MAC layer protocols. Distributed MAC protocols allow sensor nodes to compete to access the wireless medium channel, which may introduce more collisions.

Existing works mainly focus on the congestion caused by buffer overflow in node-level congestion. To reduce this type of congestion, traffic control is employed as the major technique. In [11], the authors provided a comprehensive review on traffic congestion and proposed a scheme to avoid congestion based on congestion detection, hop-by-hop backpressure and multi-source regulation. The receiver monitors the traffic and the current buffer occupancy. The traffic information will be sent through backpressure messages to upstream neighbors to limit the packet sending rate. Furthermore, the multi-source regulation provides a congestion control through the end-to-end communication. In [33], the authors proposed a mechanism named Fusion based on three congestion mitigation techniques, including hop-by-hop flow control, limiting source rate, and prioritized medium access control. These three congestion techniques could mitigate the congestion by preventing the transmission to the congested nodes. Then, Chen and Yang [14] proposed a congestion-avoidance scheme based on light-weight buffer management using hop-by-hop flow control. It employs a $1/k$ buffer solution to prevent hidden terminals from causing traffic congestion.

Several MAC layer protocols [12, 13, 34] have been proposed to reduce the link-level congestion. In [13], the authors proposed a modified carrier sense multiple access protocol (CSMA) to improve the network performance. The protocol aims to reduce the cost of channel state checking, and adds a machine learning approach to predict the probability of a successful reception. In [34], the authors proposed a power back-off scheme to resolve collisions by limiting the transmission power. And the authors in [12] proposed an enhanced p-persistent CSMA. They proposed a method to calculate a proper p for CSMA based on the topology information of partial network. However, these proposed algorithms mainly focus on modifying the existing CSMA protocols in which the requirements and assumptions are not practical in WSNs.

Besides traffic control strategies, routing based congestion-avoidance protocols are also effective methods to reduce the congestion in networks. The main idea of existing works is to reroute packets to bypass congestion areas. The idea is employed in [35] to reduce the congestion by throttling or rerouting the traffic. The authors in [36] introduced some virtual sinks with a longer range multi-radio in WSNs. The authors assumed sensors can communicate with a long range communication radio to bypass potential congestion areas. [10] proposed a congestion control scheme by calculating the mean of the packet generation rate. LACAR routing scheme in [37] was designed to probabilistically avoid congestion by choosing lightly loaded nodes according to relative location information. In [38], a traffic-aware dynamic routing algorithm was proposed to route the packets around the congestion area and scatter packets to light loaded relay nodes to alleviate buffer flow. These routing algorithms need either topology information or a long range communication radio, which is not practical in WSNs.

1.2.2 Summary of Major Limitations

- Traffic control based schemes are designed to limit transmission rate or reduce traffic at source node, which may affect the validity of data processing results.

- Routing based schemes need either topology information or a long range communication radio which is not practical for WSNs.
- The messages are delivered to a centralized sink node. Lack of optional relay nodes in a region close to sink node may aggravate congestion.
- MAC layer based schemes require limiting the transmission power or acquisition of topology information in partial network which is not practical for WSNs.

1.3 Urban Sensing Networks

Traditional sensor networks rely on a large number of sensor nodes normally deployed statically in a target area. The recent advances in embedded system design for mobile devices make the human-carried devices feasible for environment monitoring. People-centric urban sensing has been envisioned as a novel urban sensing paradigm. It relies on sensors embedded in human-carried mobile devices or vehicular electrical devices to collect and report sensing data. Sensor nodes embedded in these mobile systems can take advantages of powerful computational resources and rechargeable battery power. The new paradigm of sensor networks also makes people not only data consumers but also data contributors. The ubiquitous electrical devices carried by human and vehicles are gradually replacing the traditional static sensor networks for many urban area applications.

1.3.1 People-Centric Urban Sensing Networks

People-centric urban sensing network, also known as participatory sensing network, differs significantly from traditional wireless sensor network. First, participatory sensor nodes are embedded in rechargeable mobile devices, such as smart phone, iPad, laptop and auto computer. The powerful resources equipped in these devices enhance their capabilities in computation, sensing, data storage, reliable data communication, and energy lifetime dramatically. Hence, the energy efficiency is no longer as critical as in traditional wireless sensor

networks. Second, in urban sensing networks, sensing data collection and reporting no longer rely on fixed infrastructure. The data can be forwarded by mobile nodes to the sink either directly or indirectly in multiple hops. Due to mobility, network topology structure constantly changes, which make end-to-end communication delay, message delivery ratio and quality of service (QoS) some of the most essential performance evaluation metrics in urban sensing networks. Third, these devices are owned and operated by individuals. Instead of being only data consumers, these devices could also collect sensing data. It makes data collection more directly related to people's lives and hence privacy becomes one of the major concerns of participating users. In fact, the data collecting and reporting services put users' privacy in jeopardizing since both the delivery nodes and the wireless access points are able to identify the data owner through direct communications. The uploaded sensor reading is required to be collected with spatial-temporal information to provide accurate and high quality service for data users. The spatial-temporal information related to collectors can be used to recover the trajectory of them, which can seriously jeopardize participating collectors' privacy. Side information attack has been studied in recent research. Adversaries may obtain this kind of information from side channels, such like video cameras, social networks and published information. It can divulge source identities in spite of usage of existing pseudonym schemes. As a result, private location information combining with side information can be used to recover the trajectory of participating users.

1.3.2 Existing Solutions for Location Privacy in Urban Sensing Networks

The participatory sensing concept was firstly proposed in [39]. The concept then is extended to urban sensing and people-centric sensing. The key idea is that the network relies on the people-carried mobile devices to collect the sensing data in urban environments. It enables the public and professional users to collect and share the sensed data. The authors in [40] proposed an architecture named *MetroSense* for urban-scale people-centric sensing for the first time. The paper provided detailed design principles and a network model for

people-centric urban sensing networks. The network is composed of traditional static sensors, mobile sensors embedded in the mobile devices, gateways and a server. The sensor nodes deliver collected data to the server through the gateways which is considered as physical infrastructure in the network. The paper also mentioned the trajectory privacy problem. However, the proposed solution is based on an insufficient adversarial model.

The first implementation for privacy protection was proposed in [41]. In this paper, the location is blurred based on tessellation and clustering against adversaries. The reported data are eventually aggregated to improve the privacy. This idea of data aggregation is also applied in [42, 43]. In [43], the proposed PriSense is designed based on the concept of data slicing and mixing. It can support a wide range of statistical additive and non-additive aggregation functions with accurate aggregation. The sensing data are divided and distributed to cover nodes to hide the identity information of source nodes. The data are eventually aggregated by the cover nodes and delivered to the server. However, aggregation may also hide the accurate sensing information contained in each individual sensing data and sacrifice the precision of service quality.

Another optional solution based on mix-zones and pseudonyms were proposed in [44–47]. In these algorithms, mix-zones are first constructed and placed in some regions of the network. Then, the pseudonyms are assigned to users as the communication identities when they enter into the mix-zones. This method is designed to achieve k-anonymity to prevent discovering user's real identity. In [47], the authors divided the sensing area into sensitive areas and non sensitive areas. Different pseudonyms are assigned to a user when he enters into and departures from the mix zone. However, the mix zone relies on a trusted third party, which may not be always true. And they cannot be placed through the entire network to protect trajectory privacy.

Spatial cloaking [48] was proposed to enable data collectors to adjust the resolution of location information along spatial or temporal dimensions to avoid exposure of user's exact location. This methodology was further studied in [49–51]. These works mainly focus on

the selection of anonymous locations and trade-off between quality service and anonymity. However, the privacy protection is achieved by sacrificing the resolution of either spatial or temporal dimensions.

Dummy location was studied in [52–54]. The fundamental idea is to report dummy locations to conceal the actual location of the reported data. Suppression based techniques [55] was also proposed to blur the reported locations by converting the database of trajectories. [56] proposed to construct a cluster in a nearby neighborhood and then transform each cluster into a anonymity set. In these methods, the privacy can be protected by obscuring the exact locations, which may induce information loss for data service.

Encryption based algorithms and data exchange schemes were proposed in [57–59]. In [57], the sensed data are encrypted and disseminated to replica sensors. The replica sensors then store the received data and relay them upon receiving inquiries. As a consequence, the source node identity can be concealed by the replica sensors. Nevertheless, the shared key may either help the operator to identify the source node or enable the malicious replica nodes to decrypt the data contents. In [58], the collected sensor readings are exchanged between participants within wireless communication range. The data can be exchanged multiple times to prevent adversaries from correlating the data and its identity. [60] proposed to forward the collected data from friends to friends of the source user until the required number of hops has been reached. In these schemes, source node may be directly identified by intermediate nodes through wireless communications. Additionally, malicious intermediate nodes can also reveal and tamper with data contents through the forwarding procedure. There is little flexibility in delivery ratio when the data are being dropped or tampered with.

1.3.3 Summary of Major Limitations

- Location privacy may be achieved by yielding the accuracy of collected data.
- Privacy protection service may not be provided over the entire network.

- Encryption based methods may leak the identity information of the participating user by exchanging shared keys.
- The collected data may be tampered with and dropped by the malicious intermediate nodes.
- The assumption that there exists a trusted third party is not sufficient for adversarial model.
- Malicious delivery nodes may collude to derive the privacy information.
- The information loss by collecting side information is not quantitatively analyzed.

1.4 Proposed Research Direction

Due to inherent characteristics, WSNs protocol design has to consider several essential design issues concurrently, which may be conflicting with each other. In this dissertation, we analyze the relationship among these conflicting design issues and develop algorithms to preserve location privacy from a cost-aware perspective under various trade-off constraints. They can provide diverse options that can be analogous to delivering of US Mail through USPS: express mail is more expensive than regular mail; however, mails can be delivered with less time needed. The proposed schemes also provide a secure message delivery option under the cost-aware design-off framework.

1.4.1 Source Location Privacy Protection in Wireless Sensor Networks

In this dissertation, we propose a secure and efficient Cost-Aware SEcure Routing (CASER) protocol that can address network lifetime and routing security concurrently in WSNs.

In CASER protocol, each sensor node needs to maintain the energy levels of its immediate adjacent neighboring grids in addition to their relative locations. Using this information, each sensor node can create varying filters based on the expected design trade-off between security

and network lifetime. Each sensor node also needs to maintain the location information of neighbor nodes. CASER allows messages to be transmitted using two routing strategies, random walking and deterministic routing. The two routing strategies are applied based on the lifetime filter. The distribution of these two strategies is determined by specified security requirements.

We then discover that the energy consumption is severely disproportional to the uniform energy deployment for the given network topology, which greatly reduces the lifetime of the sensor networks. To solve this problem, we propose an efficient non-uniform energy deployment strategy to optimize the lifetime and message delivery ratio under the same energy resource and security requirement. CASER is also updated to adapt the non-uniform energy deployment.

In addition, we also give quantitative secure analysis on the proposed routing protocol based on the criteria proposed in [32]. The simulations are also provided to show that CASER can provide excellent energy balance and routing security.

CASER protocol has two major advantages: (i) It ensures balanced energy consumption of the entire sensor network so that the lifetime of the WSNs can be maximized. (ii) CASER protocol supports multiple routing strategies based on the routing requirements, including fast/slow message delivery and secure message delivery to prevent routing traceback attacks and malicious traffic jamming attacks in WSNs.

1.4.2 Congestion-Aware Routing (CAR) Algorithm in Wireless Sensor Networks

In this dissertation, we propose a congestion-aware routing scheme to reduce the potential congestion in the subsequent packet forwarding by monitoring the traffic in the MAC layer.

In CAR, each sensor node selects the relay node based on two different routing strategies: the shortest path forwarding and the congestion-aware forwarding. In the shortest path forwarding, the relay node selection follows the geographic routing strategy [61] based on

the geographic location. In the congestion-aware forwarding algorithm, each sensor node selects the relay node based on the channel competing results. When traffic congestion is not detected, the shortest path routing algorithm will be used and congestion-aware transmission algorithm is used otherwise. The shortest path routing algorithm ensures an efficient end-to-end message transmission from the source node to the sink node. CAR can effectively reduce end-to-end message communication delay and improve the system throughput by reducing traffic congestion.

1.4.3 Location Privacy Protection in Urban Sensing Networks

We propose a novel delay-aware privacy-preserving (DAPP) data reporting scheme to preserve the trajectory privacy of participating users based on a combination of Shamir's secret sharing and two-phase routing. In this dissertation, we begin with analyzing the design trade-off among communication delay, delivery ratio and security. We then propose a scheme that can provide flexible message delivery options to meet various security and performance requirements, such as communication delay and delivery ratio.

In DAPP, the data reporting includes two independent forwarding phases. In the first phase, participating user first generates a unique pseudonym for each sensor reading. Then, the sensor reading is decomposed into n pieces based on Sharmir's secret sharing and these data pieces are forwarded to randomly selected delivery nodes. In the second phase, the selected delivery node relays its received data piece to the application data server through a nearby wireless access point. Upon receiving k or more data pieces, the application data server is able to reconstruct the original collected data. To ensure integrity of the recovered data, both the original data and its hash value will be transmitted together.

Secret sharing can ensure confidentiality and integrity of the reported data. We propose a dynamic pseudonym scheme to guarantee anonymity of the source node. DAPP can also provide redundancy for error tolerance under additional computational overhead, which ensures a high message delivery ratio for data transmission. This design makes both security

and communication delay adjustable based on selection of the (n, k) scheme.

1.5 Overview of the Dissertation

1.5.1 Design Goals

Our design goal for the secure routing algorithm in traditional wireless sensor networks can be summarized as follows:

- To maximize the sensor network lifetime, we ensure that the energy consumption of all sensor grids is balanced.
- To achieve a high message delivery ratio, our routing protocol should try to avoid message dropping when an alternative routing path exists.
- The adversaries should not be able to get the source location information by analyzing the traffic pattern.
- The adversary should not be able to get the source location information if he is only able to monitor a certain area of the WSN and compromise a few sensor nodes.
- Only the sink node is able to identify the source location through the message received. The recovery of the source location from the received message should be very efficient.
- The routing protocol should maximize the probability that the message is being delivered to the sink node when adversaries are only able to jam a few sensor nodes.

For the congestion-aware routing algorithm, our design goals are described as follows:

- The end-to-end communication delay caused by congestion should be effectively alleviated.
- The proposed scheme should rely on the existing MAC layer protocols without requiring extra physical equipment and further modification.

- The energy efficiency should be addressed in the proposed scheme.
- The proposed scheme should be able to mitigate congestion caused by the traffic routed to the centralized sink node.

We also want to achieve the following goals for the transmission scheme in urban sensing networks:

- Adversaries should not be able to obtain real identities of participating users without side information.
- The malicious delivery node should not be able to discover spatial-temporal information of the reported data.
- Adversaries should not be able to recover data trajectory by collecting side information.
- The proposed scheme should provide data integrity verification for the recovered data.
- The proposed scheme should be able to provide a high delivery ratio in case some data pieces are dropped or tampered with by malicious delivery nodes.
- The proposed scheme should provide flexibility and diversity in protocol design.

1.5.2 Major Contributions

Our contributions on routing algorithm design in WSNs can be summarized as follows:

1. We propose a secure and efficient Cost-Aware SEcure Routing (CASER) protocol for WSNs. In this protocol, cost-aware based routing strategies can be applied to address the message delivery requirements.
2. We devise a quantitative scheme to balance the energy consumption so that both the sensor network lifetime and the total number of messages that can be delivered are maximized under the same energy deployment.

3. We develop theoretical formulas to estimate the number of routing hops in CASER under varying routing energy balance control and security requirements.

4. We quantitatively analyze the security of the proposed routing algorithm.

5. We provide an optimal non-uniform energy deployment strategy for the given sensor network based on the energy consumption ratio. Our theoretical and simulation results both show that under the same total energy deployment, we can increase the lifetime and the number of messages that can be delivered by more than four times in the non-uniform energy deployment scenario.

Our contributions on congestion-aware routing algorithm can be described as follows:

1. We propose a congestion aware routing algorithm to address communication delay and energy efficiency.

2. We analyze the congestion in one-hop network and extend it to a scenario of multi-hop network. We give the bounds for the communication delay under congestion scenarios.

3. We evaluate the performance of the proposed CAR routing algorithm on communication delay.

4. The simulation results demonstrate the proposed CAR can reduce the communication delay very close to the ideal case.

Our contributions on forwarding scheme design in people-centric urban sensing networks can be summarized as follows:

1. We propose a delay-aware privacy preserving (DAPP) data forwarding scheme to protect trajectory privacy of participating users in urban sensing networks.

2. We devise a secret sharing based secure message delivery option that can provide data integrity verification of the recovered data and maximize the message delivery ratio by introducing redundancy in reported data.

3. We present a dynamic pseudonym scheme to defend against side information attacks.

4. The proposed scheme is able to achieve a trade-off among security, communication delay and delivery ratio through adjustable parameters.

5. We quantitatively analyze performance of the proposed scheme on security, communication delay and delivery ratio.

1.5.3 Thesis Organization

The dissertation is structured as follows.

Chapter 2 proposes CASER protocol for source location protection.

Section 2.1 serves as an introduction for this chapter. In Section 2.2, we present the network model and adversarial assumptions. We propose CASER algorithm based on energy balance routing strategy and security routing strategy in Section 2.3. In this section, we also derive formulas to decide the energy consumption of balancing routing strategy and security routing strategy.

In Section 2.4, we introduce a security evaluation model and present a quantitative security analysis to demonstrate CASER can preserve the source location privacy. In addition, the security analysis also shows that CASER can effectively defend against jamming attacks and detect compromised nodes. Finally, in Section 2.5, we present the performance evaluations and simulation results.

Chapter 3 proposes the non-uniform energy deployment through the entire network.

In Section 3.1, we investigate the energy consumption under uniform energy deployment. Both theoretical analysis and simulation results demonstrate that the energy consumption is severely disproportional through the entire network. The energy consumption is balanced in a localized area. To solve this problem, in Section 3.2, we propose a non-uniform energy deployment to extend the lifetime of the entire network, while updating the proposed CASER to adapt the non-uniform energy deployment. The simulation results in this section show

the non-uniform energy deployment can significantly extend the lifetime through the entire network under various security requirements. The overall energy consumption of networks is well balanced, and thereby significantly extends the network lifetime.

Chapter 4 presents a congestion-aware routing algorithm to reduce the communication delay under congestion scenarios.

Section 4.1 gives an introduction of this chapter. The system model and assumptions are presented in Section 4.2. In Section 4.3, we describe CAR routing algorithm in detail. We conduct the analysis for the performance of communication delay in Section 4.4. We derive a formula to decide the communication delay in the ideal case and the worst case for the proposed CAR routing algorithm. The evaluation and simulations are provided in Section 4.5, which demonstrate CAR routing algorithm can effectively reduce the communication delay. We conclude in Section 4.6.

Chapter 5 introduces a novel delay-aware and privacy preserving data forwarding scheme.

Section 5.1 gives an introduction to the whole chapter. Section 5.2 presents system models and adversarial assumptions. In Section 5.3, we provide details of DAPP scheme. In this section, a dynamic pseudonym scheme and a Shamir's secret sharing based scheme are proposed to ensure the data integrity and anonymity of the source node. The security analysis is presented in Section 5.4. It quantitatively demonstrates DAPP can protect the trajectory privacy of participating users. It also shows DAPP can effectively defend against collusion attack and guarantee data integrity. Performance evaluation and simulation results are provided in Section 5.5. We conclude this chapter in Section 5.6.

Chapter 6 summarizes the contributions and concludes the dissertation. An outline of related future work is also provided.

CHAPTER 2

COST-AWARE SECURE ROUTING: DESIGN AND ANALYSIS

In this chapter, we propose a cost-aware secure routing protocol to achieve a trade-off between security and network lifetime through two adjustable parameters: energy balance control (EBC) and security level. CASER can create various filters based on EBC parameter to balance energy consumption and thereby increase the network lifetime. Security level can determine the probabilistic distribution of random walking to make the routing path dynamic and unpredictable, which can prevent adversaries from estimating direction of the messages and defend against jamming attacks. CASER combines random walking and geographic based deterministic routing strategy to ensure secure and efficient delivery of the collected data to the sink node. In this chapter, we develop theoretical formulas to measure routing efficiency through estimating the number of routing hops under varying routing energy balance control parameters and security requirements. Quantitatively security analysis and simulation results are provided to demonstrate the security properties and performance.

2.1 Introduction

In WSNs, sensor nodes are equipped with low power radios to send and receive messages through wireless medium, which makes data uploading rely on hop by hop transmission. Routing protocols are designed to ensure successful delivery of the collected data. Due to the inherent characteristics of WSNs, a properly designed routing algorithm should not only ensure a high message delivery ratio, but also guarantee low energy consumption and maximize the network lifetime. Existing routing algorithms, such as geographic routing algorithms, can determine a shortest routing path to increase the energy efficiency. However, the static routing strategy may drain the energy of sensor nodes along the shortest routing path quickly. A few of existing works have focused on providing alternative routing paths to

balance the energy consumption and at the same time extend the network lifetime. However, there is still a lack of robust quantitative measurement on the trade-off between energy consumption and energy balance.

Source location privacy is an important security issue. Location of source may expose significant amount of information about the objects being monitored by sensor nodes. While confidentiality of the message can be ensured through content encryption, it is much more difficult to adequately address the source-location privacy. Privacy service in WSN is further complicated since the sensor nodes are designed to operate unattended for long periods of time and only consist of low-cost and low-power radio devices. Battery recharging or replacement may be infeasible or impossible. Hence, computationally intensive cryptographic algorithms, such as public-key cryptosystems and large scale broadcasting-based protocols, are not suitable for WSNs. This makes privacy preserving transmission in WSNs an extremely challenging research task.

There are three major techniques for adversaries to obtain source location information in WSNs, which are *correlation-based source identification attack*, *routing based traceback attack*, *reducing source space attack*.

Correlation-based source identification has been well studied in [28] by using a dynamic ID assignment scheme. Both routing traceback attack and reducing source attack are carried out through traffic pattern analysis. In existing works, there are mainly two approaches that can protect the source-location privacy from traffic analysis attacks in WSNs, which are broadcast-based and routing-based. For the broadcasting schemes [31, 62–65], source-location privacy is provided through broadcasting or injection of dummy packets. In these schemes, each node broadcasts message consistently or at a predefined probabilistic model so that the adversary cannot distinguish the meaningful messages from dummy messages. However, these schemes may decrease network lifetime significantly. In fact, it has been demonstrated in [66] that the power consumption for transmission of one bit is about as much as executing 800-1000 instructions.

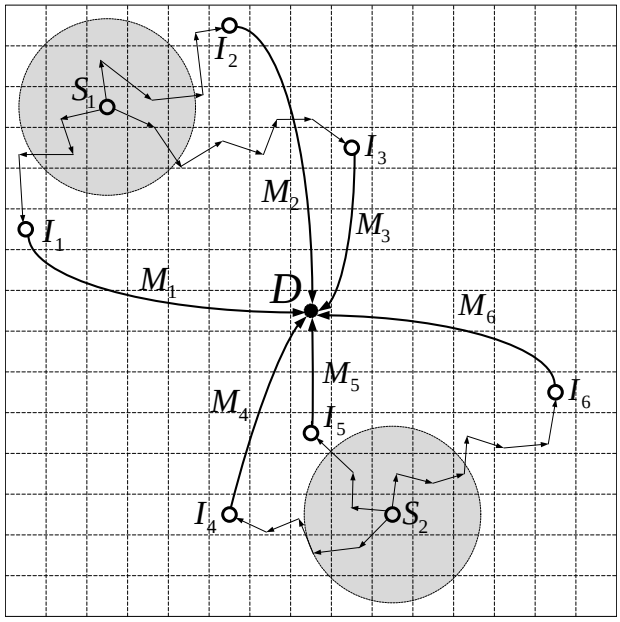

Figure 2.1 Illustration of RSIN

Routing based approach can provide source location privacy through dynamic routing so that it is infeasible for adversaries to trace back to the source node through traffic monitoring and analysis. The main idea is to, first, route sensor readings to a randomly selected intermediate node away from the real source, then the relay node forwards this packet to the sink using a static routing strategy. In this way, routing path can at most lead adversaries to the randomly selected intermediate nodes instead of the real source based on the general adversarial model. Some existing research has proposed to use random walking to provide routing privacy. However, as has been analyzed, random walking is very inefficient in message forwarding. In general, if you transmit a message for h hops using random walking, our analysis shows that the end nodes of paths will be located about $h/5$ hops from real source nodes. If the same strategy is used repeatedly, then the end messages distribution can be used to identify the source, as shown in Figure 1.1. To increase the efficiency, direct walking has been proposed in [26, 27]. Phantom routing protocols in [26, 27, 67] present strategies to select intermediate nodes through either sector-based approach or hop-based approach. However, direct walking may still divulge direction information of routing message. In [28], routing through a randomly selected intermediate node (RSIN) was proposed to transmit

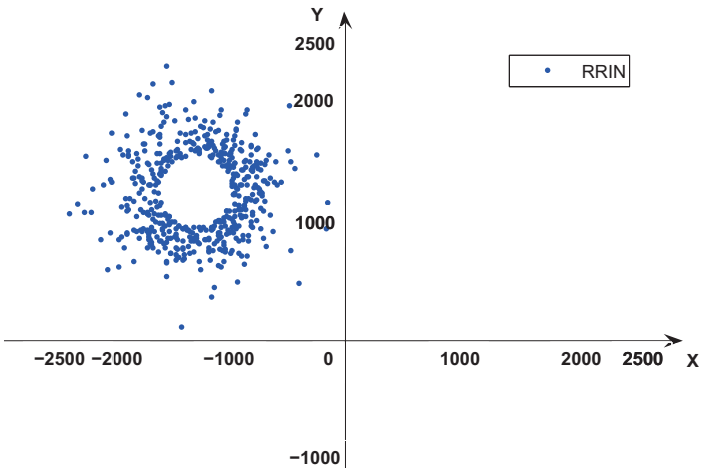

Figure 2.2 Distribution of the intermediate nodes in RSIN

each message to overcome the security weaknesses. RSIN makes the source node S randomly selects a relay node, which is away from the source node for a minimum distance $d_{\min}$ based on the relative locations of sensor nodes. The source node can be deduced into a local area by direction analysis. The energy consumption is still unbalanced in a local area which may decrease network lifetime, shown in Figure 2.2.

The existing routing algorithms may focus on security, energy efficiency and network lifetime individually. Unfortunately, they are generally designed to address and optimize one of these key issues without providing diversity and flexibility to satisfy various demands of data services. There is still a lack of a characterization framework and quantitative analysis on the performance trade-off among security, energy balance and energy efficiency.

In this chapter, we propose a geographic-based secure and efficient Cost-Aware SEcure routing (CASER) protocol for WSNs without relying on flooding. In Section 2.3, CASER algorithm is introduced to address lifetime and security concurrently through two adjustable parameters: energy balance control (EBC) and probabilistic-based random walking. This section also provides quantitative analysis of relationships among these conflicting security and performance issues. In Section 2.4, security analysis of the proposed scheme is conducted based on the criteria proposed in [32]. Section 2.5 provides performance analysis of the

proposed CASER.

2.2 Models and Assumptions

2.2.1 System Model

We assume that the WSNs are composed of a large number of sensor nodes and a sink node. The sensor nodes are randomly deployed throughout the sensor domain. Each sensor node will have a very limited and non-replenishable energy resource. The sink node is the only destination that every sensor node will send message packets to through a multi-hop routing strategy. The information of the sink node is made public.

For security management purpose, each sensor node may also be assigned a node ID corresponding to the location where this message is generated. To prevent adversaries from recovering the source location from the node ID, dynamic ID can be used. In addition, the content of each message can also be encrypted using the shared secret key between the node/grid and the sink node.

We also assume that each sensor node knows its relative location in the sensor domain and has knowledge of its immediate adjacent neighboring grids and their energy levels. The information about the relative location of the sensor domain may be broadcasted in the network for routing information update [68, 69].

The key management, including key generation, key distribution and key update, is beyond the scope of this dissertation. However, the interested readers are referred to reference such as [70] for more information.

2.2.2 Adversarial Model

In WSNs, the adversary may try to recover the message source node or jam the packet from being delivered to the sink node. The adversaries would try their best to equip themselves with advanced equipment, which means they would have some technical advantages over

the sensor nodes. In this dissertation, the adversaries are assumed to have the following characteristics:

- The adversaries will have sufficient energy resources, adequate computation capability and enough memory for data storage. On detecting an event, they could determine the immediate sender by analyzing the strength and direction of the signal they received. They can move to this sender's location without too much delay. The adversaries may also compromise some sensor nodes in the network. We assume that the adversaries will never miss any event close to them.

- The adversaries will not interfere with the proper functioning of the network, such as modifying packets, altering the routing path, or destroying sensor devices, since such activities can be easily identified. However, the adversaries may carry out passive attacks, such as eavesdropping on the communications.

- The adversaries are able to monitor the traffic in an area that is important to them and get all of the transmitted messages. However, we assume that the adversaries are unable to monitor the entire network. In fact, if the adversaries could monitor the entire wireless sensor networks, then they can monitor the events directly without relying on the sensor network.

2.3 The Proposed CASER Scheme

We now describe the proposed CASER protocol. Under the CASER protocol, routing decisions can vary to emphasize different routing strategies. In this dissertation, we will focus on two routing strategies for message forwarding: shortest path message forwarding, and secure message forwarding through random walking to create routing path unpredictability for source privacy and jamming prevention. As described before, we are interested in routing schemes that can balance energy consumption.

2.3.1 Overview of the Proposed Scheme

In our scheme, the network is evenly divided into small grids. Each grid has a relative location based on the grid information. The node in each grid with the highest energy level is selected as the head node for message forwarding. In addition, each node in the grid will maintain its own attributes, including location information, remaining energy level of its grid, as well as the attributes of its adjacent neighboring grids. The information maintained by each sensor node will be updated periodically. We assume that the sensor nodes in its direct neighboring grids are all within its direct communication range. We also assume that the whole network is fully connected through multi-hop communications.

While maximizing message source location privacy and minimizing traffic jamming for communications between the source and the destination nodes, we can optimize the sensor network lifetime through a balanced energy consumption throughout the sensor network.

In addition, through the maintained energy levels of its adjacent neighboring grids, it can be used to detect and filter out the compromised nodes for active routing selection.

2.3.2 Assumptions and Energy Balance Routing

In the CASER protocol, we assume that each node maintains its relative location and the remaining energy levels of its immediate adjacent neighboring grids. For node A, denote the set of its immediate adjacent neighboring grids as $\mathcal{N}_A$ and the remaining energy of grid i as $\mathcal{E}r_i$, $i \in \mathcal{N}_A$. With this information, the node A can compute the average remaining energy of the grids in $\mathcal{N}_A$ as $\mathcal{E}_a(A) = \frac{1}{|\mathcal{N}_A|} \sum_{i \in \mathcal{N}_A} \mathcal{E}r_i$.

In the multi-hop routing protocol, node A selects its next hop grid only from the set $\mathcal{N}_A$ according to the predetermined routing strategy. To achieve energy balance among all the grids in the sensor network, we carefully monitor and control the energy consumption for the nodes with relatively low energy levels by configuring A to only select the grids with relatively higher remaining energy levels for message forwarding.

For this purpose, we introduce a parameter $\alpha \in [0, 1]$ to enforce the degree of the *energy*

balance control (EBC). We define the candidate set for the next hop node as $\mathcal{N}_A^\alpha = \{i \in \mathcal{N}_A \,|\, \mathcal{E}r_i \geq \alpha \mathcal{E}_a(A)\}$ based on the EBC α. It can be easily seen that a larger α corresponds to a better EBC. It is also clear that increasing of α may also increase the routing length. However, it can effectively control energy consumption from the nodes with energy levels lower than $\alpha \mathcal{E}_a(A)$.

We summarize the CASER routing protocol in Algorithm 1.

Algorithm 1 Node A finds the next hop routing grid based on the EBC $\alpha \in [0, 1]$

1: Compute the average remaining energy of the adjacent neighboring grids: $\mathcal{E}_a(A) = \frac{1}{|\mathcal{N}_A|} \sum_{i \in \mathcal{N}_A} \mathcal{E}r_i$.

2: Determine the candidate grids for the next routing hop: $\mathcal{N}_A^\alpha = \{i \in \mathcal{N}_A \,|\, \mathcal{E}r_i \geq \alpha \mathcal{E}_a(A)\}$.

3: Send the message to the grid in the $\mathcal{N}_A^\alpha$ that is closest to the sink node based on its relative location.

It should be pointed out that the EBC parameter α can be configured in the message level, or in the node level based on the application scenario and the preference. When α increases from 0 to 1, more and more sensor nodes with relatively low energy levels will be excluded from the active routing selection. Therefore, the $\mathcal{N}_A^\alpha$ shrinks as α increases. In other words, as α increases, the routing flexibility may reduce. As a result, the overall routing hops may increase. But since $\mathcal{E}_a(A)$ is defined as the average energy level of the nodes in $\mathcal{N}_A$, this subset is dynamic and will never be empty. Therefore, the next hop grid can always be selected from $\mathcal{N}_A^\alpha$.

2.3.2.1 Probability Analysis

The parameter EBC enforces the route to bypass the grids with lower remaining energy levels to extend the lifetime of network. To analyze the effect, the network is divided into small grids, as shown in Figure 2.3. When the source node has a message to forward to the sink node, the source node selects a relay grid from its neighbor grids based on both hop distance and the remaining energy level. We divide the entire sensor domain into four

$\frac{\pi}{2}$ sections i $(i = 1, 2, 3, 4)$ corresponding to F(orward), U(pper), D(own) and B(ackward). The distance from the section G_i to the sink node is denoted as d_i. We also denote the remaining energy level of section i as $\mathcal{E}_i$ $(i = 1, 2, 3, 4)$. Since the initial energy distribution each grids and the events distribution are both random variables, the remaining energy level $\mathcal{E}_i$ is also a random variable and independent and identically distributed (iid). Let $f(e_i)$ be the probability distribution function (PDF) of $\mathcal{E}_i$. Based on Algorithm 1 and remaining energy distribution, the probability that section i is not selected as a candidate direction can be derived as follows:

$$\begin{aligned} P(Z_i) &= P\left(\mathcal{E}_i < \alpha \times \frac{\Sigma_{i=1}^{4}\mathcal{E}_i}{4}\right) \\ &= P\left(\frac{4 \cdot \mathcal{E}_i}{\alpha} - \Sigma_{i=1}^{4}\mathcal{E}_i < 0\right),\ i = 1, \cdots, 4, \end{aligned} \tag{2.1}$$

where Z_i is the event that grid G_i is not selected as the candidate grid due to its relatively low remaining energy level.

Denote P_i as the probability that grid G_i is selected as the relay grid for message forwarding. Suppose $d_1 \leq ... \leq d_4$, then we have

$$P_i = \prod_{j=1}^{i-1} P(Z_j) \cdot [1 - P(Z_i)],\ i = 1, \cdots, 4, \tag{2.2}$$

where $P(Z_i) = \int_{-\infty}^{0} f(z_i)\, dz_i$, and $f(z_i)$ is the PDF of random variable Z_i.

2.3.2.2 Analysis on Energy Distribution

Assume that each sensor node is initially deployed with equal initial energy. The energy level decreases when the sensor node forwards message. The remaining energy level of each node is based on the events distribution. Since the event is a random variable in the network, we assume the remaining energy levels of the sensor nodes are iid random variables.

Since the network is randomly deployed, the number of sensor nodes in each grid is determined by the size of the grid. So the number of sensor nodes in each grid also follows iid. We assume that the number of sensor nodes in each grid is large enough so that the

initial energy of each girds should follow the normal distribution according to the central limit theorem. For each layer, the energy consumption for sensing and forwarding also follow the normal distribution. So the remaining energy level $\mathcal{E}_i$ shall follow the normal distribution, that is $\mathcal{E}_i \sim N(\mu_i, \sigma_i^2)$, where μ_i is the mean of the remaining energy level of each grid, σ_i is the standard derivation of energy distribution. Then

$$Z_i \sim N\left(\mu_i', \sigma_i'^2\right), \tag{2.3}$$

$$f(Z_i) = \frac{1}{\sqrt{2\pi}\sigma_i'} e^{-\frac{1}{2}\frac{(z_i-\mu_i')^2}{\sigma_i'^2}}, \tag{2.4}$$

$$P(Z_i) = \int_{-\infty}^{0} \frac{1}{\sqrt{2\pi}\sigma_i'} e^{-\frac{1}{2}\frac{(z_i-\mu_i')^2}{\sigma_i'^2}} dz_i, \tag{2.5}$$

where $\mu_i' = \frac{4}{\alpha}\mu_i - \Sigma_{j=1}^{4}\mu_j$ and $\sigma_i'^2 = (\frac{4}{\alpha}-1)^2\sigma_i^2 + \Sigma_{j=1,j\neq i}^{4}\sigma_j^2$.

2.3.2.3 The Hop Distance Estimation

As shown in Figure 2.3, we divide the whole sensor domain into four equal size sections F, B, U and D. Let P_F, P_B, P_U and P_D be the probabilities that the message is forwarded to the sections F, B, U and D, respectively. Then we have the following theorem.

Theorem 1. *Assume that the network is randomly deployed and each sensor node is initially deployed with equal initial energy. We also assume that data generation in each sensor node is a random variable. Then the number of routing hops in the dynamic routing protocol can be estimated by the following equation*

$$\frac{h\sqrt{1+\left(\frac{P_U+P_L}{P_F-P_B}\right)^2}}{P_F-P_B}. \tag{2.6}$$

where h is the shortest hop distance between the source and the sink.

Proof. Since the network is randomly deployed, the number of sensor nodes in each grid is determined by the size of the grid. So the number of sensor nodes in each grid follows iid.

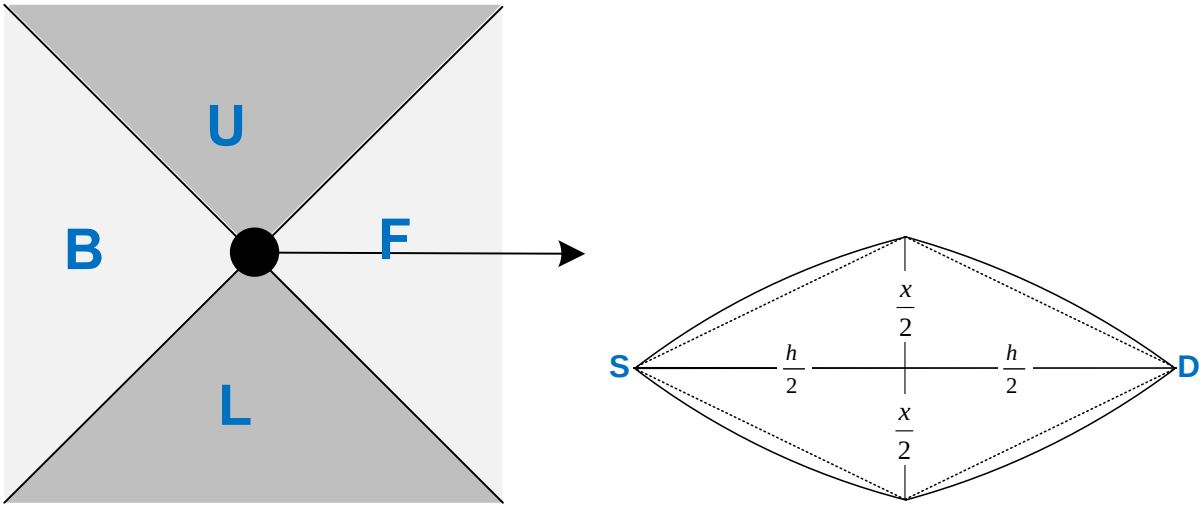

(a) Next hop node distribution (b) Routing path

Figure 2.3 Routing path and length estimation.

When the number of sensor nodes in each grid is large enough, the sum of the energy in each grid should follow the normal distribution according to the central limit theorem. Therefore, the energy consumption for each grid is also the iid and follows the normal distribution.

In dynamic routing algorithm, the next forwarding node is selected based on the routing protocol. As shown in Figure 2.3, since the probability of P_U and P_D have similar effect, while the $P_F - P_B$ needs to move the message forward h hops, therefore we have estimation $(P_F - P_B) : (P_U + P_D) = h : x$, where x is the routing hops that the message is routed in the perpendicular direction, which can be calculated as

$$x = \frac{h(P_U + P_D)}{P_F - P_B}.$$

Therefore, the entire routing path length can be estimated as

$$h\sqrt{1 + \left(\frac{P_U + P_D}{P_F - P_B}\right)^2}, \tag{2.7}$$

and the total number of routing hops can be estimated by

$$\frac{h\sqrt{1 + \left(\frac{P_U + P_D}{P_F - P_B}\right)^2}}{P_F - P_B}.$$

□

According to Section 2.3.2.1, in our case G_1, G_2, G_3 and G_4 correspond the sections F, B, U and D, respectively. Therefore, we have $P_F = P_1, P_U = P_2, P_D = P_3, P_B = P_4$. Based on Theorem 1, the total number of routing hops can be estimated according to the following corollary.

Corollary 1. *Assume that the network is randomly deployed and each sensor node is initially deployed with equal initial energy. We also assume that data generation in each sensor node is a random variable. Then for a given EBC parameter α and the hop distance h for $\alpha = 0$, the number of routing hops can be estimated from the following equation:*

$$\frac{h\sqrt{1+\left(\frac{P_2+P_3}{P_1-P_4}\right)^2}}{P_1-P_4}. \tag{2.8}$$

Table 2.1 Routing hops for different EBC parameters ($\mu' = 200$, $\sigma' = 50\sqrt{2}$)

EBC parameter α	Average hops in simulations	Estimated CASER hops
0	10	10
0.1	10.26	10.05
0.2	10.38	10.09
0.3	10.63	10.18
0.4	11.02	10.34
0.5	11.15	10.64

Our simulation results conducted using OPNET network performance analysis tool demonstrate that Corollary 1 provides a very good approximation on the actual number of routing hops, as shown in Table 2.1.

2.3.3 Secure Routing Strategy

In the previous section, we only described the shortest path routing grid selection strategy. However, in CASER protocol, we can support other routing strategies. In this section,

we propose a routing strategy that can provide routing path unpredictability and security. The routing protocol contains two options for message forwarding: one is a deterministic shortest path routing grid selection algorithm, and the other is a secure routing grid selection algorithm through random walking.

In the deterministic routing approach, the next hop grid is selected from $\mathcal{N}_A^\alpha$ based on the relative locations of the grids. The grid that is closest to the sink node is selected for message forwarding. In the secure routing case, the next hop grid is randomly selected from $\mathcal{N}_A^\alpha$ for message forwarding. The distribution of these two algorithms is controlled by a *security level* called $\beta, \beta \in [0, 1]$, carried in each message.

When a node needs to forward a message, the node first selects a random number $\gamma \in [0, 1]$. If $\gamma > \beta$, then the node selects the next hop grid based on the shortest routing algorithm; otherwise, the next hop grid is selected using random walking. The security level β is an adjustable parameter. A smaller β results in a shorter routing path and is more energy efficient in message forwarding. On the other hand, a larger β provides more routing diversity and security.

2.3.4 CASER Algorithm

Based on the previous description, the CASER algorithm can be described in Algorithm 2. While providing routing path security, security routing will add extra routing overhead due to an extended routing path.

When β increases, the probability for the next hop grid to be selected through random walking also increases. Accordingly, the routing path becomes more random. In particular, when $\beta = 1$, then random walking becomes the only routing strategy for the next hop grid to be selected. The existing research [1, 28] has demonstrated that the message may never be delivered from the source node to the destination node in this case.

When $\beta < 1$, since CASER mixes random walking with deterministic shortest path routing, the deterministic shortest path routing guarantees that the messages are sent from

Algorithm 2 Node A finds the next hop routing grid based on the given parameters $\alpha, \beta \in [0, 1]$

1: Compute the average remaining energy of the adjacent neighboring grids: $\mathcal{E}_a(A) = \frac{1}{|\mathcal{N}_A|} \sum_{i \in \mathcal{N}_A} \mathcal{E}r_i$.

2: Determine the candidate grids for the next routing hop: $\mathcal{N}_A^\alpha = \{i \in \mathcal{N}_A \,|\, \mathcal{E}r_i \geq \alpha \mathcal{E}_a(A)\}$.

3: Select a random number $\gamma \in [0, 1]$.

4: **if** $\gamma > \beta$ **then**

5: Send the message to the grid in the $\mathcal{N}_A^\alpha$ that is closest to the sink node based on its relative location.

6: **else**

7: Route the message to a randomly selected grid in the set $\mathcal{N}_A^\alpha$.

8: **end if**

the source node to the sink node. However, the routing path becomes more dynamic and unpredictable. In this way, it is more difficult for the adversary to capture the message or jam the traffic. Therefore, the delivery ratio can be increased in a hostile environment. While providing routing security, routing hop distance increases with the security level β. Corollary 2 provides a quantitative estimation of the routing hops in this scenario.

Corollary 2. *Assume that the network is randomly deployed and each sensor node is initially deployed with equal initial energy. We also assume that data generation in each sensor node is a random variable. Then the average number of routing hops for a message to be transmitted from the source to the sink nodes can be estimated as follows:*

$$\frac{h\sqrt{1 + \left(\frac{\beta}{2(1-\beta)}\right)^2}}{1 - \beta}, \tag{2.9}$$

where h is the required number of hops when the security level $\beta = 0$ (i.e., when no security is enforced).

Proof. For a security level β, the probability that the message is routed forward using the deterministic shortest path routing strategy is $1 - \beta$. For probability β, the message is forwarded using random walking. At each source, similar to Theorem 1, we can divide the

Table 2.2 Routing hops for various security parameters. The simulation was performed using OPNET.

Security parameter β	Average hops in simulations	Estimated CASER hops
0	10.00	10.00
0.125	11.97	11.46
0.25	14.51	13.52
0.375	17.98	16.70
0.5	23.34	22.36

entire domain into four $\frac{\pi}{2}$ sections, correspond to F, U, D, B with probability $P_F = 1 - \frac{3\beta}{4}, P_U = P_D = P_B = \frac{\beta}{4}$. The rest part of the proof is straight according to Theorem 1. □

Table 2.2 compares the average number of routing hops between simulation results and the estimation based on Corollary 2 for various security parameters .

Remark 1. *Corollary 1 and Corollary 2 are derived based on the assumption that the sensor nodes are randomly deployed. However, in our case, the remaining energy levels for the sensor nodes decrease exponentially when message are being transmitted based on distance between the sensor nodes and the sink node. Therefore, the actual number of routing hops should be slightly longer than this estimation.*

2.3.5 Determine Security Level Based on Cost Factor

Based on Corollary 2, for a given routing budget, we can also find the maximum routing security level. This result is given in the following theorem.

Theorem 2. *Assume that the network is randomly deployed and each sensor node is initially deployed with equal initial energy. We also assume that data generation in each sensor node is a random variable. Then for a given routing cost factor f, the optimal security level can be estimated from the following quartic equation:*

$$4fx^4 - 5x^2 + 2x - 1 = 0, \tag{2.10}$$

where $x = 1 - \beta$.

Proof. According to Corollary 2, we have

$$\frac{\sqrt{1 + \left(\frac{\beta}{2(1-\beta)}\right)^2}}{1-\beta} = f.$$

Multiply both sides with $1 - \beta$, we have

$$\sqrt{1 + \left(\frac{\beta}{2(1-\beta)}\right)^2} = f(1-\beta).$$

Square of both sides, we get

$$1 + \left(\frac{\beta}{2(1-\beta)}\right)^2 = f^2(1-\beta)^2.$$

Equivalently, we have

$$4(1-\beta)^2 + \beta^2 = 4f^2(1-\beta)^4.$$

Let $1 - \beta = x$, we can derive

$$\beta^2 = (1-x)^2 = x^2 - 2x + 1,$$

reorganize the above equation, we get

$$4f^2x^4 - 5x^2 + 2x - 1 = 0. \tag{2.11}$$

□

Equation (2.11) can be solved using Ferrari's method [71] following Algorithm 3 to recover $s = 1 - \beta$. The security level β can be recovered as: $\beta = 1 - s$.

Example 1. *Suppose we want to deliver a message with cost factor* $f = 1.5$. *To find the maximum routing security level, we need to find the security parameter* β. *We can compute* $s = 1 - \beta$ *as follows:*

1: $a \leftarrow 9; c \leftarrow -5; d \leftarrow 2; e \leftarrow -1;$

Algorithm 3 Solve equation $4f^2x^4 - 5x^2 + 2x - 1 = 0$.

1: $a \leftarrow 4f^2; c \leftarrow -5; d \leftarrow 2; e \leftarrow -1;$

2: $A \leftarrow \frac{c}{a}; B \leftarrow \frac{d}{a}; C \leftarrow \frac{e}{a};$

3: $p \leftarrow -\frac{1}{12}A^2 - C; q \leftarrow -\frac{A^3}{108} + \frac{AC}{3} - \frac{B^2}{8};$

4: $r \leftarrow -\frac{q}{2} + \sqrt{\frac{q^2}{4} + \frac{p^3}{27}};$

5: $u \leftarrow \sqrt[3]{r};$

6: $y \leftarrow -\frac{5}{6}A + u - \frac{p}{3u}; w \leftarrow \sqrt{A + 2y};$

7: $s \leftarrow \frac{-w + \sqrt{-3A - 2y + 2B/w}}{2}.$

2: $A \leftarrow -0.556; B \leftarrow 0.222; C \leftarrow -0.111;$

3: $p \leftarrow 0.0854; q \leftarrow 0.016;$

4: $r \leftarrow 0.001;$

5: $u \leftarrow 0.110;$

6: $y \leftarrow 0.314; w \leftarrow 0.270;$

7: $s \leftarrow 0.684.$

Therefore, we have $\beta = 1 - s = 0.316$*, which means 31.6% of the routing strategies should be based on random walking for message forwarding.*

2.4 Security Analysis

In CASER, the next hop grid is selected based on one of the two routing strategies: shortest path routing or random walking. The selection of these two routing strategies is probabilistically controlled by the security level β. The security level of each message can be determined by the message source according to the message priority or delivery preference. As β increases, the routing path becomes more random, unpredictable, robust to hostile detection, interception and interference attacks.

While random walking can provide good routing path unpredictability, it has poor routing performance [1, 26, 28]. CASER provides an excellent balance between routing security and efficiency.

2.4.1 Quantitative Security Analysis of CASER

In [32], we introduced criteria to quantitatively measure source-location privacy for WSNs.

Definition 1 ([32] Source-location Disclosure Index (SDI)). SDI *measures, from an information entropy point of view, the amount of source-location information that one message can leak to the adversaries.*

For a routing scheme, to achieve good source-location privacy, *SDI* value for the scheme should be as close to zero possible.

Definition 2 ([32] Source-location Space Index (SSI)). SSI *is defined as the set of possible network nodes, or area of the possible network domain, that a message can be transmitted from.*

For a source-location privacy scheme, *SSI* should be as large as possible so that the complexity for an adversary to perform an exhaustive search of the message source is maximized.

Definition 3 ([32] Normalized Source-location Space Index (NSSI)). NSSI *is defined as the ratio of the* SSI *area over the total area of the network domain. Therefore,* $NSSI \in [0, 1]$*, and we always have* $NSSI = 1 - \delta$ *for some* $\delta \in [0, 1]$*. The* δ *is called the local degree.*

Based on these criteria, we can evaluate security of the CASER routing protocol.

Theorem 3. *Assume that the network is randomly deployed and each sensor node is initially deployed with equal initial energy. We also assume that data generation in each sensor node is a random variable. Then the CASER routing protocol can achieve perfect source node location information protection when* $\beta > 0$*, that is*

$$SDI \simeq 0.$$

Proof. First, in CASER, according to our assumption, a dynamic ID is used for each message, which prevents the adversary from linking multiple messages from the same source or linking the message to the source direction using correlation based techniques.

Second, for $\beta > 0$, due to probabilistic distribution of random walking and deterministic routing, at each intermediate node, neither the original packet source direction, nor the hop distance can be determined through routing traceback analysis. In fact, the adversary is infeasible to determine the previous hop source node through routing traceback analysis. Moreover, the probability for the adversary to receive multiple messages from the same source node continuously is negligible for large sensor networks. Therefore, we have

$$SDI \simeq 0.$$

□

Theorem 4. *Assume that the network is randomly deployed and each sensor node is initially deployed with equal initial energy. We also assume that data generation in each sensor node is a random variable. Then the source location that can be provided by the CASER routing protocol is probabilistically proportional to the distribution of the random walking. That is*

$$NSSI \simeq 1.$$

Proof. When an adversary intercepts a message m while the message is being transmitted from node A to node B, there are two possible scenarios: (i) the message is transmitted using random walking, or (ii) the message is transmitted using deterministic routing.

For scenario (i), suppose message m is transmitted from S_i to D_i, the previous source node is located in shaded area, as shown in Figure **??**, based on the routing scheme and routing hop distance, where the angle of the shaded circular sector with horizontal lines is $\frac{\pi}{2}$ and symmetric to the S_iD_i.

Since each node routes the message forward with probability $1 - \beta$ using deterministic routing and with probability β using random walking. It can be derived that the probability

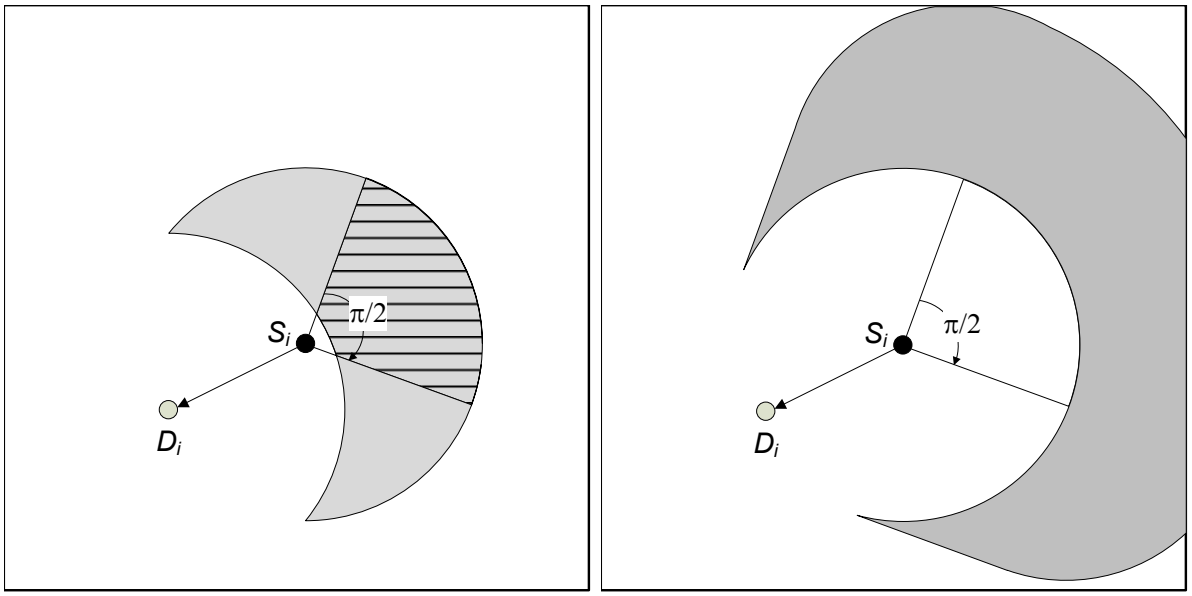

(a) Random walking (b) Deterministic routing

Figure 2.4 Routing source traceback analysis.

for the immediate previous hop node to be located in the shaded sector is $1-\beta+\frac{\beta}{4} = 1-\frac{3}{4}\beta$, and to be located in the rest of the shaded area is $\frac{3}{4}\beta$.

The probability advantage for the immediate previous hop node to be in the shared sector area with horizontal lines is,

$$1 - \frac{3}{4}\beta - \frac{1}{4} = \frac{3}{4}(1-\beta).$$

However, when the traceback analysis continues, we will not be able to get any probability advantage for the next previous hop routing source node, except that the node will be located in the shaded area, given in Figure **??**, based on the hop distance.

Since the hop distance between the actual source node and the current intercepted node is unknown, this makes it impossible for the actual source node to be located in the sensor domain, with a negligible exception of a small area around the node D_i. Therefore, we have

$$NSSI \simeq 1.$$

□

Remark 2. *From the proof of Theorem 4, we can see that the adversary can only get probability advantage* $\frac{3}{4}(1-\beta)$ *of one hop source node. In particular, when* $\beta = 1$*, that is the case of random walking, the adversary is unable to get any probability advantage.*

2.4.2 Dynamic Routing and Jamming Attacks

For security level β, the distribution between random walking and the shortest path routing for the next routing hop is β and $1-\beta$. β can vary for each message from the same source. In this way, the routing path becomes dynamic and unpredictable. In addition, when an adversary receives a message, he is, at most based on our assumption, able to trace back to the immediate source node that the message was transmitted. Since the message can be sent to the previous node by either of the routing strategies, it is infeasible for the adversary to determine the routing strategy and find out the previous nodes in the routing path.

Figure 2.5 gives the routing path distribution for four different security levels using OPNET. The messages are transmitted from a single source located at $(332, 259)$ to the fixed sink node located at $(1250, 1250)$. The source node and the destination node are 10 hops away in direct distance. In the figures, each line represents a routing path used by at least one message. This figure demonstrates that the routing path distribution width increases with the energy balance control α and the security parameter β.

In fact, if we assume that the minimum number of hops between the source node and the sink node is h for $\beta = 0$, then for $\beta > 0$, the total number of random walking is about $\frac{h\beta}{1-\beta}$ hops. The routing path can be spread largely in the area of width $\frac{h\beta}{1-\beta}$ centered around the path for security level $\beta = 0$. Therefore, for a larger security level, more effort is required to intercept a message since it triggers more random walking, which will create a wider routing path distribution and a higher routing robustness under hostile attacks. As a result, the adversary has to monitor a larger area in order to intercept/jam a message. As an example, when $\beta = 0.5$, the width of the routing path is about the same as the length of the routing path, as shown in Figure 2.5(d).

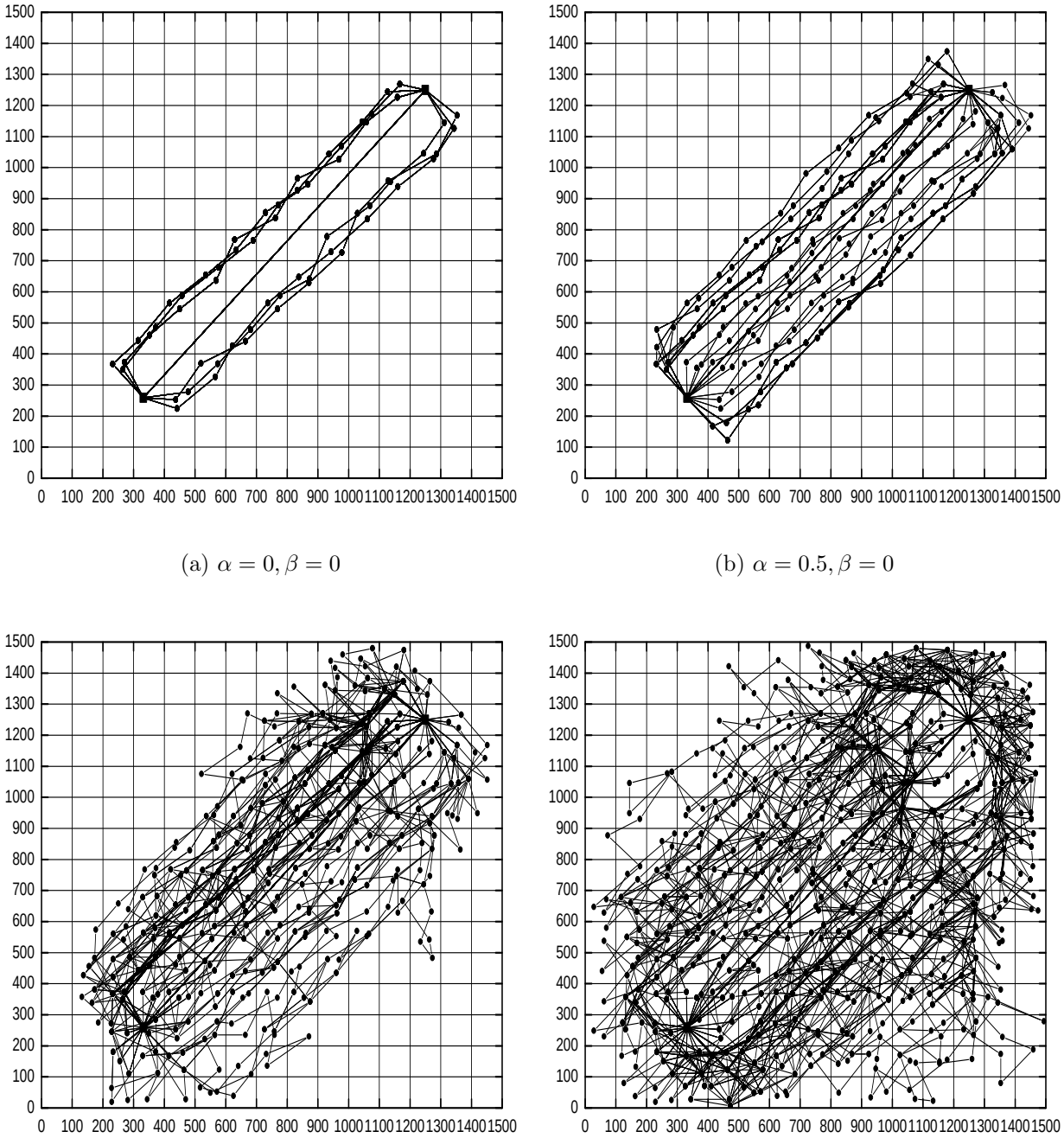

(a) $\alpha = 0, \beta = 0$

(b) $\alpha = 0.5, \beta = 0$

(c) $\alpha = 0.5, \beta = 0.25$

(d) $\alpha = 0.5, \beta = 0.5$

Figure 2.5 Routing path distribution statistics for various energy balance control α and security parameters β. In all simulations, the target area is 1500×1500. The source node is located at $(332, 259)$ and sink is located at $(1250, 1250)$.

Jamming attacks have been extensively studied [72, 73]. The main idea is that the jammers try to interfere with normal communications between the legitimate communication parties in the link layer and/or physical layer. However, a jammer can perform attacks only when the jammer is on the message forwarding path. As discussed in [73], dynamic routing is an effective method to minimize the probability of jamming.

The CASER routing algorithm distributes the routing paths in a large area based on our above analysis due to the random and independent routing selection strategy in each forwarding node. This makes the likelihood for multiple messages to be routed to the sink node through the same routing path very low, even for the smart jammers that have knowledge of the routing algorithm.

2.4.3 Energy Level and Compromised Nodes Detection

Since we assume that each node has knowledge of energy levels of its adjacent neighboring grids, each sensor node can update the energy levels based on the detected energy usage. The actual energy is updated periodically. For WSNs with non-replenishable energy resources, the energy level is a monotonically decreasing function. The updated energy level should never be higher than the predicated energy level, since the predicted energy level is calculated based on only the actually detected usage. If the updated energy level is higher than the predicted level, the node must have been compromised and should be excluded from its list of the adjacent neighboring grids.

We also compared the CASER algorithm with the RSIN algorithm in [1] on path distribution under the similar energy consumption. The results show that the CASER can achieve better and more uniform path distribution, as shown in Figure 2.6. Our simulation results show that the average number of routing hops for the two schemes are 14.51 and 15.27, respectively.

In addition, for a node with a low energy level that is caused by excessive usage due to security attacks, according to our design, these nodes will be filtered out of the pool

for active routing selection. Therefore, the CASER design can minimize the possibility for denial-of-service (DoS) attacks.

2.5 Performance Evaluation and Simulation Results

In this chapter, the simulation results illustrate the distribution of the routing path for different security levels that makes it impossible to perform traceback attack for adversaries. Then, we analyze the performance of the proposed CASER algorithm for routing efficiency and energy balance. All our simulations were conducted in a targeted sensor area of size 1500×1500 meters. The targeted area is divided into grids of 15×15. We randomly spread 1000 sensor nodes in the this domain.

2.5.1 Routing Efficiency and Delay

For routing efficiency, we conduct simulations of the proposed CASER protocol using OP-NET to measure the average number of routing hops for four different security levels. We randomly deployed 1000 sensor nodes in the entire sensing domain. We also assume that the source node and destination node are 10 hops away in direct distance. The routing hops increase as the number of the transmitted messages increase. The routing hops also increase with the security levels.

We performed simulations with different α and β values as shown in Tables 2.1 and 2.2. In all cases, we derived consistent results showing that the average number of routing hops derived in this dissertation provides a very close approximation to the actual number of routing hops. As expected, when the energy level goes down, the routing path spreads further wider for better energy balance.

We also provided simulation results on end-to-end transmission delay in Table 2.3.

Table 2.3 Delay results for various security parameters from simulation

Security Parameter	0	0.125	0.25	0.375	0.5
Average Delay (Sec)	0.0148	0.0177	0.0214	0.0265	0.0344

2.5.2 Energy Balance

The CASER algorithm is designed to balance the overall sensor network energy consumption in all grids by controlling energy spending from sensor nodes with low energy levels. In this way, we can extend the lifetime of the sensor networks. Through the EBC α, energy consumption from the sensor nodes with relatively lower energy levels can be regulated and controlled. Therefore, we can effectively prevent any major sections of the sensor domain from completely running out of energy and becoming unavailable.

In the CASER scheme, the parameter α can be adjusted to achieve the expected efficiency. As α increases, better energy balance can be achieved. Meanwhile, the average number of routing hops may also increase. Accordingly, the overall energy consumption may go up. In other words, though the energy control can balance the network energy levels, it may increase the number of routing hops and the overall energy consumption slightly. This is especially true when the sensor nodes have very unbalanced energy levels.

In our simulations, shown in Figure 2.7, the message source is located at (332, 259) and the message destination is located at (1250, 1250). The source node and the destination node are 10 hops away in direct distance. There are three nodes in each grid, and each node is deployed with energy to transmit 70 messages. We show the remaining energy levels of the sensor nodes under two different α levels. The darker gray-scale level corresponds to a lower remaining level. Figure **??**, we set $\alpha = 0$ and there is only one source node. The energy consumption is concentrated around the shortest routing path and moves away only until the energy runs out in that area. In Figure **??**, we set $\alpha = 0.5$, then the energy consumption is spread over a large area between this node and the sink. While maximizing the availability

of the sensor nodes, or lifetime, this design can also guarantee a high message delivery ratio until the energy runs out for all of the available sensor nodes in the area.

2.6 Summary

In this chapter, we present a decentralized routing algorithm CASER to balance energy consumption and increase network lifetime. CASER is also designed to provide source location privacy and defend against jamming attacks. We provide a quantitatively security analysis and derive formulas to show the relationship among security, energy consumption balance and energy efficiency. It also has the flexibility to support multiple routing strategies in message forwarding to extend the lifetime while increasing routing security. Both theoretical analysis and simulation results show that CASER can achieve a trade-off between energy balance and security under a given energy consumption.

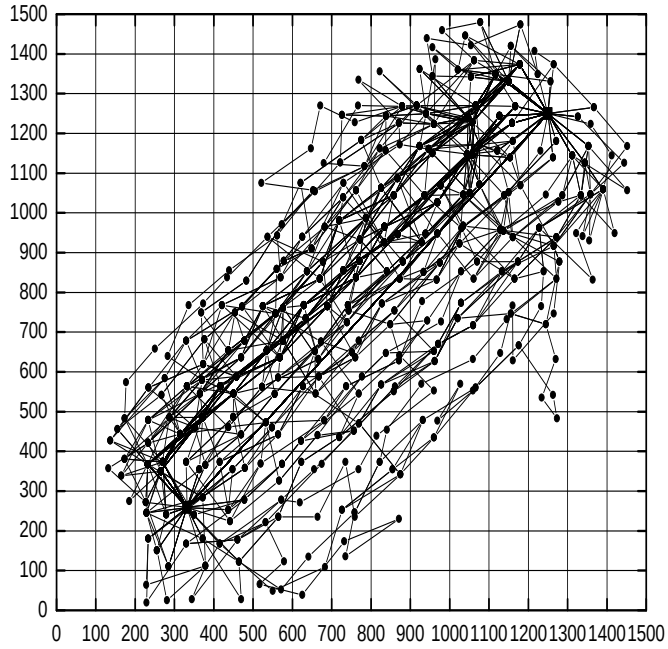

(a) CASER

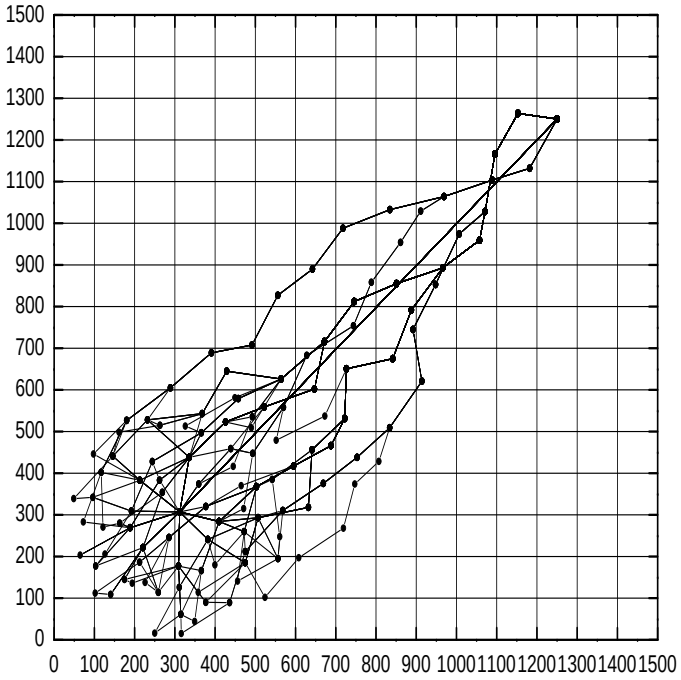

(b) RSIN

Figure 2.6 Routing path distribution statistics for energy balance control $\alpha = 0.5$ and security parameters $\beta = 0.25$ and RSIN in [1] with parameters: $d_{min} = 100, \rho = 3$.

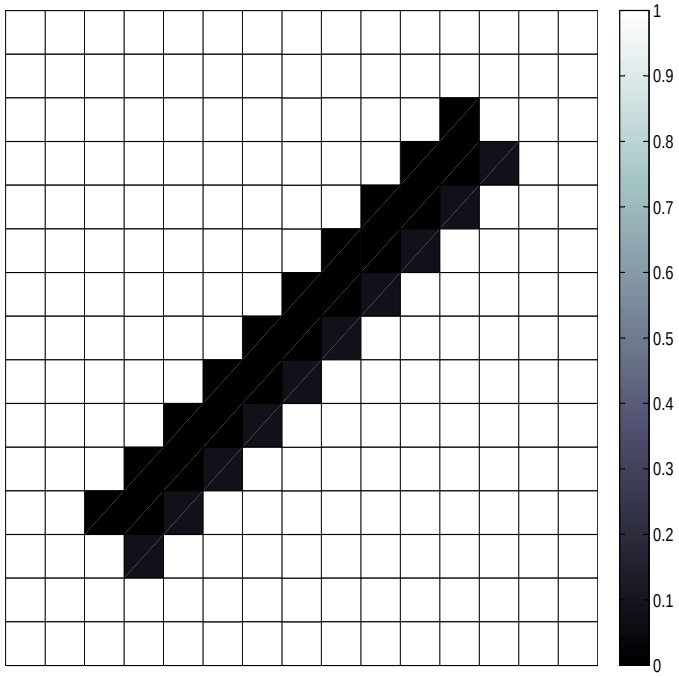

(a) $\alpha = 0$

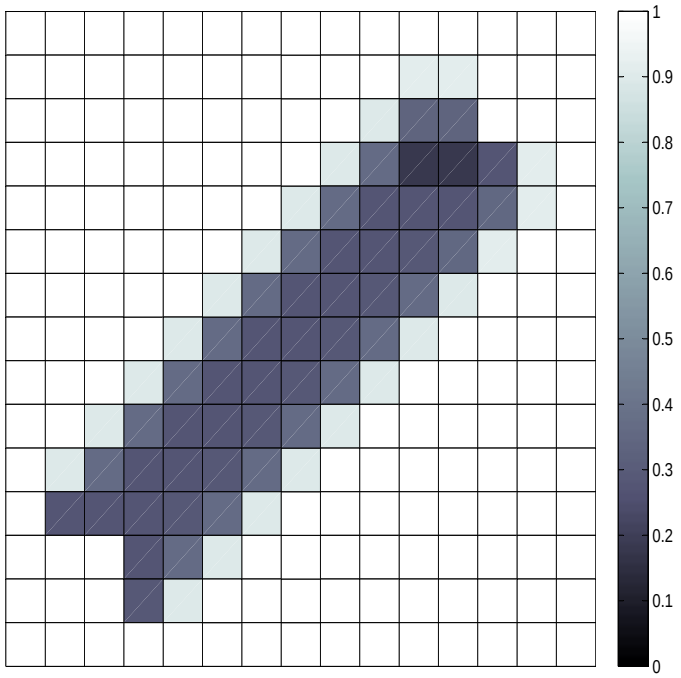

(b) $\alpha = 0.5$

Figure 2.7 Remaining energy distribution statistics after the source transmitted about 600 messages.

CHAPTER 3

COST-AWARE ENERGY DEPLOYMENT: DESIGN AND ANALYSIS

In this chapter, we propose a cost-aware energy deployment to extend the lifetime of wireless sensor networks. We also update the proposed CASER under this energy deployment strategy to preserve source location privacy. We investigate the energy consumption for CASER scheme with uniformly distributed events. The theoretical analysis and simulations show that CASER can balance the energy consumption in a local area, however the overall energy consumption through the entire network is still severely imbalanced based on the distance to the sink node under a uniform energy deployment. To solve this problem, we propose a non-uniform energy deployment to extend the lifetime of WSN while updating CASER under this energy deployment to preserve source location privacy.

3.1 Uniform Energy Deployment

3.1.1 Energy Consumption Analysis

In the multi-hop sensor network, the messages are generated at the source and forwarded hop by hop through the relay nodes to the sink. The relay node closer to the sink node consumes more energy than the outer layer sensor nodes on relaying. Assume the events are uniformly distributed in the entire network. We could have the following theorem.

Theorem 5. *Assume that all sensor nodes transmit messages to the sink node at the same frequency, the initial energy level of each grid is equal, then the average energy consumption for the grid with distance i to the sink node is:*

$$\frac{n^2 + n + i - i^2}{2i}, \tag{3.1}$$

where n is the distance between the sink node and the outmost grid.

Proof. Since all messages will be sent to the sink node, the energy consumption for the grids with distance i to the sink node can be measured based on message forwarding for grids with distance larger than i and message transmission for grids with distance i. The number of grids with distance j to the sink node is $8j$. The total energy consumption of the grids with distance i to the sink can be calculated as $\sum_{j=i}^{n} 8j$. The average grid energy consumption is therefore:

$$\frac{\sum_{j=i}^{n} 8j}{8i} = \frac{n^2 + n + i - i^2}{2i}.$$

□

3.1.2 Energy Balance of CASER

We also conduct simulations to evaluate the energy consumption for dynamic sources in Figure 3.1. The events are uniformly distributed through the entire network. Each sensor node has equal probability to generate packets and acts as a source node. We assume that the only sink node is located in the center of the target area located at (750,750), which makes the target area symmetrical to show the energy consumption. Similar to the previous simulation, we assume there are three nodes in each grid, and each node is deployed with energy to transmit 70 messages. The maximum direct hop distance between the source node and sink is 7. The simulation results shows the average energy consumption for the node is related to the distance i to the sink.

Figure 3.1 gives the remaining energy levels close to the sink node when the sensor nodes run out almost the entire energy, where $n = 7, \alpha = 0.5, \beta = 0.5$. The color evenness in each layer of the grids demonstrates the energy usage balance enforced through the EBC α.

In fact, according to equation (3.1), we can calculate the total number of messages that can be transmitted from the outmost grid when the innermost grid runs out of energy as $210/((n^2 + n)/2) = 210/((7^2 + 7)/2) = 7.5$. In this case, the overall energy consumption is only $7.5 \times \sum_{i=1}^{n} 8j^2 = 8400$, when the sensor networks become unavailable. Recall that the overall energy units deployed are $210 \times ((2n + 1)^2 - 1) = 47040$. Therefore, the energy

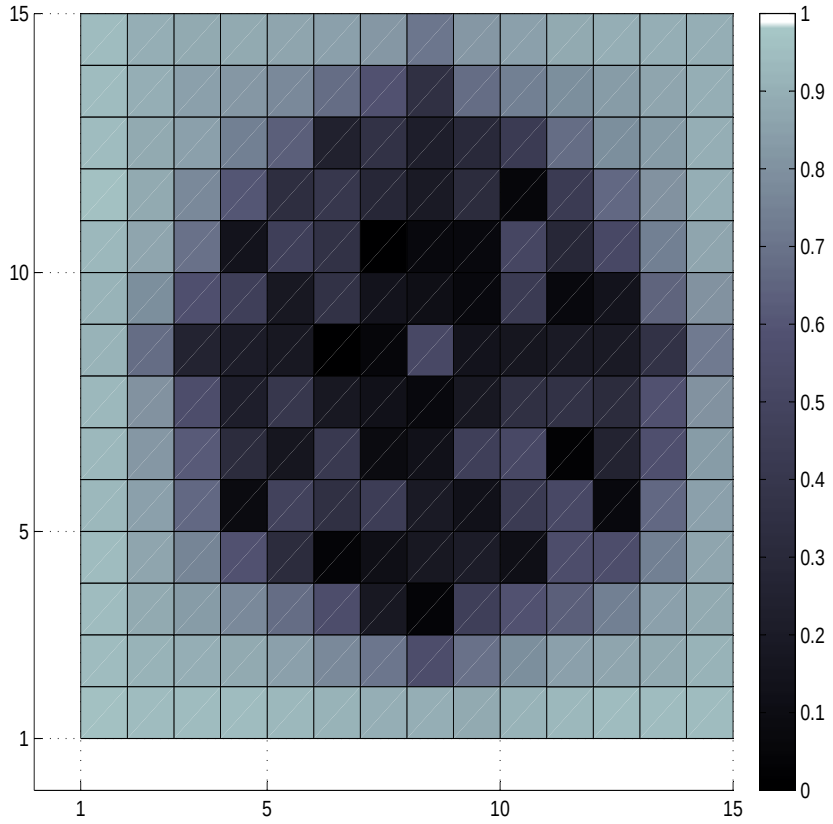

Figure 3.1 The remaining energy levels of the sensor nodes in the sensor domain when the innermost grid almost runs out of the energy, where $\alpha = 0.5, \beta = 0.5$.

consumption is only $8400/47040 = 5/28 \approx 17.86\%$ when the innermost grids run out of energy and become unavailable.

3.1.3 Delivery Ratio

One of the major differences between our proposed CASER routing protocol and the existing routing schemes is that we try to avoid having any sensor nodes run out of energy while the energy levels of other sensor nodes in that area are still high.

We implement this by enforcing a balanced energy consumption for all sensor nodes so that all sensor nodes will run out of energy at about the same time. This design guarantees a high message delivery ratio until energy runs out from all available sensor nodes at about the same time. Then the delivery ratio drops sharply. This has been confirmed through our

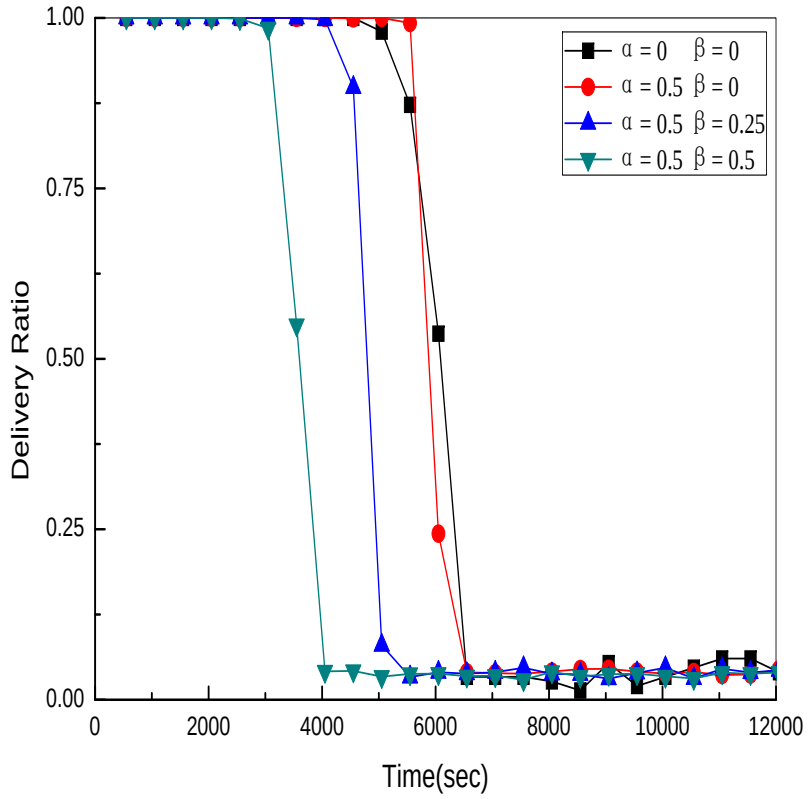

Figure 3.2 Delivery ratio under different EBC α and security level β.

simulations, shown in Figure 3.2.

3.2 CASER Optimal Non-Uniform Energy Deployment

CASER is designed to balance the energy consumption of sensor nodes and thereby extends the lifetime of the sensor networks. However, as we have described in Section 2.5.2, the energy consumption is uneven in sensor networks. The energy consumption for the sensor nodes closer to the sink node is much higher than the nodes that are away from the sink node. In fact, the average energy consumption for the node with distance i to the sink node can be calculated according to equation (3.1). Therefore, the best that we can do is to balance the energy of the grids with the same radius to the sink node, as shown in Figure 3.1.

In this section, we will explore the optimal, non-uniform initial energy deployment strategy that can maximize the lifetime of the sensor networks. Suppose the original energy

distribution for each grid is the same, and we denote the energy level as u. We also assume that the largest distance between the sink node and the outmost grid is n, then the total energy unit is $u((2n+1)^2-1)$.

3.2.1 Node Energy Deployment

For the optimal energy deployment, the energy allocation of the grids should be proportional to the energy usage. We still assume that the sink node is in the center of the sensor domain. All sensor nodes transmit messages at the same frequency. The distance between the outmost grid and the sink node is n according to equation (3.1), the energy allocation for the grids with hop distance i to the sink node should be:

$$\frac{n^2+n+i-i^2}{2i}v,$$

where v is the basic energy unit for energy deployment. Accordingly, from the outmost to the innermost, the energy assignment should be:

$$v, \frac{2n-1}{n-1}v, \frac{3(n-1)}{n-2}v, \cdots, \frac{(n+2)(n-1)}{4}v, \frac{(n+1)n}{2}v.$$

The total energy units should be:

$$v\left(\frac{8}{3}n^3+4n^2+\frac{4}{3}n\right).$$

To maintain the same amount of energy, we let:

$$u((2n+1)^2-1) = v\left(\frac{8}{3}n^3+4n^2+\frac{4}{3}n\right).$$

Then we have:

$$v = \frac{3n}{(2n+1)(n+1)}u. \tag{3.2}$$

Example 2. *We still assume that $n = 7$, and each grid has $u = 210$ energy units originally. According to equation (3.2), we can derive that:*

$$v = \frac{3u}{2n+1}u = 42.$$

Therefore, the non-uniform energy deployment for all of the grids from the outmost to the innermost can be calculated as:

$$42, 91, 151, 231, 350, 567, 1176.$$

With this energy deployment, we maintained the same overall amount of energy deployment units, 47040, in the non-uniform energy deployment. However, under our assumption, the energy consumption should be 100% before the sensor network runs out of energy and dies. Recall that in the uniform energy deployment scenario, the sensor network dies when only about 17.86% of the energy is consumed. Therefore, under non-uniform deployment, the efficiency of a sensor network's energy usage can be roughly $100/17.86 = 5.6$ times compare to the uniform energy deployment. The efficiency can be measured by the total number of messages that can be delivered, or the lifetime of the sensor network under the same transmission frequency.

3.2.2 Routing in Non-Uniform Energy Deployment

Algorithm 4 Node A finds the next hop routing grid based on the given parameters $\alpha, \beta \in [0, 1]$

1: Compute the average remaining energy of the adjacent neighboring grids: $\mathcal{E}_a(A) = \frac{1}{|\mathcal{N}_A|} \sum_{i \in \mathcal{N}_A} \frac{\mathcal{E}r_i}{\frac{n^2+n+i-i^2}{2i}}$.

2: Determine the candidate grids for the next routing hop: $\mathcal{N}_A^\alpha = \{i \in \mathcal{N}_A \,|\, \mathcal{E}r_i \geq \alpha \mathcal{E}_a(A)\}$.

3: Select a random number $\gamma \in [0, 1]$.

4: **if** $\gamma > \beta$ **then**

5: Send the message to the grid in the $\mathcal{N}_A^\alpha$ that is closest to the sink node based on its relative location.

6: **else**

7: Route the message to a randomly selected grid in the set $\mathcal{N}_A^\alpha$.

8: **end if**

Under the new energy deployment, we have to redefine the way we calculate the average remaining energy of the adjacent neighboring grids since otherwise, the messages will always be routed to the nodes that are closer to the sink node, at least initially. In this way, the number of possible nodes for the next hop can be greatly limited and security routing may become trivial.

For the non-uniform energy deployment case, the energy assignment is proportional to the energy consumption. In other words, the energy assignment is constant when divided by the energy consumption factor $\frac{n^2+n+i-i^2}{2i}$, where $i = 1, 2, \cdots, n$. Therefore, we can define the average remaining level as:

$$\mathcal{E}_a(A) = \frac{1}{|\mathcal{N}_A|} \sum_{i \in \mathcal{N}_A} \frac{\mathcal{E}r_i}{\frac{n^2+n+i-i^2}{2i}}. \tag{3.3}$$

Accordingly, we have the updated Algorithm 4.

3.2.3 Simulation Results

We conducted simulations using OPNET to compare the message delivery ratio of uniform energy deployment (noED) and non-uniform energy deployment (ED) for different α values when $\beta = 0$. The simulation settings are similar to Figure 3.1. However, each node is deployed with a different energy level according to Algorithm 4. From the simulation results in Figure 3.3, we can see that the delivery ratio increases with α. Comparing to uniform energy deployment, the delivery ratio for non-uniform energy deployment is much higher than the uniform energy deployment with the same α.

We also compared the total number of messages that can be delivered in the two scenarios. Our statistics are based on the message delivery ratio that is 95% or above. In uniform energy deployment, when $\alpha = 0$, the number of messages that can be delivered is 1510. When $\alpha = 0.25$, the number of messages that can be delivered increases to 1624. The increase is 7.55%. We found that when we further increase α, the number of messages that

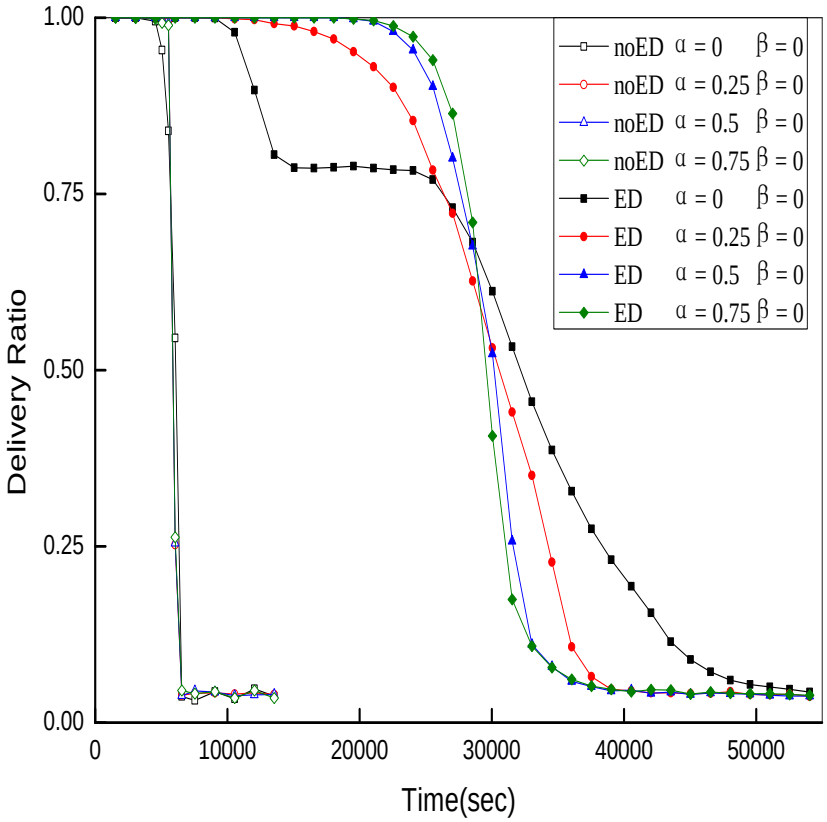

Figure 3.3 Message delivery ratio: $\beta = 0$ and varying α

can be transmitted increases slightly. At this point, all the nodes around the sink have run out of energy and no more messages can be transmitted.

For the non-uniform deployment, when $\alpha = 0, 0.25, 0.5$ and 0.75, the ratio of the number of messages that can be delivered between non-uniform and uniform is 2.37, 4.2, 5.16 and 5.38, respectively. The simulation results demonstrate that the proposed CASER and non-uniform energy deployment can significantly increase the delivery ratio and the lifetime of the WSN.

When $\beta \neq 0$, from Figure 3.4 we can see that the message delivery ratio drops as β increases. This is because the overall energy consumption increases as the required security level increases. We also found that under the proposed CASER protocol, non-uniform energy deployment can increase the energy efficiency and network lifetime even when security is required in WSNs.

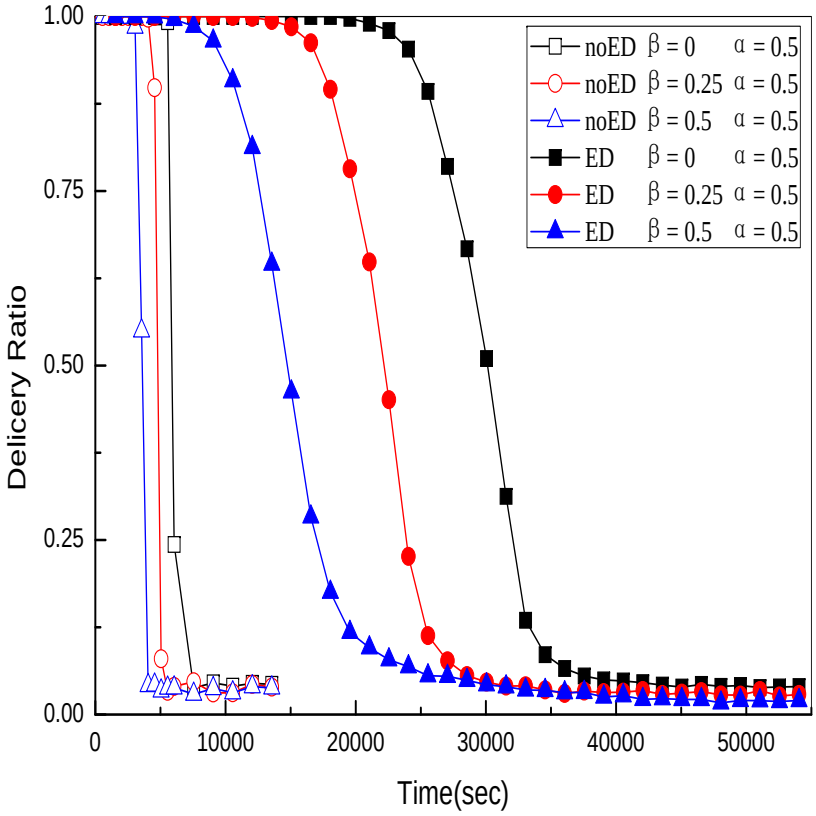

Figure 3.4 Message delivery ratio: $\alpha = 0$ and varying β

Figure 3.5 provides the message delivery ratio in a more realistic scenario. Since the different messages may have different importance, we select both security parameters and energy balance levels randomly for non-uniform and uniform energy deployment in this simulation. The results demonstrate that non-uniform energy deployment can achieve a much higher delivery ratio while extending the lifetime of the WSN.

Figure 3.6 shows the energy consumption of the WSN for non-uniform energy deployment. Comparing the two results, we conclude that CASER can achieve excellent energy balance. All sensor nodes run out of energy at about the same time, while in uniform energy deployment, the energy consumption is very unbalanced, as shown in Figure 3.1.

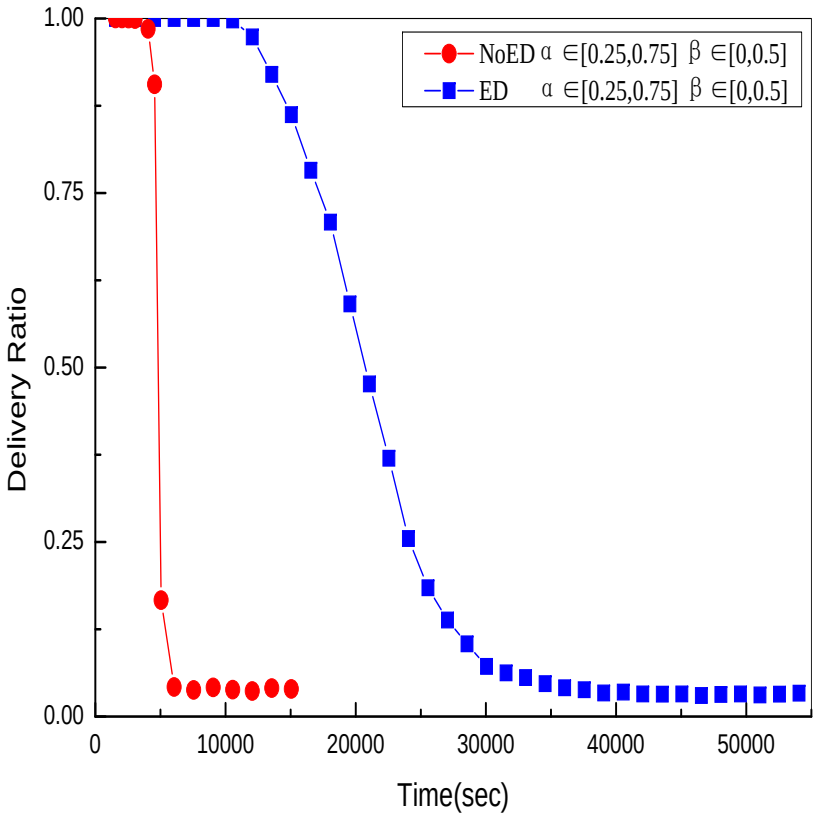

Figure 3.5 Message delivery ratio: dynamic changed β for various messages

3.3 Summary

In Chapter 2 and 3, we present a secure and efficient Cost-Aware SEcure Routing (CASER) protocol for WSNs to balance the energy consumption and increase network lifetime. CASER has the flexibility to support multiple routing strategies in message forwarding to extend the lifetime while increasing routing security. Both theoretical analysis and simulation results show that CASER has an excellent routing performance in terms of energy balance and routing path distribution for routing path security. We also propose a non-uniform energy deployment scheme to maximize the sensor network lifetime. Our analysis and simulation results show that we can increase the lifetime and the number of messages that can be delivered under the non-uniform energy deployment by more than four times under uniform energy deployment.

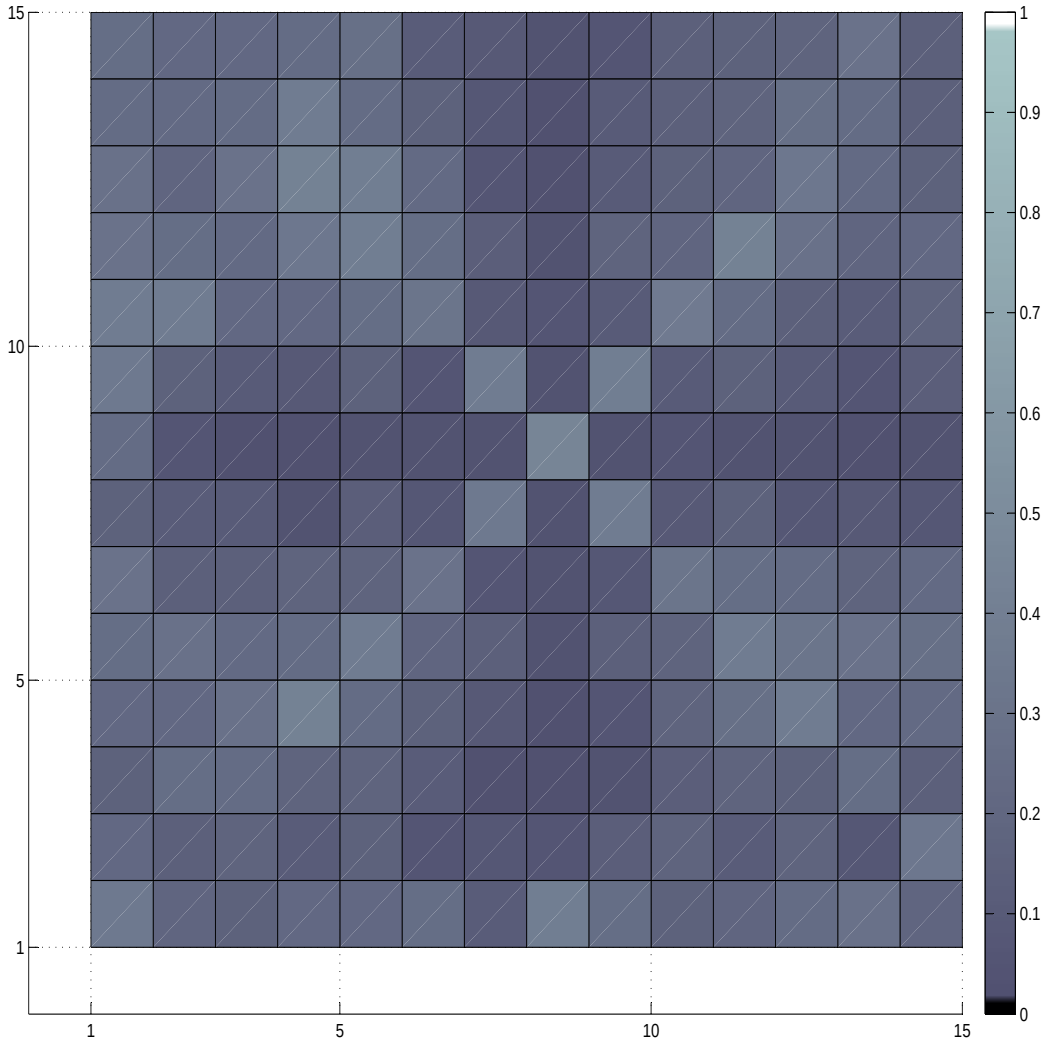

Figure 3.6 A snapshot of energy distribution when the remaining energy is about 10% in the sensor nodes, where $\alpha = 0.5, \beta = 0.5$.

CHAPTER 4

CONGESTION-AWARE ROUTING (CAR): DESIGN AND ANALYSIS

WSNs are designed to collect and transmit sensed data to one or more sink nodes. The information of the sensed data is critical for real-time processing and decision-making in both military and civilian applications, such as monitoring the forest fire and target locating. For these applications, end-to-end transmission delay is one of the most significant design issues for WSNs. In this chapter, we propose a congestion-aware routing scheme to reduce congestion by monitoring the traffic in the MAC layer. In CAR routing scheme, each node selects the relay node based on two different routing strategies: the shortest path forwarding and the congestion-aware forwarding. In the shortest path forwarding, the relay node applies geographic routing strategy [61] based relative locations, ensures an efficient message delivery through hop by hop transmission. In congestion-aware forwarding strategy, each node selects the relay node based on the competing results of wireless medium channel, which can effectively reduce the end-to-end message transmission delay.

4.1 Introduction

WSNs consist of a large number of untethered and unattended sensor nodes. Sensor nodes are equipped with low-power radio devices to send and receive messages. The messages are forwarded hop by hop from source nodes to the sink node, which may greatly create significant traffic congestion in the area close to the sink node. Burst events may also develop a significantly amount of traffic in a localized area. The unbalanced traffic volume in WSNs may increase the communication delay and energy consumption in WSNs while decreasing the network lifetime.

In traditional networks, the existing research on congestion mainly focuses on the traffic control in both end-to-end and hop-by-hop communications. These algorithms are mainly

applied to the transport layer or the Medium Access Control (MAC) layer. They are designed to avoid congestion by limiting the transmission rate or reducing traffic in the network. However, the aforementioned strategies are unsuitable for event-driven WSNs, which has been mentioned in Chapter 1.

The existing routing algorithms mainly focus on the end-to-end communication delay. They generally assume that delay between two nodes is constant. However, when the number of sink nodes is low in the networks, the traffic close to the sink nodes will be concentrated. As a result, the end-to-end transmission delay increases due to congestion. In addition, the distributed routing protocols may introduce the congestion in the MAC layer. In [74], the author has investigated the performance of CSMA/CA distributed coordination function comprehensively. It has demonstrated that the congestion condition would deteriorate significantly with increasing the number of simultaneous transmissions. In a distributed routing protocol, the routing path is decided independently based on routing strategies, such as geographic based routing protocols [61, 75]. Due to lack of cooperation, source nodes would select relay nodes independently to forward the messages locally. As shown in Figure 4.1, the congestion occurs when the sensor nodes in the set of A_1 attempts to transmit messages simultaneously in the source area. Then, in the subsequent packet transmission, MAC layer congestion cannot be avoided when these selected relay nodes try to forward the packets to the next hop simultaneously through channel i. Since all the packets are forwarded to one centralized sink in the network, congestion would occur hop-by-hop.

To solve this problem, we propose CAR routing scheme to reduce the potential congestion in the subsequent packet forwarding by monitoring the traffic in the MAC layer. In the proposed routing scheme, each sensor node selects the relay node based on two different routing strategies: the shortest path forwarding and the congestion-aware forwarding. In the shortest path forwarding, the relay node selection follows the geographic routing strategy [61] based on the geographic location. In the congestion-aware forwarding algorithm, each sensor node selects the relay node based on the channel competing results. When congestion is not

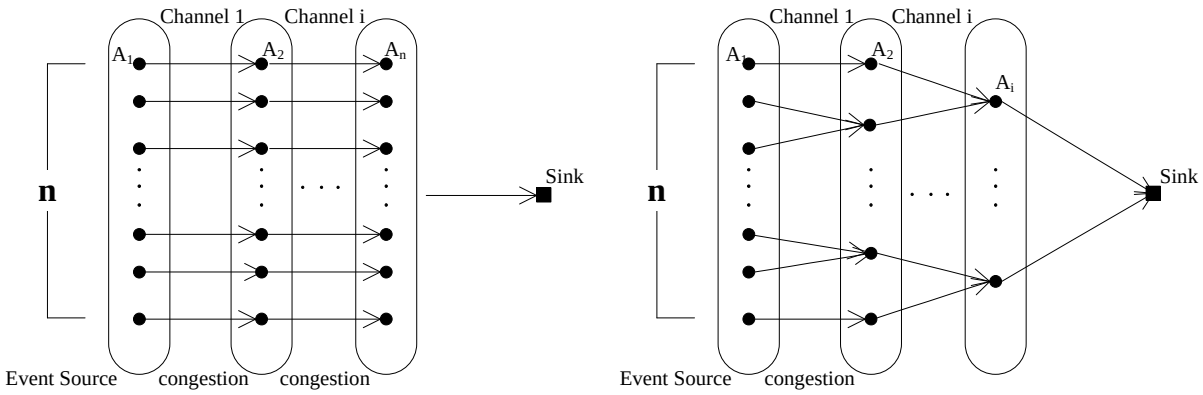

(a) Congestion

(b) CAR

Figure 4.1 The link layer congestion: (a) General distributed routing algorithms that may lead to congestion in subsequent forwarding; (b) Illustration of the CAR routing algorithm

detected, the shortest path routing algorithm will be used and congestion-aware transmission algorithm is used otherwise. The shortest path routing algorithm ensures an efficient end-to-end message transmission from the source node to the sink node. The congestion-aware forwarding can effectively reduce end-to-end message transmission delay and improve the system throughput by effectively mitigating congestion.

4.2 System Model and Assumptions

4.2.1 System Model

We assume that WSNs are composed of a large number of sensor nodes and a sink node. The sensor nodes are randomly deployed throughout the sensor domain. The sink node is the only destination for all sensor nodes to forward messages through a multi-hop routing strategy. The information of the sink node is made public. We also assume that each sensor node knows its relative location in the sensor domain and has knowledge of its immediate adjacent neighboring nodes. The information about the relative location of the sensor domain may be broadcasted in the network for routing information updating [69]. Each sensor node is

able to monitor the local traffic information. It can obtain information of the transmitted packets through monitoring the physical channel within its communication range.

4.2.2 MAC Layer Protocol

Carrier sense multiple access with collision avoidance (CSMA/CA) is one of standard medium access control protocols in WSNs. In CSMA/CA mechanism, the exponential backoff scheme is employed as the major backoff scheme. Each node starts to monitor the physical channel once it has a packet to transmit. Before each attempt of transmission, the tag node with packet to transmit keeps monitoring the channel for a period of Distributed Inter Frame Spacing (DIFS). If the channel is sensed busy, the tag node defers its transmission until the channel is idle for DIFS. Then the station generates a random backoff interval before transmitting. The time following an idle DIFS is divided into slots, and each slot is equal to σ which depends on the physical layer.

In each stage of backoff, the backoff window will be uniformly chosen in the range $(0, w-1)$. The value of w will be initially set equal to CW_{min} and doubled after a failure of transmission up to $CW_{max} = 2^m CW_{min}$. CW_{min} is denoted as the minimum contention window and m is the contending window size. The value of w will be equal to $2^i CW_{min}$ after the ith transmission attempt. The stage between the ith transmission attempt and the $(i+1)$th attempt is called as the ith stage. Once the packet is successfully transmitted by the tag node, the value of w will be set equal to the initial value.

The backoff time counter decreases when the physical channel is detected idle. It stops counting once the channel is busy for a successful transmission or a collision. When the channel is sensed idle, the counter will be reactivated and decremented. Once the counter reaches zero, the tag node transmits its packet immediately. There will be a period of Short Inter-Frame Spacing (SIFS) before the receiver sends back an acknowledgement (ACK) to the tag node.

The four-way handshaking technique, known as request-to-send/clear-to-send (RTS/CTS)

mechanism, is also utilized in the MAC layer as an access mechanism. This mechanism can increase the system performance by solving the hidden node problem.

4.3 The Proposed Routing Scheme

We now describe the proposed routing scheme. The algorithm consists of two strategies for routing path selection: the shortest path forwarding based on geographical information, and the congestion-aware forwarding based on physical channel competing results.

4.3.1 Overview of the Proposed Routing Scheme

In CAR, we assume that each node maintains the relative locations of its immediate adjacent neighboring nodes. Each node selects the relay node based on the shortest path forwarding and congestion-aware forwarding. Firstly, the source node A composes a candidate set for the relay node selection. The candidate set includes its all immediate adjacent neighboring nodes that are closer to the sink node than itself. We denote this set as $\mathcal{N}_A$. In the shortest path forwarding, the node A selects the node B that is closest to the sink node as the relay node when it has packets to forward when no traffic congestion is detected. Otherwise, A selects a relay node based on the congestion-aware forwarding scheme. If node A fails to access the channel, it will monitor the physical channel to obtain the channel competing results. Assume that A's neighboring node C has successfully accessed the channel and forwarded its packet to its relay node D. Then, if $D \in \mathcal{N}_A$, node A reselects D as its relay node in the congestion-aware forwarding.

In the shortest path forwarding, each sensor node independently selects the relay node according to the relative location which might increase the number of relay nodes. The number of potential transmissions may increase with the number of relay nodes in a local area. The number of the forwarding nodes may increase traffic congestion for the subsequent packet delivery [74]. The results may also introduce more transmission collision and

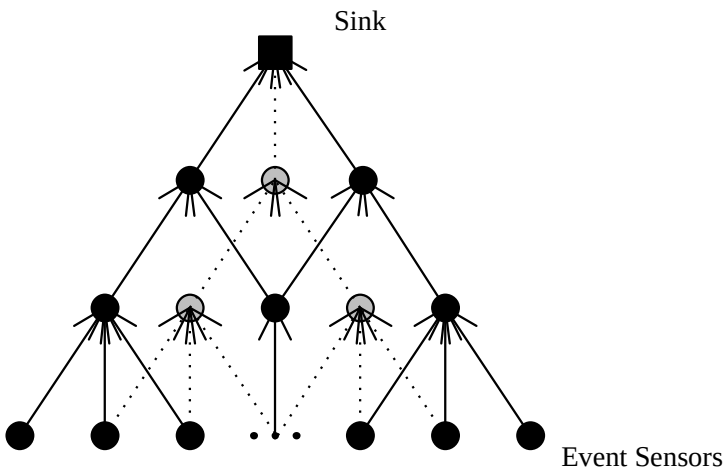

Figure 4.2 Dynamic tree formation

significantly prolong the congestion delay. Our proposed CAR scheme enables the sensor nodes to utilize the traffic condition and channel competing results to reselect relay nodes in a congested area. In this way, we can reduce the number of concurrent transmissions in the subsequent forwarding by decreasing the number of relay nodes. While decreasing end-to-end transmission delay, the CAR routing strategy can also increase the network throughput at the same time.

In addition, the proposed CAR routing scheme can reduce the energy consumption that introduced by congestion. Instead of keeping trying to transmit the packets in a congested area and consuming more energy, CAR can reduce the congestion by decreasing the number of contending nodes. As a result, the number of transmission attempts for each node also be reduced. The proposed CAR can also balance the energy consumption in congested areas. Since the channel competing results should be uniformly distributed in the available forwarding nodes, the forwarding nodes may take turns to be selected for message forwarding. As shown in Figure 4.2, the black nodes might be selected as the forwarding nodes for the current message forward. However, the gray nodes can provide more options for relay nodes selection when burst events occur.

4.3.2 Congestion-Aware (CAR) Routing Algorithm

Based on the previous description, we summarize the proposed CAR routing scheme in Algorithm 5.

Algorithm 5 Node A derives the next hop routing node based on the MAC layer congestion condition

1: Node A determines the candidate set for the next hop node selection by choosing all its neighboring nodes that are closer to the sink node than itself. Denoted the set as $\mathcal{N}_A$.

2: Selects node B in the set $\mathcal{N}_A$ that is closest to the sink node as the next hop node based on its relative location.

3: **if** the packet fails to be delivered to the next hop node, **then**
4: Node A monitors the channel from the MAC layer to obtain the information of the packet that can be successfully transmitted.

5: Suppose C is the node that successfully transmits the packet to its relay node D.

6: **if** the destination node D is in the set $\mathcal{N}_A$ **then**
7: Node A reselects node D as the next hop node.

8: **end if**

9: **end if**

4.4 The Analysis on Congestion through End-to-End Transmission

The proposed CAR algorithm mainly focuses on solving the congestion problem caused by the burst events. Firstly, we will give the analysis on the congestion in one hop. In the one hop domain, the sensor nodes may keep collecting data and forward the data to the sink node during occurrences of the burst events. Secondly, we will further analyze the end-to-end transmission delay from the source node to the sink node through the multi-hop packet delivery.

4.4.1 One Hop Congestion Analysis

Definition 4 (End-to-end transmission delay)**.** *The end-to-end transmission delay is defined as the average time duration from the time the packet is generated at bottom of the MAC queue of the source node until the sink node receives the packet successfully through the multi-hop delivery.*

Definition 5 (Contending delay)**.** *The contending delay is defined as the average time duration from the time the packet is at the top of the MAC queue to the ACK that the packet is received by the transmitting node in the one hop domain.*

The propagation delay is a constant based on the physical layer settings. In our analysis, it is included in the contending delay as defined in Definition 5. The CSMA/CA adopts the exponential backoff scheme to minimize the collision probability. In [74] and [76], the authors have studied the collision probability and saturation throughput for Distributed Coordinate Function (DCF) mechanism which is one of mechanisms in CSMA/CA. We shall follow the definitions and analysis results to derive the mean access delay that a single packet is successfully transmitted to its destination in the one hop area. Suppose that the packet is successfully transmitted in the jth transmission attempt. In [76], the authors derived the average delay per stage as follows:

$$E[D_j] = T_s + j \cdot T_c + E[slot]\Sigma_{i=0}^{j}(\frac{W_i - 1}{2}), \tag{4.1}$$

$$E[slot] = (1 - P_{tr})\sigma + P_{tr}P_sT_s + P_{tr}(1 - P_s)T_c. \tag{4.2}$$

where $\frac{W_i-1}{2}$ is the average number of slot times that the station defers in the stages, T_c is the time duration the channel is detected busy when the tag node meets a collision and jT_c is the time duration that the packet waits for collisions until it reaches the jth stage, T_s is the time duration that the packet is transmitted successfully in the jth stage, and $E[slot]$ is the average time that a station defers in a slot. σ is the period of an empty unit slot. T_s is the time duration when the tag node monitors a successful transmission. P_{tr} is

the probability that at least one station other than the tag node transmits in the a random chosen slot which is defined differently from [74], since the analysis mainly focuses on the transmission delay for a given tag node. Let P_{tr} denote the probability that the tag node can successfully monitor transmissions and collision in the channel. Then it is calculated as follows:

$$P_{tr} = 1 - (1 - \tau)^{n-1}, \tag{4.3}$$

where n is the number of contending sensor nodes within the one hop range and τ is the probability that the node transmits a packet in a randomly chosen slot time.

Let P_s be the probability that the tag station can monitor a successful transmission when at least one node other than tag node transmits. It can be derived as:

$$P_s = \frac{(n-1) \cdot \tau \cdot (1-\tau)^{n-2}}{P_{tr}}. \tag{4.4}$$

In [74], the probability τ was derived based on a Markov model as follows:

$$\tau = \frac{2 \cdot (1-2p) \cdot (1-p)^{m+1}}{W \cdot (1-(2p)^{m+1})(1-p) + (1-2p)(1-p^{m+1})}, \tag{4.5}$$

where p is the conditional probability that each packet meets a collision at each transmission attempt, regardless of the number of retransmissions suffered in one hop. The p can be calculated as follow:

$$p = 1 - (1 - \tau)^{n-1}. \tag{4.6}$$

Combining equation (4.5) and equation (4.6), the probabilities τ and p can be solved by numerical methods. Since p is the function of n, we denote $p(n)$ instead of p in following analysis.

In this chapter, we mainly focus on the analysis of the mechanism of RTS/CTS. The analysis procedure can also be applied to the base CSMA/CA mechanism. According to the backoff mechanism, the time duration of T_s and T_c can be expressed by following equations based on RTS/CTS:

$$T_s = RTS + SIFS + \delta + CTS + SIFS +$$

$$\delta + PHY_{head} + MAC_{head} + L + SIFS + \tag{4.7}$$

$$\delta + ACK + DIFS + \delta,$$

$$T_c = DIFS + RTS + SIFS + CTS, \tag{4.8}$$

where RTS, CTS, PHY_{head}, MAC_{head} and L are the transmission delay for the RTS, CTS, physical layer header, MAC layer header and the data payload respectively, and δ is the propagation delay.

Furthermore, the contending delay $C_i[D]$ in ith hop delivery can be calculated by

$$C_i[D] = \Sigma_{j=0}^{m} E[D_j] \cdot P_j. \tag{4.9}$$

where P_j is the probability of a successful transmission in jth stage, and can be calculated as follows:

$$P_j = \frac{(1-p)p^j}{1-p^{m+1}}. \tag{4.10}$$

The average number of transmission attempts for a successful transmission can be derived as follows:

$$E[N_i] = \Sigma_{j=0}^{m} P_j \cdot j. \tag{4.11}$$

In this section, we will further analyze the congestion in multi-hop networks and evaluate the performance of the proposed CAR. Suppose the sensor node can directly communicate with the sensor node within its communication range. We suppose the burst event only occurs in a local domain. And it can be detected by sensors within the sensing range. Suppose the burst event is located at the center of the domain D, and the radius of the domain D is the sensing range of sensor nodes. Then the burst event can be detected by the sensors in the domain D. The sensors in the center of the domain will encounter a serious

congestion. In fact, the number of sensor nodes competing for the channel access is $\lambda \cdot S(D)$, where λ is the density of sensor nodes and $S(D)$ is the area of D. In the subsequent packet delivery, the number of contending nodes may vary that is dependent on the topology and the area of burst events. The probability that there is at least one collision in the multi-hop delivery can be derived as:

$$P_h = 1 - \Sigma_{i=1}^{h}(1 - p(n_i)), \tag{4.12}$$

where h denotes the hop distance from the source node to the sink node and n_i is the number of contending nodes in the ith hop.

In the ith hop transmission, the average transmission delay is calculated according to equation (4.9). Then the end-to-end transmission delay through the delivery from the source node to the sink node can be calculated using the following equation:

$$E[D] = \Sigma_{i=1}^{h} C_i[D]. \tag{4.13}$$

In addition, the energy of sensor nodes is largely consumed by the message transmitting and receiving. The number of transmission attempts is one of the important issues for energy consumption. In fact, the number of transmission attempts depends on the number of contending nodes. Based on the aforementioned results, the average number of transmission attempts for a successful transmission from the source node to the sink node in the multi-layer network can be computed as follows:

$$\mathcal{N} = \Sigma_{i=1}^{h} N_i, \tag{4.14}$$

where N_i is the average number of transmission attempts in the ith hop.

4.4.2 Numerical Results

In this section, we will give numerical results based on the theoretical analysis. Since the number of contending nodes depends on the topology and area of events, we consider two extreme cases for the multi-hop network: the worst case and the ideal case.

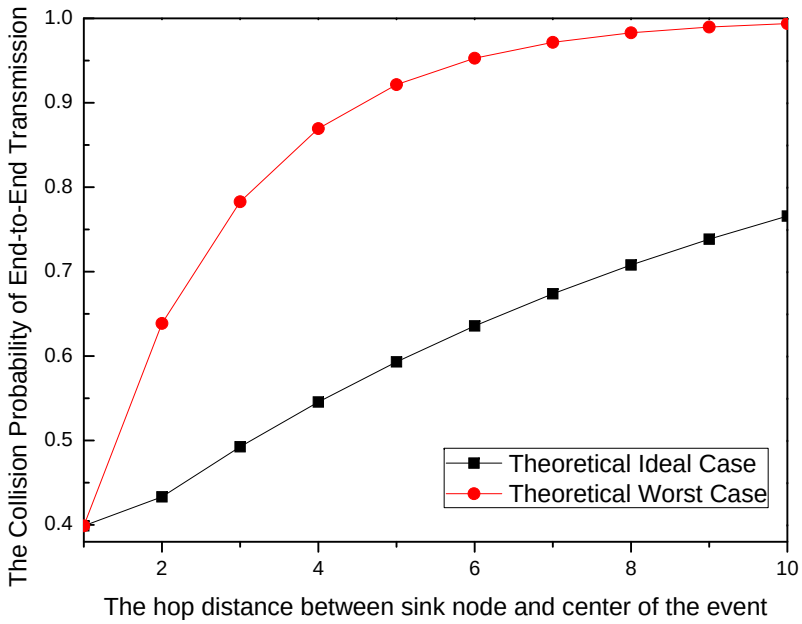

Figure 4.3 The end-to-end collision probability in multi hops. There are 20 contending nodes in the event area.

We divide the network into multi layers as shown in Figure 4.1. There is only one burst event in the network. The number of source nodes is determined by the density and the sensing range of the sensor nodes. In the worst case, the number of the contending nodes remains the same as the number of source nodes, that is $\lambda \cdot S(D)$. The packet confronts congestion hop-by-hop from the source node to the sink node. In the ideal case, the number of contending nodes in the source area cannot be reduced since the number of source nodes cannot be reduced. However, an ideal routing algorithm, the source nodes selects only one relay node in the next layer. Therefore, the number of contending nodes is minimal. Ideally, the number of contending nodes in subsequent forwarding can be reduced to three, includeing the previous hop relay node, the current relay node, and the next hop relay node. In addition, in the last hop of the delivery, there are only two contending nodes in the communication range. The end-to-end transmission delay in the worst case and ideal case can be calculated using equation (4.13).

In Figure 4.3, it shows the end-to-end collision probability for a particular packet that experiences at least one collision from the source node to the sink node in both the ideal case

and the worst case. It shows that in the ideal case, a properly designed routing algorithm can reduce the number of contending nodes in subsequent transmission, therefore, it can effectively decrease the end-to-end collision probability.

Then we give the numerical results of both end-to-end transmission delay and the number of retransmission. The results are present in Figure 4.4 and Figure 4.5. The parameters in the numerical results are listed in Table 4.1.

Table 4.1 Parameter setting of numerical results

Physical header	40 bits
MAC header	48 bits
RTS	40 bits
CTS	48 bits
Payload	250 bits
Channel bit rate	250k bits/s
Propagation delay, δ	1 μs
Slot time, σ	20 μs
SIFS	20 μs
DIFS	50 μs
Minimum CW, W	32
Number of CW size, m	5

4.5 Performance Analysis and Simulation Results

In this section, we provide theoretical evaluation and simulation results to demonstrate performance of the proposed CAR routing scheme. Since congestion increases the transmission delay and decreases packet receiving rate, we will mainly focus on the end-to-end transmission delay and the network throughput.

4.5.1 Performance Metrics

We will define two metrics to quantitatively evaluate the network performance.

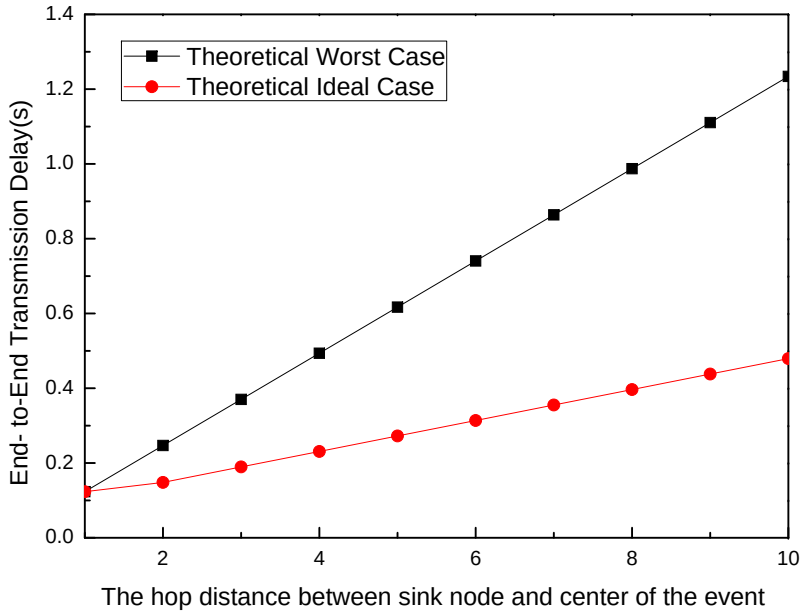

Figure 4.4 The end-to-end transmission delay in multi hops. There are 20 contending nodes in the event area.

4.5.1.1 End-to-End Packet Transmission Delay (Δ)

The end-to-end transmission delay is composed of processing delay, transmission delay, propagation delay and congestion delay. In the simulation, the end-to-end transmission delay is defined by the following equation:

$$\Delta = \frac{\sum_{i \in \mathcal{I}} (T_{r_i} - T_{s_i})}{|\mathcal{I}|},$$

where $\mathcal{I}$ is the set of packets received, T_{s_i} is the time the packet is being sent out, T_{r_i} is the time the packet is being received, and $|\mathcal{I}|$ is the cardinality of the set $\mathcal{I}$.

4.5.1.2 Network Throughput ($\mathfrak{T}$)

Network throughput is another important metric to evaluate the routing scheme performance. Let $\mathfrak{T}$ be the normalized system throughput, then $\mathfrak{T}$ can be defined as follows:

$$\mathfrak{T} = \frac{B}{T},$$

where B is the total number of bits being delivered, and T is the total time consumption.

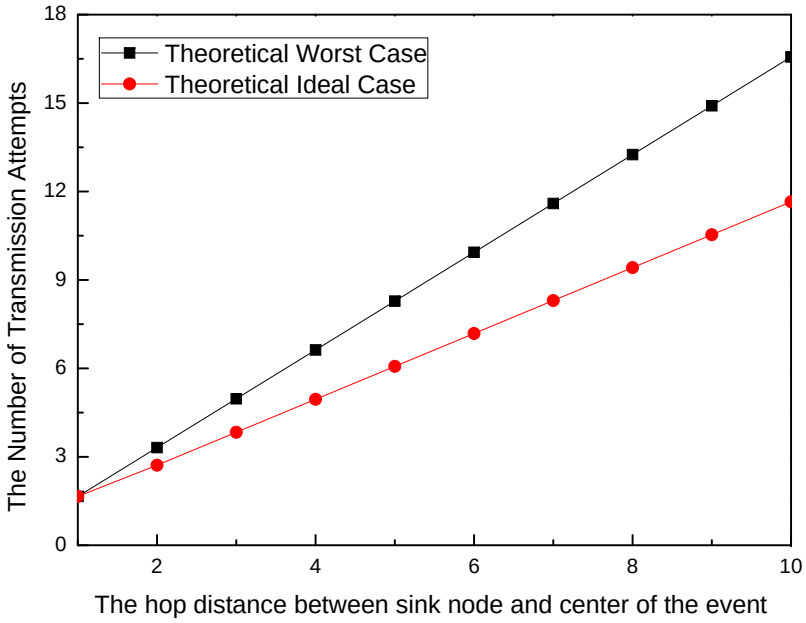

Figure 4.5 The number of retransmission through end-to-end transmission in multi hops. There are 20 contending nodes in the event area.

In the next subsection, our simulation results demonstrate that our proposed CAR routing scheme can achieve a performance close to the ideal scenario.

4.5.2 Simulation Results

We conduct simulations using OPNET in different scenarios to show the performance of the proposed routing scheme. The results will be compared with a representative geographic based routing protocol. We denote the proposed routing protocol as CAR and the geographic based routing as *MinRoute* in the following simulation results.

4.5.2.1 Simulation Setup

The proposed CAR routing scheme is designed to reduce the link-level congestion. To show the performance of CAR routing protocol, we conduct simulations with different event source locations.

The sensing range is different from the communication range. Each sensor is able to

sense the event within the sensing range. The number of the sensor nodes that sensed the burst events is determined by the topology and the sensing range. The actual number of contending nodes is less than or equal to the number of source nodes due to the difference between communication range and sensing range. The detailed simulation configurations are summarized in Table 4.2, and two different simulation scenarios are described in Table 4.3 and Table 4.4.

Table 4.2 Simulation parameter setting

Area Size	$100m \times 100m$
Deployment Type	Random
Network Architecture	Homogeneous sensor nodes with one sink node
Number of Nodes	600
Sink Coordinate	(90,90)
Communication Range	10m

Table 4.3 Simulation scenario 1: various event locations

Application Type	Event-driven
Event Location	(80,80); (70,70); (60,60); (50,50); (40,40); (30,30); (20,20)
Event Sensing Range	10m
Number of Source Nodes	18; 21; 18; 22; 16; 21; 18

Table 4.4 Simulation scenario 2: various sensing ranges

Application Type	Event-driven
Event Location	(20,20)
Event Sensing Range	2m; 4m; 6m; 8m; 10m 12m; 14m; 16m; 18m 20m;
Number of Source Nodes	2; 7; 16; 18; 27; 39; 49; 64 ; 76;

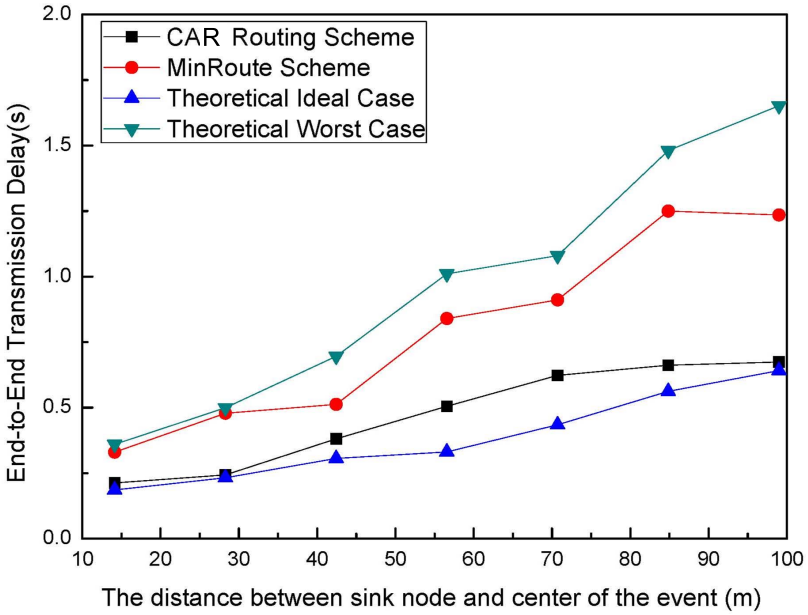

Figure 4.6 Average end-to-end transmission delay with varying burst event locations

4.5.2.2 Source Event Location

In Figure 4.6, we compare the average packets end-to-end transmission delay between the two routing protocols that have the burst event located in different places, as detailed in Table 4.1 and Table 4.3. In the simulation, the number of source nodes depends on the topology. We also compare the simulation results with the numerical results. The numerical results in ideal case and the worst case are computed based on the topology in the simulation.

Figure 4.6 shows that the *MinRoute*, as a distributed routing algorithm, experiences more congestion due to more potential concurrent transmissions through hop-by-hop delivery. Its end-to-end transmission delay is closer to the worst case. On the contrary, the end-to-end transmission delay in the CAR is closer to the ideal case. It also shows that the CAR can effectively decrease the end-to-end transmission delay by reducing the number of contending nodes in the subsequent packet delivery. With the increasing of distance from the event source to the sink, the CAR has a much shorter end-to-end transmission delay than the *MinRoute*.

4.5.2.3 Sensing Range

For a given node density, extending the event sensing range can increase the number of source nodes. However, the number of contending nodes in event source area not only depends on the number of source nodes but also on the communication range. The number of contending nodes in the source area is determined by the sensing range and node density if the sensing range is less than the communication range. If the sensing range is larger or equal to the communication range, the number of contending nodes in the source area is equal to $\lambda \cdot S(D)$. However, in the multi-hop delivery, the number of contending nodes in the subsequent forwarding can be affected by the number of source nodes since all the packets are sent to the only sink node in the wireless sensor network. Therefore, increasing sensing range leads to more link-level congestion for forwarding packets other than in the source event area.

We conduct simulations for a fix event center to verify the impact of sensing range on the performance of the CAR routing scheme. The settings of the simulations are detailed in Table 4.4. In Figure 4.7 and Figure 4.8, the source event center is located at $(80, 80)$ and the sensing range increases from $2m$ to $20m$. The number of source nodes increases with the increment of the sensing range. It is also detailed in Table 4.4. In Figure 4.7, we compare the end-to-end transmission delays between the CAR and the $MiniRoute$. We have similar results as in Figure 4.6. CAR can effectively reduce the end-to-end transmission delay with increasing the number of source nodes. In addition, the end-to-end transmission delay is almost the same when there are only two source nodes that can hardly introduce congestion. The gap of the end-to-end transmission delays between the two compared routing schemes increases with the number of source nodes. The number of source nodes is equal to the number of contending nodes before the sensing range reaches $10m$. Furthermore, the end-to-end transmission delay of $MiniRoute$ increases rapidly when the event sensing range is larger than the communication range $10m$. It shows that the $MiniRoute$ introduces much more congestion after the turning point. Since the $MiniRoute$ is initially designed as a distributed

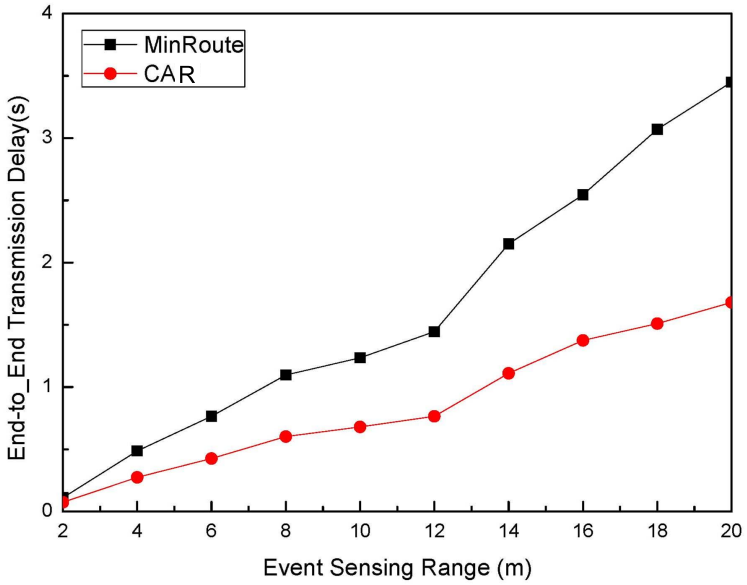

Figure 4.7 Average end-to-end transmission delay with varying event sensing ranges

routing algorithm, the sensor node selects relay node independently. The only sink node in the network makes the traffic more and more concentrated as the packets approach the sink node. On the contrary, the end-to-end transmission delay in the CAR only increases linearly. The Figure 4.7 shows that the proposed CAR has a stable performance. It can effectively alleviate the congestion in the subsequent hop delivery. The simulation results on end-to-end throughput is shown in Figure 4.8. It compares the results when the sensing range is larger than the communication range.

4.6 Summary

In this chapter, we present a congestion-aware routing (CAR) scheme for WSNs to reduce the link layer congestion. CAR routing utilizes the MAC layer traffic information to select next hop relay node. The simulation results show that our proposed CAR routing scheme can reduce the end-to-end packet transmission delay by more than 50% while increasing the network throughput for more than two times in our settings.

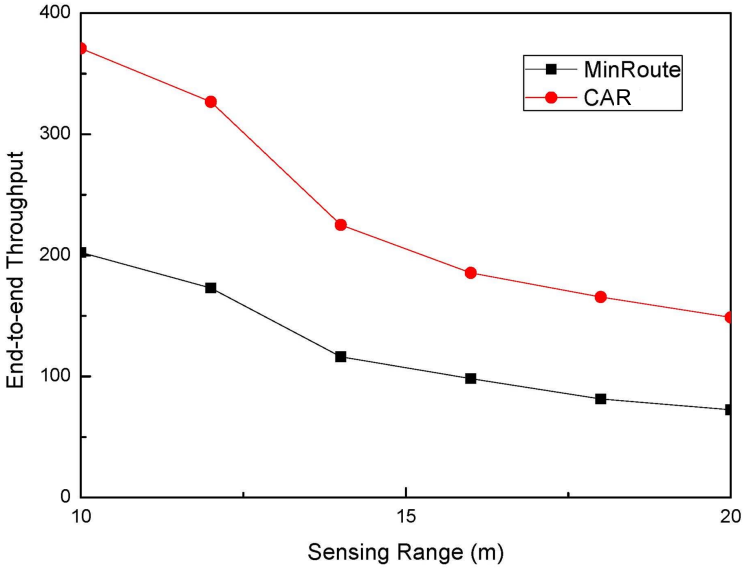

Figure 4.8 Network throughput with varying event sensing ranges

CHAPTER 5

DELAY-AWARE AND PRIVACY PRESERVING DATA FORWARDING: DESIGN AND ANALYSIS

In this chapter, we propose a decentralized data forwarding scheme to preserve trajectory privacy of participating users based on a combination of two-phase forwarding and secret sharing. DAPP provides a design trade-off framework to address security, communication delay and delivery ratio based on the selection of a (k, n) secret sharing scheme. The quantitative analysis and numerical results on security, communication delay and delivery ratio will also be provided in this chapter.

5.1 Introduction

Urban sensing networks are designed to monitor urban environment. Recent technological advances make urban sensing network feasible to rely on the sensors embedded in human-carried mobile devices or vehicular electrical devices to collect and report data. As urban sensing is more related to individuals, the location information collected with data may be used to jeopardize users' privacy. As mentioned in Chapter 1, the existing works for location privacy protection can be divided into three categories, which are *pseudonym based scheme*, *compression based scheme* and *routing based scheme*.

Pseudonym based schemes proposed in [44–47] mainly rely on a trusted third party to dynamically assign pseudonyms to participating users to conceal their real identities. Pseudonyms can be only used within mix-zones constructed by a trusted third party. The assumption of the trusted third party cannot be always true. In addition, the mix-zones cannot be placed through the entire network to preserve trajectory privacy.

Alternatively, compression based schemes in [41–43, 48–51] are designed to pre-process the uploaded data to blur the reported location. The authors employed the techniques, such

as compression, aggregation, tessellation and dummy copies, to blur, suppress and even hide the reported location contained in the collected data. The privacy protection is achieved by sacrificing the resolution of either spatial or temporal dimensions, which may seriously cause a loss for system QoS.

In routing based schemes [57–59], uploaded sensor readings are relayed by intermediate nodes to the application data server hop by hop. In [58, 59], the proposed scheme is a lack of protection for data confidentiality and vulnerable to side information attack. The data relayed by intermediate nodes can be easily dropped and tampered with. Encryption methods in [57] have been used to provide confidentiality of the collected data. However, secret keys may introduce more security concerns. The secret keys may be possessed by all sensor nodes or only shared between application data server and the source node. Hence, either the application data server can identify the source node based key information or data readings are made public to intermediate nodes.

Existing solutions may preserve location privacy of participating users, but without considering security from a cost-aware perspective. Few of them provide a quantitative analysis on security and the relationship between security and its cost. In this dissertation, we propose a novel delay-aware privacy-preserving data forwarding scheme to address the two key design issues, source location privacy and communication delay. DAPP is designed based on a Sharmir's secret sharing scheme and a two-phase forwarding algorithm. We also propose a dynamic pseudonym scheme to conceal the identities of source nodes. DAPP cannot only ensure data confidentiality and preserve location privacy, but also provide a data integrity verification and defend against collusion attacks. The details of DAPP are presented in Section 5.3. In Section 5.4, we conduct the quantitative analysis on security. The performance evaluation and numerical results are provided in Section 5.5.

5.2 Models and Assumptions

5.2.1 System Model

Urban sensing network relies on a set of sensor nodes embedded in mobile devices or vehicular systems for data sensing and reporting. These devices can get wireless Internet access intermittently through wireless access points (APs) in the sensing area. The APs, such as WiFi access points, may be owned and operated by the government, organizations or individuals. They are directly connected to the application data server. In this network, the surrounding environment information is collected by the participating mobile devices and eventually sent to the application data server.

The application data server provides environmental sensing services for data consumers and disseminates the requested tasks to mobile devices carried by participants. Mobile devices can join the system at will to participate in data sensing. They are required to report the collected data to the application data server once they accept tasks. To provide precise services to data consumers, the data are required to be collected with spatial-temporal information. Here we may use the term "report location" to indicate the spatial-temporal information. The data format is $\{{}_p\mathsf{ID}, (\hat{x}, \hat{y}), \hat{T}_d\}$, where ${}_p\mathsf{ID}$ is the pseudonym of the data source, $(\hat{x}, \hat{y})$ is the coordinator where data is collected, and $\hat{T}_d$ is the collecting time. This information may divulge details about the participating user's location. Due to the characteristics of opportunistic sensing and physical infrastructure of the network, we only deal with sensing data that is delay tolerant.

5.2.2 Adversarial Model

Our adversary model is similar to [42]. It can be summarized as follows:

- The adversary can be any parties in the network, including individual sensing nodes, wireless access points, and even the application data servers.

- Adversaries are generally assumed to be honest but curious. We also assume that they may drop or tamper with the reported data due to their own interests.
- The collected data are eventually forwarded to the application data server, which enables it to disclose their reported location. The application data server may try to uncover source identities of the received data and the trajectory.
- The participating user list is kept secret to delivery nodes and public, however, the application data server can access the list due to its administrative right.
- Intermediate delivery nodes can obtain the source pseudonym of their received data. They may collude to obtain the location privacy information or forge collected data to fool the application data server.

5.2.3 Side Information Attack

Side information attack includes both direct side information attack and indirect side attack. The *direct side information* refers to the information that an adversary can acquire based on direct access to the communication. In our case, the direct side information may include information $\{{}_p\mathsf{ID}, (\hat{x}, \hat{y}), \hat{T}_d\}$ of a particular event. In particular, the adversary can record the set of identities $\mathscr{I}$ appear within its communication range. The nature of wireless communications makes adversary able to extrapolate the source node located within its communication range. If $\mathscr{I}$ is small enough by combining direct side information obtained, the adversary may derive the actual ID and correlate it to the ${}_p\mathsf{ID}$.

The *indirect side information* is defined as the information that an adversary can obtain through indirect channels, such as media, video and web blog published on the internet, of a particular event. In DAPP scheme, an adversary may receive data d, which contains $\{{}_p\mathsf{ID}, (\hat{x}, \hat{y}), \hat{T}_d\}$. To derive the actual source identity ID of ${}_p\mathsf{ID}$, it may search through the public domain to find the people who have visited location $(\hat{x}, \hat{y})$ at time $\hat{T}_d$. In this way, the adversary may either completely identify the actual ID or limit it to a smaller subset.

5.2.4 Mobility Model

In urban sensing networks, sensor nodes are embedded in the mobile devices carried by people or vehicles. In this dissertation, we apply the Manhattan street pedestrian model described in [77]. The analysis for vehicular networks is similar based on mobility mode presented in [78]. The Manhattan street model is proposed to emulate the movement pattern of pedestrian on the streets. In this model, sensor nodes move on a two-way street segment. The street segment can be modeled as a real street between two intersections. The arrivals and departures of mobile nodes occur at the endpoints of the street segment. The velocities of the mobile sensor nodes are independent and identically distributed (iid) random variables with a probability density function $f_v(v)$. The direction and speed of a node remain constant in one segment. Participating users arriving at both endpoints can be modeled as a Poisson Process [79]. The total arrival rate is denoted as λ. At each endpoint, the mobile node may alter its direction with a predetermined probability. The four directions at a cross road are expressed as f(orward), l(eft), r(ight) and b(ackward), respectively. The probability for going these directions at the intersection are P_f, P_r, P_l, P_b. This model assumes that communications between two nodes in different street segments is not possible. As a result, an existing connection breaks at the endpoints.

5.3 The Proposed DAPP Scheme

In this section, we present a novel delay-aware privacy-preserving (DAPP) data reporting scheme based on a combination of Shamir's secret sharing and two-phase routing. It can ensure data confidentiality and also provide a data integrity verification option for the reported data. We also propose a dynamic pseudonym scheme to guarantee anonymity of the source node.

Table 5.1 Notation definition

Notation	Definition
Δ	Communication range of the mobile device
t_α	Time interval between two consecutive transmissions
ℓ	Length of a street segment
λ	Arrival rate of participating users
$f(v)$	Probability density function of v
d/d_i	Sensing data d / i^{th} data piece of data d
d_L	Location information of data d being discovered
d_I	Identity information of data d being discovered
$\{(\hat{x}, \hat{y}), T_d\}$	Data d is reported from location $(\hat{x}, \hat{y})$ at time T_d
X/Y	Estimated source identity set prior to/after data transmission event
$X^A/X^D/X^S$	Evaluation metrics X for APs (A) / delivery node (D) / application data server (S)
$\widetilde{X}$ / $\bar{X}$	Direct/Indirect side information attack of X
$P(d_I)/P(d_L)$	Probability of identity/location information loss of d
$I(X;Y)$	Mutual information between X and Y
P_T	Joint identity and location privacy information leakage
$H(\cdot)$	One way hash function

5.3.1 Overview of the Proposed Privacy Scheme

To transmit collected data, the source node generates n data pieces from the collected data based on the Shamir's secret sharing scheme. It then generates a unique pseudonym for each data piece as its identity to conceal the source information. The data pieces are then forwarded to n randomly selected participating users, named as delivery nodes, within the communication range. Delivery nodes relay the received data pieces to the application data server through nearby APs. Upon receiving k or more data pieces, the application data server is able to reconstruct the original collected data. To ensure integrity of the recovered data, both the original data and its hash value will be transmitted together.

5.3.2 Secret Sharing

In Shamir's (k, n) secret sharing scheme, to share a secret S, the secret holder picks a random $k-1$ degree polynomial $f(x) = a_0 + a_1 x + a_2 x^2 + \cdots + a_{k-1} x^{k-1}$ over a finite field $\mathbb{Z}_q$, where $a_0 = S$ and $q > \max(S, n)$ is a prime number. $\mathcal{H}$ generates n data pieces $S_i = (i, f(i)),\ i = 1, \cdots, n$. The secret holder distributes the n data pieces to n individual users.

The secret S can be recovered by k or more available data components using Barycentric Lagrange Interpolation. The computational complexity to recover the secret S is only $\mathcal{O}(n)$. More specifically, for k available data components, S can be recovered as follows:

1. For any k out of n secret pieces $(i, f(i))$, without loss of generality, we assume $i = 0, \cdots, k-1$. Define $l(x) = (x - x_0)(x - x_1) \cdots (x - x_{k-1})$.

2. Compute the weight
$$w_j = \frac{1}{\prod_{i=0, i \neq j}^{k} (x_j - x_i)}. \tag{5.1}$$

3. Let
$$l_j(x) = l(x) \frac{w_j}{x - x_j}$$
and
$$L(x) = l(x) \sum_{j=0}^{k} \frac{w_j}{x - x_j} y_j. \tag{5.2}$$

4. The shared secret is $S = L(0)$.

5.3.3 Dynamic Pseudonyms

Pseudonyms have been widely used to prevent adversaries from obtaining source identities. However, adversaries may use side information to link multiple pseudonyms or correlate the pseudonyms to the actual identity. To solve this problem, we propose a new method to generate dynamic pseudonyms using an ID-hash-chain. Instead of simply using hash functions, we enable the source node to employ a secret key in the hash chain.

Suppose ID is the real identity of a participating user. To conceal it, the user replaces ID with a dynamic changing pseudonym ${}_p\mathsf{ID}_i$ for each message transmission, where i is related to the order of message. Each pseudonym is generated using a one way hash function $H(\cdot)$ based on the previous pseudonym and the secret key. The ID-hash-chain $\{{}_p\mathsf{ID}_1, {}_p\mathsf{ID}_2, ...\}$ for the participating user ID is generated as follows:

$$\begin{aligned} {}_p\mathsf{ID}_1 &= H(\mathsf{ID}, K) \\ {}_p\mathsf{ID}_2 &= H({}_p\mathsf{ID}_1, K) \\ &\cdots \end{aligned}$$

where K is a secret key of the message source. Without knowing the secret key and the real identity, establishing a linkage between pseudonyms, or between a pseudonym and the real identity are both infeasible.

5.3.4 DAPP Scheme

In DAPP, to ensure security of the reporting data d, we generate n data pieces based on Shamir's secret sharing scheme. Each data piece is then forwarded to a randomly selected delivery node. In this way, the original data can be concealed among n trustworthy secret holders. The shared data d can be recovered by any k or more data pieces. Since we assume the delivery nodes may tamper with the reporting data, the application server may receive incorrect data pieces. Therefore, the application data server may not be able to recover the original data. To deal with this issue, the proposed scheme is designed to be able to verify the integrity of the recovered data.

We assume the source node $\mathcal{H}$ has data d to transmit. It first computes the hash value $H(d)$, where $H(\cdot)$ is a one way hash function. d and $H(d)$ are treated as two independent secret data pieces. We randomly select two (k, n) secret sharing schemes to share d and $H(d)$ separately. The polynomial computation is operated over $\mathbb{Z}_q$. The procedure is described as follows:

1. $\mathcal{H}$ chooses a prime $q > \max(d, n)$.

2. $\mathcal{H}$ constructs two coefficient sets, $\mathcal{A}$ and $\mathcal{B}$. Each set contains $k-1$ randomly selected coefficients, $\mathcal{A} = \{a_0 = d, a_1, ..., a_{k-1}\}$ and $\mathcal{B} = \{b_0 = H(d), b_1, ..., b_{k-1}\}$ from $\mathbb{Z}_q$.

3. $\mathcal{H}$ generates two random polynomials over $\mathbb{Z}_q$ as follows:

$$f_a(x) = \sum_{i=0}^{k-1} a_i x^i, \tag{5.3}$$

$$f_b(y) = \sum_{i=0}^{k-1} b_i y^i. \tag{5.4}$$

4. $\mathcal{H}$ computes n components $f_a(i), f_b(i)$ from d and $H(d)$, respectively, $i = 1, \cdots, n$.

5. The i^{th} data piece for d and $H(d)$ is $(i, f_a(i), f_b(i))$, $i = 1, \cdots, n$.

The proposed data distribution scheme is summarized in Algorithm 6.

Algorithm 6 Data Distribution

1: Choose a prime $q > \max(d, n)$.
2: Construct two coefficient sets $\mathcal{A}$ and $\mathcal{B}$ from $\mathbb{Z}_q$ randomly.
3: Based on $\mathcal{A}$ and $\mathcal{B}$, construct two polynomials $f_a(x) = \sum_{i=0}^{k-1} a_i x^i$, and $f_b(y) = \sum_{i=0}^{k-1} b_i y^i$ over $\mathbb{Z}_q$ to share d and $H(d)$, respectively, as two secret values.
4: Compute n data pieces $d_i = (i, f_a(i), f_b(i), q)$, $i = 1, \cdots, n$.
5: Generate a pseudonym ${}_p\mathsf{ID}$ for d using ID-hash-chain.
6: **for** each $i \in [1, n]$ **do**
7: Send d_i to a randomly selected neighboring node M_i.
8: Insert an interval t_α before sending d_{i+1}.
9: The neighboring node M_i forwards d_i to a wireless access point.
10: **end for**

DAPP includes two phases in data forwarding. In the first phase, the generated n data pieces are distributed to n randomly selected delivery nodes before being relayed to the application server. The data source may choose to add a time interval t_α between transmissions

of two consecutive data pieces. A properly selected t_α can effectively control the probability for any single delivery node to receive multiple data pieces, especially in sparse networks. Since delivery nodes may not be completely trusted, integrity of the reconstructed data has to be verified. The reconstruction algorithm follows the Barycentric Lagrange Interpolation. It is described in Algorithm 7.

Algorithm 7 Data Reconstruction and Verification

1: Suppose the server has received at least k out of n data pieces $(i, f_a(i), f_b(i))$ for data $(d, H(d))$.

2: The application data server reconstructs the original data using the Barcentric Lagrange Interpolation algorithm described in Equations (5.1) and (5.2).

3: The application data server verifies integrity of the reconstructed data by checking whether $D = H(d)$ holds true.

5.4 Security Analysis

Source privacy information can be specified by two equally essential parts: spatial-temporal information and identity information. Only when both are exposed, the complete privacy information is disclosed.

In this section, we will provide quantitative analysis that DAPP can provide both identity and spatial-temporal information from being disclosed to adversaries. We first introduce several definitions and metrics.

5.4.1 Definitions and Security Metrics

Definition 6 (Identity information leakage)**.** *The identity information leakage for data d is defined as the probability that an adversary is able to derive the source identity d_I of data d. We denote it as $P(d_I)$.*

Definition 7 (Location information leakage)**.** *The location information leakage for data d is defined as the probability that an adversary is able to derive the spatial-temporal information d_L of data d. The probability is denoted as $P(d_L)$.*

To measure identity information loss of the received data, we introduce mutual information.

Definition 8 (Identity information loss)**.** *Let X be the set of possible identities estimated by adversaries prior to receiving a message, and Y be the set of estimated source identities after receiving the message. The identity information loss for forwarding the message event is defined as the mutual information between the X and Y. That is*

$$I(X;Y) = H(Y) - H(Y|X). \tag{5.5}$$

Notice that source privacy information consists of both spatial-temporal information and its correlated identity. We introduce the following metric to measure the joint information loss.

Definition 9 (Joint information leakage)**.** *The joint identity and location privacy information leakage P_T for data d is defined as the joint probability that the adversary obtains the spatial-temporal information and the identity of data d. That is*

$$\begin{aligned} P_T(d) &= P(d_L, d_I) \\ &= P(d_L|d_I)P(d_I) \\ &= P(d_I|d_L)P(d_L), \end{aligned} \tag{5.6}$$

where d_I and d_L denote the the identity and location information of data d, respectively.

5.4.2 Identity Information Loss

The identity Information loss can be derived by the following theorem.

Theorem 6. *Assume an adversary is able to limit the message source node to a potential subset $Y \subset X$ attack after receiving a message. Then the identity information loss is*

$$I(X;Y) = \log|X| - \log|Y|, \tag{5.7}$$

where $|X|, |Y|$ denote the cardinalities of X and Y, respectively.

Proof. In set X, if each node can be the source node with equal probability, then the probability for each node in the set to be selected as the source node is $\frac{1}{|X|}$. After a message is received, the adversary may limit the message source node to set Y. If each node in set Y can be the source node with equal probability, the probability for each node in Y to be selected as the source node is $\frac{1}{|Y|}$. The identity information loss can be calculated by the following equation:

$$\begin{aligned} I(X;Y) =& H(X) - H(X|Y) \\ =& -\sum p(x)\log p(x) + \sum_{y\in Y} p(y) \sum p(x|y)\log p(x|y) \\ =& -|X| \cdot \frac{1}{|X|}\log\frac{1}{|X|} + \sum_{y\in Y} p(y)(|Y| \cdot \frac{1}{|Y|}\log\frac{1}{|Y|}) \\ =& \log|X| - \log|Y|. \end{aligned}$$

□

5.4.2.1 Without Side Information Attack

For security attack without side information, based on Definition 6, Definition 8 and Theorem 6, we have the following corollary.

Corollary 3. *The proposed DAPP scheme can achieve unconditional message source privacy protection for participating users under message* ID *based attack. That is the set of possible source node X prior to data transmission is the same as the set of the possible source node Y after message transmission. As a result, we have $I(X;Y) = 0$.*

Proof. DAPP introduces a two-phase message forwarding: distribution of data pieces to randomly selected delivery nodes, and message forwarding to the application server through the APs. Assume an adversary receives a data piece d_i with a unique pseudonym ${}_p\mathsf{ID}$. Prior to receiving d_i, the potential set for data source can be arbitrary nodes in the entire set of population in the urban area of the delivery nodes since they are not entitled to access the list of the participating users. For the application data server, since it has access to the participating user list, the priori estimated set is the same as the participating users.

Through message forwarding, the adversary obtains ${}_p\mathsf{ID}$ instead of ID of d_i. The proposed dynamic pseudonym makes it infeasible for adversaries to derive ID from ${}_p\mathsf{ID}$ without secret key K. Hence, the posterior estimated identity set Y based on message forwarding event is also equal to X. Therefore, $I(X;Y) = 0$. □

5.4.2.2 Side Information Attack

Side information attack is envisioned as one of the major threats to data privacy. It may divulge part or even the entire source identity information.

Corollary 4. *For DAPP, through direct side information attack, the identity information loss to the delivery node ($\widetilde{I}^D$), the AP ($\widetilde{I}^S$) and the application data server ($\widetilde{I}^A$) can be derived as follows:*

$$\widetilde{I}^D(X;Y) = \log|X| - \log|Y|, \tag{5.8}$$

$$\widetilde{I}^S(X;Y) = \widetilde{I}^A(X;Y) = 0, \tag{5.9}$$

where $|X|, |Y|$ denote the cardinalities of X and Y, respectively.

Proof. Direct side information is obtained through traffic monitoring during message forwarding. The data pieces are relayed to the application data server by randomly selected delivery nodes. The application data server and APs may possibly collect direct side information only about delivery nodes rather than the source node. Therefore, they are unable

to reduce the size of X. As a consequence, $X = Y$. Therefore, we have

$$\widetilde{I}^S(X;Y) = \widetilde{I}^A(X;Y) = 0. \tag{5.10}$$

The potential event set X is the same as the total population in the network. Since the delivery node can acquire direct side information about the source node, after the message is being transmitted, the delivery node may be able to limit the message source to a subset Y, which is equal to the population in the communication rage of source. Based on Theorem 6, we have

$$\widetilde{I}^D(X;Y) = \log|X| - \log|Y|.$$

□

Corollary 5. *Through indirect side information attack, the identity information loss to the delivery node, the AP and the application data server can be derived as follows:*

$$\bar{I}^S(X;Y) = \log|X| - \log|Y|, \tag{5.11}$$

$$\bar{I}^D(X;Y) = \bar{I}^A(X;Y) = 0. \tag{5.12}$$

Proof. The indirect side information can be used to derive the source identity by exploring the matched spatial-temporal information through public information. The key procedure of this attack lies in the recovery of the reported location $\{(\hat{x}, \hat{y}), T_d\}$ in d. However, DAPP applies secret sharing to ensure confidentiality, which makes it infeasible to reveal the data content by single data piece. Thus, neither an AP nor a delivery node can reveal the source identity of the received data piece. The identity information loss to them is

$$\bar{I}^D(X;Y) = \bar{I}^A(X;Y) = 0. \tag{5.13}$$

In addition, data pieces are eventually sent to the application data server, which enables it to recover the reported location. Due to access right, application data sever can acquire the participating user list, thus, the estimated identity set X is equal to the list of participating

users. Based on indirect side information, it can limit X into a subset Y, which is depended on the accuracy of indirect side information.

$$\bar{I}^S(X;Y) = \log|X| - \log|Y|.$$

□

5.4.3 Location Information Leakage

Spatial-temporal information is equally essential for source privacy. In the subsequent analysis, we will discuss the location information leakage of DAPP. We first prove that the data distribution process follows Poisson process.

Theorem 7. *The process of data distribution in the first forwarding phase of the proposed DAPP scheme is a Poisson process.*

Proof. In the Manhattan street model, the node arrival and departure at an endpoint of a street segment is a Poisson process. It is straightforward to derive that the arrival process at any points in the street segment parallelizing the endpoint is also a Poisson process. Suppose that the participant A encounters n participants when it stays at the point (x_i, y_i). And it stays at the point for a time duration $\delta\,(\delta \to 0)$. The node arrival rate at this point is λ. So the probability that A meets n participants is

$$p(N(\delta + t) - N(t) = n) = e^{-\lambda\delta} \cdot \frac{(\lambda\delta)^n}{n!}, \tag{5.14}$$

where $N(t)$ is the number of participants that node A has encountered from time 0 to time t.

Suppose A needs T seconds to move from (x_i, y_i) to (x_j, y_j). So the process for A to encounter other participants for time duration T is the sum of encounter processes from location (x_i, y_i) to (x_j, y_j). These meeting processes are mutually independent. Since the number of the independent Poisson processes is $\frac{T}{\delta}$, the sum of multiple Poisson processes is

still a Poisson process. Hence, the new arrival rate of the Poisson process can be computed by the following equation

$$\lambda_{\text{sum}} = \sum_{i=1}^{T/\delta} \lambda_i = \frac{T}{\delta} \cdot \lambda. \tag{5.15}$$

The probability that A meets n participants in time duration T can be calculated as

$$\begin{aligned} p(N(t+T) - N(t) = n) &= e^{-\lambda_{\text{sum}} \cdot \delta} \cdot \frac{(\lambda_{\text{sum}} \cdot \delta)^n}{n!} \\ &= e^{-\lambda \cdot T} \cdot \frac{(\lambda \cdot T)^n}{n!}. \end{aligned}$$

Therefore, it is a Poisson process. The data distribution is actually equal to the encountering Poisson process. The probability to forward one data piece in a given time duration t_d is

$$p(N(t+t_d) - N(t) = 1) = e^{-\lambda t_d}(\lambda t_d). \tag{5.16}$$

However, the source node will insert an interval between two data distributions in the first forwarding phase. Suppose the data piece d_i is forwarded to the delivery node at time t, and the source node insert an interval t_α before the forwarding of d_{i+1}. Since Poisson process is a memoryless process, the number of arrivals occurring in any bounded interval of time after time t is independent of the number of arrivals occurring before time t. So the probability to forward d_{i+1} in a given time duration t_d is

$$p(N(t+t_d+t_\alpha) - N(t+t_\alpha) = 1) = e^{-\lambda t_d}(\lambda t_d). \tag{5.17}$$

Therefore, the data distribution process in the proposed scheme is a Poisson process. □

5.4.3.1 The Location Information Leakage to Individual Delivery Node

In this dissertation, Manhattan street model is applied to analyze the location information leakage to a malicious delivery node. In this model, we denote ℓ as the length of a street segment. Assume S is the source node and M is a malicious node. v_S and v_M are the velocities of S and M, respectively. Denote the probability density function for v as $f(v)$.

Let t_M be the time duration that a malicious node stays in the source node communication range Δ. Then we have $t_M = \frac{2\Delta}{z}$, where $z = |v_M - v_S|$. We also use $P(t_M > kt_\alpha)$ to denote the probability that a sensor node stays in the source node communication range at least kt_α seconds. Let P_M be the probability that a malicious node M is selected as the delivery node in one data piece distribution, and c be the number of times that M has been selected as the delivery node.

Theorem 8. *Assume velocities of the malicious node and the source node are two independent and identically distributed (i.i.d.) random variables, then the location information leakage to the malicious delivery node can be derived as follows:*

$$P^D(d_L) = \int_{-\frac{2\Delta}{kt_\alpha}}^{\frac{2\Delta}{kt_\alpha}} f(z)dz \times \sum_{i=k}^{n} \left[\left(\frac{1}{4}\right)^{\left\lfloor \frac{2it_\alpha v_S}{\ell} \right\rfloor} \binom{n}{i} P_M^i (1-P_M)^{n-i} \right], \tag{5.18}$$

where $f(z)$ is the joint probability density function of $z = |v_M - v_S|$.

Proof. Since the data content can be closely related to the reporting location, leakage of message content may inadvertently expose the source location. To deal with this potential security issue, DAPP utilizes secret sharing to ensure data confidentiality by generating multiple seemingly meaningless data pieces and delivers each piece through a randomly selected delivery node. In this way, the malicious node will not be able to get the content of the data unless it is capable of collecting up to k or more data pieces.

There are two possible scenarios for a malicious node to obtain k data pieces: (i) The malicious node comes across the data source node at least k times to collect the data pieces from the source node during the entire duration of the message transmission; and (ii) The malicious node stays in the communication range of the source node at least kt_α seconds.

In the first case, since velocities of the participating users are independent, the spatial dependence degree of two arbitrary nodes is approximately 0 according to [80], which means

that the probability for two nodes to meet for the second time is approximate to 0 within a limited short time duration. Thus, probability for the first case can be viewed as 0.

The success of the malicious node is determined by the likelihood of the second case. Assume $f(z)$ is the joint probability density function of $z = |v_M - v_S|$, then we have

$$\begin{aligned} P(t_M \geq kt_\alpha) &= P\left(\frac{2\Delta}{z} \geq kt_\alpha\right) \\ &= P\left(z \leq \frac{2\Delta}{kt_\alpha}\right) \\ &= \int_{-\frac{2\Delta}{kt_\alpha}}^{\frac{2\Delta}{kt_\alpha}} f(z)dz. \end{aligned} \tag{5.19}$$

The success of case (ii) requires the malicious node to be selected as the delivery node at least k times. In DAPP, the source node selects delivery nodes based on the principle of randomness, thus each node in the source communication range can be selected as delivery node with equal probability $P_M = \frac{1}{|X|}$, where $|X|$ is the total number of participants in the communication range of S. Based on Theorem 7, the process of the participating users' arrival and departure can be modeled as $M/G/\infty$ based on *Theory of Queues*. In this model, the source node can be denoted as the service node. t_M is actually the service time for a given participating user. Moreover, suppose λ is the arrival rate and T is the average service time. Hence, we can have

$$|X| = \lambda \cdot T. \tag{5.20}$$

Since ℓ is the length of of a street segment, we have $t_M \leq \frac{\ell}{\max[v_S, v_M]}$. Without loss of the generality, we may assume $v_S \geq v_M$, then,

$$T = 2 \cdot \int_{\frac{2\Delta v_S}{\ell}}^{\nu} \frac{2\Delta}{z} f(z)dz, \tag{5.21}$$

where $\nu = V_{\max} - V_{\min}$, $V_{\max}$ and $V_{\min}$ represent the maximum and minimum speed of the participating users.

The location information leakage in one street segment can be described as the joint probability of $t_M \geq kt_\alpha$ and $c \geq k$. That is

$$
\begin{aligned}
P^D(d_L) &= P(t_M \geq kt_\alpha, c \geq k) \\
&= P(t_M \geq kt_\alpha) P(c \geq k \,|\, t_M \geq kt_\alpha) \\
&= P(t_M \geq kt_\alpha) \sum_{i=k}^{n} \binom{n}{i} P_M^i (1 - P_M)^{n-i}.
\end{aligned} \tag{5.22}
$$

In equation (5.22), all data pieces are assumed to be distributed in one street segment. In fact, these data pieces may be distributed in several streets. S and M may change their velocities at the endpoint of the street segment. Hence, M can stay in the communication range of S only if they moves in the same direction. To simplify the analysis, we assume that the probability for each direction is equal to $\frac{1}{4}$. Thus, the probability that S and M choose same direction at an endpoint is equal to $(\frac{1}{4})^2$. Therefore,

$$
\begin{aligned}
P^D(d_L) =& P(t_M > kt_\alpha) \\
& \times \sum_{i=k}^{n} \left[\left(\frac{1}{4}\right)^{\left\lfloor \frac{2it_\alpha v_S}{\ell} \right\rfloor} \binom{n}{i} P_M^i (1 - P_M)^{n-i} \right].
\end{aligned} \tag{5.23}
$$

Combining equation (5.19) and equation (5.23), we can get equation (5.18). □

From Theorem 8, we can derive the following corollary.

Corollary 6.

$$
\lim_{kt_\alpha \to \infty} P^D(d_L) = 0. \tag{5.24}
$$

Proof. From equation (5.18), we have

$$
\begin{aligned}
P^D(d_L) =& \int_{-\frac{2\Delta}{kt_\alpha}}^{\frac{2\Delta}{kt_\alpha}} f(z)dz \\
& \sum_{i=k}^{n} \left[\left(\frac{1}{4}\right)^{\left\lfloor \frac{2it_\alpha v_0}{\ell} \right\rfloor} \binom{n}{i} P_M^i (1 - P_M)^{n-i} \right] \\
& \leq \int_{-\frac{2\Delta}{kt_\alpha}}^{\frac{2\Delta}{kt_\alpha}} f(z)dz \cdot \left(\frac{1}{4}\right)^{\left\lfloor \frac{2kt_\alpha v_S}{\ell} \right\rfloor}.
\end{aligned} \tag{5.25}
$$

Since both $\int_{-\frac{2\Delta}{kt_\alpha}}^{\frac{2\Delta}{kt_\alpha}} f(z)dz$ and $\left(\frac{1}{4}\right)^{\left\lfloor \frac{2kt_\alpha v_S}{\ell} \right\rfloor}$ are asymptotically equivalent to 0 as $kt_\alpha \to \infty$. Therefore, we have $\lim_{kt_\alpha \to \infty} P^D(d_L) = 0$. □

5.4.3.2 The Location Information Leakage to APs

In the second forwarding phase, delivery nodes transmit the data pieces to APs, which are assumed to be uniformly distributed in urban area. Thus, each AP has equal probability to receive the data piece and we have the following corollary.

Corollary 7. *The location information leakage to each AP can be computed by the following equation*

$$P^A(d_L) = \sum_{i=k}^{n} \binom{n}{i} \left(\frac{1}{\eta}\right)^i \left(1 - \frac{1}{\eta}\right)^{\eta - i}, \tag{5.26}$$

where η is the number of wireless APs in urban area. From this equation, we can see that the location information leakage to delivery node and each AP is asymptotically equivalent to 0 as $k \to \infty$.

5.4.4 Joint Identity and Location Privacy Information Leakage

We have discussed the identity information loss and the location information leakage separately. The results show that the delivery node may only obtain partial identity information that is insufficient to identify the data source. However, the reported location and the identity information may be dependent on side information attack. In order to elaborate privacy information loss, we further investigate privacy leakage when these two pieces are considered jointly.

Theorem 9. *For the joint identity and location privacy information leakage, we have*

$$\begin{aligned} \lim_{kt_\alpha \to \infty} P_T^D &= 0 \\ \lim_{\substack{k=n \\ n \to \infty}} P_T^A &= 0. \end{aligned} \tag{5.27}$$

Proof. Based on Definition 9, we have

$$\begin{aligned} P_T^D &\leq P^D(d_L), \\ P_T^A &\leq P^A(d_L). \end{aligned}$$

The equalities in above equations may hold if the adversary can collect k or more data pieces through side information attack. Thus, the joint identity and location privacy information leakages to an AP and a delivery node are both dependent on the parameters $(k, n; t_\alpha)$. Based on Corollary 6, we have

$$\lim_{kt_\alpha \to \infty} P_T^D \leq \lim_{kt_\alpha \to \infty} P^D(d_L) = 0.$$

From equation (5.26), the joint identity and location privacy information leakage to an AP can be derived as follows

$$0 \leq \lim_{\substack{k=n \\ n\to\infty}} P_T^A \leq \lim_{\substack{k=n \\ n\to\infty}} P^A(d_L) = \lim_{k\to\infty} \left(\frac{1}{\eta}\right)^k = 0.$$

□

Similarly, for the application server, we have the following corollary.

Corollary 8. *For the application data server, the joint identity and location privacy information under side information attacks can be calculated by*

$$P_T^S = \frac{1}{|Y|}.$$

5.4.5 Participating Nodes Collusion

Participating users may conspire or share information to infer privacy information of others. Assume there are κ ($\kappa \leq k_1$) malicious nodes in the network, where k_1 is the number of delivery nodes in urban sensing networks. The probability for an arbitrary delivery node to

be malicious is $\frac{\kappa}{k_1}$. Hence, the location information leakage of the reported data d is

$$P^C(d_L) = \sum_{i=k}^{n} \binom{n}{i} \left(\frac{\kappa}{k_1}\right)^i \left(1 - \frac{\kappa}{k_1}\right)^{n-i}. \tag{5.28}$$

For each data piece d_i, the malicious delivery node may record a potential identity set through traffic monitoring, $\mathscr{I}^i = \{a_0^i, \cdots, a_l^i\}$. As the direct side information can be shared, the colluding users could limit the source identity to be an element in the intersection $\bigcap_{i=0}^{k} \mathscr{I}^i$. The joint identity and location privacy information P_T^C for collusion attacks falls as the location information leakage $P^C(d_L)$ decreases. Based on equation (5.28), $P^C(d_L)$ decreases to $(\frac{\kappa}{k_1})^k$ as k increases to n. Then, P_T^C can be asymptotically equivalent to 0 as $k = n$ and $k \to \infty$. Therefore, we have the following corollary.

Corollary 9.

$$\lim_{\substack{k=n \\ n\to\infty}} P_T^C \leq \lim_{\substack{k=n \\ n\to\infty}} P^C(d_L) = \lim_{k\to\infty} \left(\frac{\kappa}{k_1}\right)^k = 0.$$

The numerical result is presented in Table 5.2. It shows that the location privacy information leakage can be minimized with increasing k for a given n. Furthermore, with a proper setting on (k, n), DAPP can defend against collusion attacks even if there is a relatively high ratio of malicious delivery nodes.

5.4.6 Data Integrity

In reality, delivery nodes may drop, tamper with and forge the received data due to their own interests. To deal with these issues, DAPP provides a mechanism to verify the integrity of the received data. The application data server needs k untampered data pieces to recover the original data d and D. In case that at least one data piece in the set of k pieces has been tampered with, we should have $H(d) \neq D$. Therefore, the recovered data can detect whether the data set contains any corrupted data pieces as well as integrity of the recovered data.

Table 5.2 Joint privacy information leakage by collusion attacks, where n=30

$Percentage\ of\ Colusion\ Nodes/P_T^C)(\%)$	$k=5$	$k=10$	$k=15$	$k=20$	$k=25$	$k=30$
1%	1.16×10^{-3}	2.50×10^{-11}	1.35×10^{-20}	2.73×10^{-31}	1.36×10^{-43}	1.36×10^{-58}
5%	1.56	1.16×10^{-4}	2.31×10^{-10}	1.76×10^{-17}	3.32×10^{-26}	9.31×10^{-38}
10%	17.5	4.54×10^{-2}	3.56×10^{-6}	1.11×10^{-11}	8.60×10^{-19}	1.02×10^{-28}
15%	47.6	9.66×10^{-1}	7.08×10^{-4}	2.14×10^{-8}	1.65×10^{-14}	1.92×10^{-23}

5.5 Performance Evaluation and Simulation Results

In urban sensing networks, QoS can be measured by communication delay and delivery ratio. In this section, we analyze the communication delay and error rate of DAPP scheme.

5.5.1 Communication Delay

DAPP scheme includes two phases for data forwarding: data forwarding from the source node to the delivery nodes, and from the delivery nodes to the application data server.

In the first phase, let the communication delay for the i^{th} data piece distribution is τ_i, which includes two parts. One part of the delay is introduced to encounter the i^{th} delivery node, denoted as γ_i. Theorem 7 proves that the data distribution process is a Poisson process. Hence, γ_i should follow Γ distribution. The probability distribution function for γ_i is given by

$$f_{\gamma_i}(t) = \lambda e^{-\lambda t} \cdot \frac{(\lambda t)^{(n-1)}}{(n-1)!}, \tag{5.29}$$

where λ is the arrival rate of Poisson process. The second part is introduced by the inserted constant interval t_α. For the i^{th} delivery node, the delay is equal to it_α.

In the second phase, the delay is the time duration from the time that the delivery node receives a data piece until it reaches the next AP. Suppose the delivery node receives one data piece at time $\hat{t}$ and T is the average time duration that the delivery node travels from one AP to the next AP. The time $\hat{t}$ should be uniformly distributed in the range of T. We denote the delay in the second forwarding phase as t_i for each data piece d_i. The total communication delay $\mathcal{T}_d$ can be computed as follows:

$$\mathcal{T}_d = \min_{1 \to k} \{\gamma_i + t_i + it_\alpha \,|i = 1, \cdots, k\}, \tag{5.30}$$

where $\gamma_i + t_i + it_\alpha$ is the delay for the application data server to receive the i^{th} data component, and $\min_{1\to k}$ is the function to find the k^{th} minimum value of a given set. Equation (5.30) shows that the overall delay is determined by k when it is large. Table 5.4 gives numerical results for various k values.

Table 5.3 The error rate for the reported data, where n=30

$P_E(\%)$	$k=5$	$k=10$	$k=15$	$k=20$	$k=25$
$p_e=1\%$	2.64×10^{-46}	1.31×10^{-33}	1.27×10^{-22}	4.59×10^{-13}	4.83×10^{-5}
$p_e=2\%$	1.70×10^{-38}	2.52×10^{-27}	7.31×10^{-18}	7.87×10^{-10}	2.51×10^{-3}
$p_e=3\%$	6.20×10^{-34}	1.15×10^{-23}	4.19×10^{-15}	5.70×10^{-8}	2.33×10^{-2}
$p_e=4\%$	1.05×10^{-30}	4.43×10^{-21}	3.65×10^{-13}	1.13×10^{-6}	1.06×10^{-1}
$p_e=5\%$	3.35×10^{-28}	4.39×10^{-19}	1.13×10^{-11}	1.10×10^{-5}	3.28×10^{-1}

5.5.2 Delivery Ratio

Due to the nature of the wireless communications, the message received may contain errors. Unreliable delivery nodes may even drop the received data pieces for their own interests. To deal with this problem, the proposed scheme introduces redundancy to minimize the error rate for the reporting data. The underlying secret sharing scheme ensures the reported data can be recovered by receiving k or more valid data pieces. The extra $n-k$ data pieces add redundancy that can be employed for data recovery under erroneous scenarios. Let p_e be the error rate or packet loss rate of a single data piece. The overall error rate P_E for the reported data can be computed by the following equation:

$$P_E = \sum_{i=n-k+1}^{n} \binom{n}{i} p_e^i (1-p_e)^{n-i}. \tag{5.31}$$

Based on equation (5.31), for a given n, the overall error rate P_E decreases when k reduces, and the overall error rate P_E can be minimized by increasing the number of redundant packets. Table 5.3 provides numerical results of the overall error rate for various k's.

5.5.3 Trade-off Design

In this dissertation, DAPP is designed to achieve trade-off among several conflicting design issues in urban sensing networks. It leverages the relationship between configurable scheme parameters and system performance to provide flexible options for system users. Based

on equation (5.18) and equation (5.30), we have the following equations to determine joint information leakage and communication delay:

$$\begin{cases} P_T^D &= P(t_s > kt_\alpha) \\ & \quad \times \sum_{i=k}^{n} \left[\left(\frac{1}{4}\right)^{\left\lfloor \frac{2it_\alpha v_S}{\ell} \right\rfloor} \binom{n}{i} P_M^i (1-P_M)^{n-i} \right] \\ \mathcal{T}_d &= \min_{1\to k}\{\gamma_i + t_i + it_\alpha \,|i = 1, \cdots, k\}, \end{cases} \tag{5.32}$$

In equation (5.32), parameter t_α is designed to prevent one single delivery node from collecting multiple data pieces in a sparse network. It can be set according to the density of population. The two equations show the trade-off between communication delay and security. For a given t_α and n, the location privacy information leakage can be minimized by increasing the value of k. On the other hand, when k increases, the communication delay also increases, as shown in Table 5.4 and Table 5.5.

Furthermore, for the trade-off between error rate and security, we have the following equations:

$$\begin{cases} P_T^D &= P(t_s > kt_\alpha) \\ & \quad \times \sum_{i=k}^{n} \left[\left(\frac{1}{4}\right)^{\left\lfloor \frac{2it_\alpha v_S}{\ell} \right\rfloor} \binom{n}{i} P_M^i (1-P_M)^{n-i} \right] \\ P_E &= \sum_{i=n-k+1}^{n} \binom{n}{i} p_e^i (1-p_e)^{n-i}. \end{cases} \tag{5.33}$$

In equation (5.33), for a given t_α and n, the error rate can be minimized by decreasing k. However, the direct joint information leakage to the delivery nodes also increase. The numerical results are provided in Table 5.3 and Table 5.5.

Table 5.4 The average communication delay and joint privacy information leakage for various k, while $n = 30$, $\lambda = 100$ and $t_\alpha = 20$

$\lambda = 1$ $t_\alpha = 20$	Location Leakage $P_T^D(\%)$	Communication Delay(s)
$k = 5$	2.37	648.7
$k = 10$	2.29×10^{-1}	1201.6
$k = 15$	3.11×10^{-2}	1749.4
$k = 20$	5.20×10^{-3}	2300.7
$k = 25$	9.67×10^{-4}	2852.3
$k = 30$	2.10×10^{-4}	3418.2

In summary, DAPP can achieve trade-off among security, communication delay and delivery ratio. By carefully setting on parameter (n, k, t_α), DAPP can provide an excellent balance between location privacy for participating users and various performance requirements of data users.

5.5.4 Computational Complexity

The computational complexity is determined by the overhead in recovery of the secret data using Barycentric Lagrange Interpolation, which is $\mathcal{O}(n)$ for reconstruction of the collected data. If the delivery nodes only drop data pieces without manipulating, then the Barycentric Lagrange Interpolation algorithm only needs to be implemented once to recover the collected data. However, if the application data server receives modified or corrupted data pieces, it may need to implement the Barycentric Lagrange Interpolation algorithm up to $\binom{n}{k}$ times in the worst case to recover the original data.

Fortunately, the parameters (k, n) with relatively small values are able to decrease the location information leakage close to 0, as shown in Table 5.5. As a consequence, it enables the application data server to rebuild the original data in a short time interval. In particular, for $n = 25$ and $k = 20$, the computer with 2.0GHz processor needs at most 0.053 seconds to reconstruct the original data.

5.5.5 Numerical Simulation Results

In numerical simulations, we assume v_i follows the uniform distribution in the range of $[V_{\min}, V_{\max}]$. The results of other distributions are similar. To emulate the reality, we set up both dense network and sparse network to show the joint information leakage to the delivery node. In the two scenarios, we select various parameters (k, n, t_α) to show the relationship between the settings and the security performance against intermediate delivery node under side information attack.

In the first scenario, we set the average number of people in the communication range of the source node as $\lambda = 10$, and $t_\alpha = 1$. With a proper setting on (k, n), P_M is small enough to make the joint information leakage approximated to 0. The joint information leakage to the delivery node is presented in Table 5.5.

In the second scenario, we consider a sparse network in the urban area. We set $\lambda = 100$. Then through equation (5.20) and equation (5.21), we can derive that the average number of people in the communication range of source node to be around 1. As a consequence, there may be only one neighbor node around the source node to be selected as delivery node. In such a scenario, the joint information leakage is determined by the value of $P(t_s \geq kt_\alpha) \cdot \left(\frac{1}{4}\right)^{\left\lfloor \frac{2kt_\alpha v_0}{L} \right\rfloor}$. To minimize this value, we raise t_α to 20 and let k increases from 5 to 30. The joint information leakage to the delivery node is shown in Table 5.3 and Table 5.5. The simulation results of the tables can be summarized as follows:

- Location privacy can be preserved in the proposed DAPP scheme under side information attack.
- With proper parameter settings, the joint information leakage can be minimized to approximately 0 for each delivery node.
- The joint information leakage, average communication delay and error rate can be adjusted by the selection on system parameters.

5.6 Summary

In this chapter we propose a delay-aware privacy preserving (DAPP) data forwarding scheme for people-centric urban sensing networks. It is developed based on Sharmir's secret sharing, dynamic pseudonyms and a two-phase data forwarding method. The two-phase forwarding method detaches the connection between the source node and the application data server. The Shamir's secret sharing based scheme prevents delivery nodes from discovering privacy information in the reported data. The proposed dynamic pseudonym scheme can provide anonymity of identity against side information attacks. Both theoretical analysis and simulation results demonstrate that the proposed DAPP can provide an excellent design trade-off among security, communication delay and delivery ratio.

Table 5.5 The average communication delay and joint privacy information leakage for various (k, n), $t_\alpha = 1$ and $\lambda = 10$

$Delay(s)$ $/P_T^D(\%)$	$k = 5$	$k = 10$	$k = 15$	$k = 20$	$k = 25$	$k = 30$
$n = 5$	$219.5/8.89 \times 10^{-4}$	-	-	-	-	-
$n = 10$	$145.2/1.45 \times 10^{-1}$	$284.8/5.28 \times 10^{-9}$	-	-	-	-
$n = 15$	140.3/1.13	$213.8/9.85 \times 10^{-6}$	$341.3/4.45 \times 10^{-14}$	-	-	-
$n = 20$	139.8/3.84	$206.9/3.77 \times 10^{-4}$	$271.8/4.21 \times 10^{-10}$	$396.6/3.76 \times 10^{-19}$	-	-
$n = 25$	139.6/8.71	$206.7/4.17 \times 10^{-3}$	$264.7/5.44 \times 10^{-8}$	$327.4/1.21 \times 10^{-14}$	$451.2/3.20 \times 10^{-24}$	-
$n = 30$	139.2/15.6	$206.2/2.40 \times 10^{-2}$	$284.3/1.58 \times 10^{-6}$	$320.3/4.15 \times 10^{-12}$	$382.7/2.75 \times 10^{-19}$	$506.1/2.78 \times 10^{-29}$

CHAPTER 6

CONCLUSIONS AND FUTURE WORK

Location privacy is an essential design and performance issue for WSNs and people-centric networks along with other constraints such as energy efficiency, lifetime and communication delay. In this dissertation, we intend to address location privacy and other conflicting design constraints in a cost-aware framework for these two types of networks.

6.1 CASER Protection Scheme

For source location privacy in traditional wireless sensor networks, we present a secure and efficient Cost-Aware SEcure Routing (CASER) protocol to balance energy consumption and increase network lifetime. We first devise an energy balance control parameter to create an adjustable filter to balance the energy consumption. We develop a security level parameter to determine the probabilistic distribution of random walking. We derive formulas to decide the energy consumption based on the energy balance control parameter and security level. For CASER, we employ two routing strategies, shortest path routing and random walking. The security level parameter can make routing paths dynamic and unpredictable. It can effectively prevent adversaries from tracing back to the source location and defend against jamming attacks. The shortest path routing strategy is used to ensure a high message delivery ratio. Both theoretical analysis and simulation results show that CASER has an excellent routing performance in terms of energy balance and routing path distribution for location privacy.

We investigate the energy consumption for CASER scheme with uniformly distributed events. The analysis and simulation results show the energy consumption is severely disproportional to uniform energy deployment. The sensor nodes closer to sink node may exhaust their residual energy for relaying messages. To solve this problem, we propose a non-uniform

energy deployment scheme to maximize the lifetime of WSNs. To provide equivalent security properties, CASER scheme is updated to adapt the non-uniform energy deployment. Our analysis and simulation results show that we can increase the lifetime and the number of messages that can be delivered under the non-uniform energy deployment by more than four times of uniform energy deployment under the same assumption.

CASER has the flexibility to support multiple routing strategies in message forwarding to extend the lifetime while increasing routing security. It can achieve a trade-off between security and network lifetime.

6.2 CAR Routing Algorithm

We introduce a congestion-aware routing (CAR) algorithm to reduce the communication delay in WSNs. We propose to monitor traffic in the wireless medium channel and utilize the channel competing results as a strategy to select a relay node.

We analyze communication delay in both the ideal case and the worst case. The theoretical analysis and simulation results demonstrate that the proposed CAR routing scheme can reduce the end-to-end packet transmission delay by more than 50% while increasing the network throughput for more than two times in our settings.

6.3 DAPP Protection Scheme

For location privacy in urban sensing networks, we introduce a delay-aware secure message forwarding scheme. We first propose a Sharmir's secret sharing based scheme to ensure confidentiality of the collected data. The proposed scheme can also provide options for integrity verification to prevent adversaries from dropping and tampering with the reported data.

A dynamic pseudonym is introduced to conceal the real identity of the source node. Through this scheme, the relationship between the source node and the pseudonyms can be

protected. It effectively defends against side information attacks.

We propose a two-phase forwarding scheme to detach the connection between source nodes and application data server. In this way, the application data server is unable to estimate the source node identity based on direct side information. Theoretical analysis shows by using dynamic pseudonym scheme and secret-sharing, the proposed scheme can preserve trajectory privacy.

We provide quantitatively analyze on the performance of the communication delay and the delivery ratio under a given security level. It shows that DAPP has the flexibility to provide a trade-off among communication delay, delivery ratio and participating user's privacy. The simulation results show that DAPP can minimize information leakage under the given communication delay constraints. The built-in redundancy in DAPP can also minimize the error rate for reporting data.

6.4 Related Future Works

The future work that directly related to this dissertation is broad and comprehensive. We are currently working on the following two issues:

Privacy Definition and Characterization In this dissertation, we defined location privacy information leakage from probability perspective. However, there is still a lack of quantitative measurement and characterization of privacy information in general. Our goal is to develop a formal methodology to characterize privacy and provide a quantitative measurement.

Measurement Criterion on Privacy Information Loss Publishing individual data records without revealing sensitive information is an important yet challenging issue. Several criteria have been proposed in existing research to measure the information loss of a privacy protection scheme, such as k-anonymity, l-diversity and t-closeness. However, k-anonymity

and t-closeness cannot provide privacy if sensitive values in an equivalence class lack diversity. l-diversity does not consider overall distribution for privacy information, which is also difficult to be realized. These criteria also are not able to provide the lower bound of privacy information loss for a published table. As a future research task, we intend to develop a general information disclosure methodology under a given privacy leakage constraint.

BIBLIOGRAPHY

BIBLIOGRAPHY

[1] Y. Li and J. Ren, "Source-location privacy through dynamic routing in wireless sensor networks," in *INFOCOM, 2010 Proceedings IEEE*, March 2010, pp. 15–19.

[2] Y. Yu, R. Govindan, and D.Estrin, "Geographical and energy-aware routing: A recursive data dissemination protocol for wireless sensor networks," UCLA Computer Science Department Technical Report, Tech. Rep., May 2001.

[3] D. P. Tommaso Melodia and I. E. Akyildiz, "Optimal local topology knowledge for energy efficient geographical routing in sensor networks," in *Twenty-third AnnualJoint Conference of the IEEE Computer and Communications Societies (INFOCOM)*, March 2004, pp. 1705–1716.

[4] G. Zhao, J. Li, X. Liu, and A. Kumar, "Lifetime-aware geographic routing in wireless sensor networks," in *Cyber-Enabled Distributed Computing and Knowledge Discovery, 2009. CyberC '09. International Conference on*, Oct 2009, pp. 355–362.

[5] M. Ye, C. Li, G. Chen, and J. Wu, "Eecs: an energy efficient clustering scheme in wireless sensor networks," in *Performance, Computing, and Communications Conference, 2005. IPCCC 2005. 24th IEEE International*, April 2005, pp. 535–540.

[6] P. Bose, P. Morin, I. Stojmenovic, and J. Urrutia, "Routing with guaranteed delivery in adhoc wireless networks," in *3rd Int. Workshopon Discrete Algorithms and methods for mobile computing and communications*, 1999, pp. 46–55.

[7] C.-C. Hung, K.-J. Lin, C.-C. Hsu, C.-F. Chou, and C.-J. Tu, "On enhancing network-lifetime using opportunistic routing in wireless sensor networks," in *Computer Communications and Networks (ICCCN), 2010 Proceedings of 19th International Conference on*, Aug 2010, pp. 1–6.

[8] J.-H. Chang and L. Tassiulas, "Maximum lifetime routing in wireless sensor networks," *Networking, IEEE/ACM Transactions on*, vol. 12, no. 4, pp. 609–619, August 2004.

[9] F. Liu, C.-Y. Tsui, and Y. J. Zhang, "Joint routing and sleep scheduling for lifetime maximization of wireless sensor networks," *Wireless Communications, IEEE Transactions on*, vol. 9, no. 7, pp. 2258–2267, July 2010.

[10] C. Ee and R. Bajcsy, "Congestion control and fairness for many-to-one routing in sensor networks," in *ACM International Conference on Embedded Networked Sensor Systems(SenSys 04)*, 2004.

[11] S. E. C.Y. Wan and A. Campbell, "Coda: Congestion detection and avoidance in sensor networks," in *ACM International Conference on Embedded Networked Sensor Systems(SenSys 03)*, 2003, pp. 266–279.

[12] C. Conti and E. Gregori, "Dynamic tuning of the ieee 802.11 protocol to achieve a theoretical throughput limit," *IEEE/ACM Transactions on Networking*, vol. 8, no. 6, pp. 785–799, December 2000.

[13] S. Eisenman and A. Campbell, "E-csma: Supporting enhanced CSMA performance in experimental sensor networks using per-neighbor transmission probability thresholds," in *IEEE INFOCOM 2007*, May 2007, pp. 1208–1216.

[14] S. Chen and N. Yang, "Congestion avoidance based on lightweight buffer management in sensor networks," *IEEE Transactions on Parallel and Distributed Systems,*, vol. 17, no. 9, pp. 934–946, Sept 2006.

[15] I. Stojmenovic and X. Lin, "Power-aware localized routing in wireless networks," *Parallel and Distributed Systems, IEEE Transactions on*, vol. 12, no. 11, pp. 1122–1133, Nov 2001.

[16] J. Li, J. Jannotti, D. S. J. D. Couto, D. R. Karger, and R. Morris, "A scalable location service for geographic ad hoc routing," in *the Sixth ACM Annual International Conference on Mobile Computing and Networking*. ACM, 2000, pp. 120–130.

[17] B. Karp and H. T. Kung, "Gpsr: Greedy perimeter stateless routing for wireless networks," in *the Sixth ACM Annual International Conference on Mobile Computing and Networking (Mobicom)*, April 2000, pp. 243–254.

[18] Y. Xu, J. Heidemann, and D. Estrin, "Geography-informed energy conservation for ad-hoc routing," in *the Seventh Annual ACM/IEEE International Conference on Mobile Computing and Networking*, 2001, pp. 70–84.

[19] D. E. N. Bulusu, J. Heidemann, "Gps-less low cost outdoor localization for very small devices," Computer science department, University of Southern California, Technical Report00-729, April 2000.

[20] C.-C. H. A. Savvides and M. Srivastava, "Dynamic fine-grained localization in ad-hoc networks of sensors," in *the Seventh ACM Annual International Conference on Mobile Computing and Networking (MobiCom)*, 2001, pp. 166–179.

[21] P. Bose, P. Morin, I. Stojmenovic, and J. Urrutia, "Routing with guaranteed delivery in ad hoc wireless networks," in *the 3rd ACM International Workshop on Discrete Algorithms and Methods for Mobile Computing and Communications (DIAL M 99)*, Seattle, WA, August 1999, pp. 48–55.

[22] Y. Li, Y. Yang, and X. Lu, "Rules of designing routing metrics for greedy, face, and combined greedy-face routing," *Mobile Computing, IEEE Transactions on*, vol. 9, no. 4, pp. 582–595, April 2010.

[23] R. Shah and J. Rabaey, "Energy aware routing for low energy ad hoc sensor networks," in *Wireless Communications and Networking Conference, 2002. WCNC2002. 2002 IEEE*, vol. 1, March 2002, pp. 350–355.

[24] H. Zhang and H. Shen, "Balancing energy consumption to maximize network lifetime in data-gathering sensor networks," *Parallel and Distributed Systems, IEEE Transactions on*, vol. 20, no. 10, pp. 1526–1539, Oct. 2009.

[25] J. Kuruvila, A. Nayak, and I. Stojmenovic, "Hop count optimal position-based packet routing algorithms for ad hoc wireless networks with a realistic physical layer," *Selected Areas in Communications, IEEE Journal on*, vol. 23, no. 6, pp. 1267–1275, June 2005.

[26] P. Kamat, Y. Zhang, W. Trappe, and C. Ozturk, "Enhancing source-location privacy in sensor network routing," in *Distributed Computing Systems, 2005. ICDCS 2005. Proceedings. 25th IEEE International Conference on*, June 2005, pp. 599–608.

[27] C. Ozturk, Y. Zhang, W. Trappe, and M. Ott, "Source-location privacy in energy-constrained sensor network routing," in *workshop on security of ad hoc and sensor networks - SASN*. ACM, May 2004, pp. 88–93.

[28] Y. Li and J. Ren, "Preserving source-location privacy in wireless sensor networks," in *Sensor, Mesh and Ad Hoc Communications and Networks, 2009. SECON '09. 6th Annual IEEE Communications Society Conference on*, June 2009, pp. 1–9.

[29] R. Shaikh, H. Jameel, B. d'Auriol, S. Lee, Y.-J. Song, and H. Lee, "Network level privacy for wireless sensor networks," in *Information Assurance and Security, 2008. ISIAS '08. Fourth International Conference on*, Sept 2008, pp. 261–266.

[30] S. Misra and G. Xue, "Efficient anonymity schemes for clustered wireless sensor networks," *Int. J. Sen. Netw.*, vol. 1, pp. 50–63, Sep. 2006.

[31] M. Shao, Y. Yang, S. Zhu, and G. Cao, "Towards statistically strong source anonymity for sensor networks," in *INFOCOM 2008. The 27th Conference on Computer Communications. IEEE*, April 2008, pp. 51–55.

[32] Y. Li, J. Ren, and J. Wu, "Quantitative measurement and design of source-location privacy schemes for wireless sensor networks," *Parallel and Distributed Systems, IEEE Transactions on*, vol. 23, no. 7, pp. 1302–1311, July 2012.

[33] K. J. B. Hull and H. Balakrishnan, "Mitigating congestion in wireless sensor networks," in *ACM International Conference on Embedded Networked Sensor Systems(SenSys 04)*, 2004, pp. 134–147.

[34] E. C. J. Colbourn, M. Cui and V. R. Syrotiuk, "A carrier sense multiple access protocol with power backoff (csma/pb)," *Ad Hoc Networks*, vol. 5, no. 8, pp. 1233–1250, November 2007.

[35] T. He, J. Stankovic, C. Lu, and T. Abdelzaher, "Speed: a stateless protocol for real-time communication in sensor networks," in *Proceedings of 23rd International Conference on Distributed Computing Systems*, May 2003, pp. 46–55.

[36] A. C. C. Wan, S. Eisenman and J. Crowcroft, "Siphon: Over-load traffic management using multi-radio virtual sinks in sensor networks," in *ACM International Conference on Embedded Networked Sensor Systems(SenSys 05)*, 2005, pp. 116–129.

[37] M. Bhuiyan, I. Gondal, and J. Kamruzzaman, "Lacar: Location aided congestion aware routing in wireless sensor networks," in *IEEE Wireless Communications and Networking Conference (WCNC)*, April 2010, pp. 1–6.

[38] F. Ren, T. He, S. Das, and C. Lin, "Traffic-aware dynamic routing to alleviate congestion in wireless sensor networks," *IEEE Transactions on Parallel and Distributed Systems*, vol. 22, no. 9, pp. 1585–1599, Sept 2011.

[39] J. Burke, D. Estrin, M. Hansen, A. Parker, N. Ramanathan, S. Reddy, and M. B. Srivastava, "Participatory sensing," in *the 1st Workshop on World-Sensor-Web*, Oct 2006, pp. 1–5.

[40] A. T. Campbell, S. B. Eisenman, N. D. Lane, E. Miluzzo, and R. A. Peterson, "People-centric urban sensing," in *Proceedings of the 2nd Annual International Workshop on Wireless Internet*, 2006, pp. 18–31.

[41] A. Kapadia, N. Triandopoulos, C. Cornelius, D. Peebles, and D. Kotz, "Anonysense: Opportunistic and privacy-preserving context collection," *Pervasive Computing*, vol. 5013, pp. 280–297, 2008.

[42] K. L. Huang, S. Kanhere, and W. Hu, "Towards privacy-sensitive participatory sensing," in *Pervasive Computing and Communications, IEEE International Conference on*, March 2009, pp. 1–6.

[43] J. Shi, R. Zhang, Y. Liu, and Y. Zhang, "Prisense: Privacy-preserving data aggregation in people-centric urban sensing systems," in *Proceedings of IEEE INFOCOM 2010*, March 2010, pp. 758–766.

[44] A. R. Beresford and F. Stajano, "Mix zones: User privacy in locationaware services," in *2nd IEEE Ann. Conf. Pervasive Computing and Communications Workshops*, 2004, pp. 127–131.

[45] J. Freudiger, M. H. Manshaei, J. Y. L. Boudec, and J. P. Hubaux, "On the age of pseudonyms in mobile ad hoc networks," in *Proceeding of IEEE INFOCOM 2010*, March 2010, pp. 1–9.

[46] X. Liu, H. Zhao, M. Pan, H. Yue, X. Li, and Y. Fang, "Traffic-aware multiple mix zone placement for protecting location privacy," in *Proceeding of IEEE INFOCOM 2012*, March 2012, pp. 972–980.

[47] S. Gao, J. Ma, W. Shi, G. Zhan, and C. Sun, "Trpf: A trajectory privacy-preserving framework for participatory sensing," *Information Forensics and Security, IEEE Transactions on*, vol. 8, no. 6, pp. 874–887, June 2013.

[48] M. Gruteser and D. Grunwald, "Anonymous usage of location-based services through spatial and temporal cloaking," in *ACM 1st Int. Conf. Mobile Systems, Applications and Services*, 2003, pp. 31–42.

[49] M. Datar, N. Immorlica, P. Indyk, and V. S. Mirrokni, "Locality-sensitive hashing scheme based on p-stable distributions," in *Proceedings of the Twentieth Annual Symposium on Computational Geometry*, 2004, pp. 253–262.

[50] T. Xu and Y. Cai, "Exploring historical location data for anonymity preservation in location-based service," in *Proceeding of IEEE INFOCOM 2008*, March 2008, pp. 547–555.

[51] K. Vu, R. Zheng, and J. Gao, "Efficient algorithms for k-anonymous location privacy in participatory sensing," in *Proceeding of INFOCOM 2012*, March 2012, pp. 2399–2407.

[52] S. Gao, J. Ma, W. Shi, and G. Zhan, "Towards location and trajectory privacy protection in participatory sensing," in *Mobile Computing, Applications and Services*, 2011, pp. 381–386.

[53] H. Lu, C. S. Jensen, and M. L. Yiu, "Pad: Privacy-area aware, dummybased location privacy in mobile services," in *7th ACM Int.Workshop on Data Engineering for Wireless and Mobile Access*, 2008, pp. 16–23.

[54] H. Kido, Y. Yanagisawa, and T. Satoh, "An anonymous communication technique using dummies for location-based services," in *9th Int. Symp. Privacy Enhancing Technologies (PETS¡¯10)*, 2005, pp. 88–97.

[55] M. Terrovitis and N. Mamoulis, "Privacy preservation in the publication of trajectories," in *Mobile Data Management, 2008. MDM '08. 9th International Conference on*, April 2008, pp. 65–72.

[56] O. Abul, F. Bonchi, and M. Nanni, "Never walk alone: Uncertainty for anonymity in moving objects databases," in *Data Engineering, 2008. ICDE 2008. IEEE 24th International Conference on*, April 2008, pp. 376–385.

[57] E. De Cristofaro and R. Di Pietro, "Adversaries and countermeasures in privacy-enhanced urban sensing systems," *Systems Journal, IEEE*, vol. 7, no. 2, pp. 311–322, June 2013.

[58] D. Christin, J. Guillemet, A. Reinhardt, M. Hollick, and S. Kanhere, "Privacy-preserving collaborative path hiding for participatory sensing applications," in *Mobile Adhoc and Sensor Systems (MASS), IEEE 8th International Conference on*, Oct 2011, pp. 341–350.

[59] ——, "Privacy-preserving collaborative path hiding for participatory sensing applications," in *Mobile Adhoc and Sensor Systems (MASS), IEEE 8th International Conference on*, Oct 2011, pp. 341–350.

[60] L. Hu and C. Shahabi, "Privacy assurance in mobile sensing networks: Go beyond trusted servers," in *Pervasive Computing and Communications Workshops, 8th IEEE International Conference on*, March 2010, pp. 613–619.

[61] B. Karp and H. T. Kung, "Gpsr: Greedy perimeter stateless routing for wireless networks," in *MobiCom's 2000*, Seattle, WA, 2000, pp. 243–254.

[62] L. Kang, "Protecting location privacy in large-scale wireless sensor networks," in *Communications, 2009. ICC '09. IEEE International Conference on*, June 2009, pp. 1–6.

[63] K. Mehta, D. Liu, and M. Wright, "Location privacy in sensor networks against a global eavesdropper," in *IEEE International Conference on Network Protocols ICNP 2007*, Oct 2007, pp. 314–323.

[64] Y. Ouyang, Z. Le, D. Liu, J. Ford, and F. Makedon, "Source location privacy against laptop-class attacks in sensor networks," in *Proceedings of the 4th International Conference on Security and Privacy in Communication Netowrks*, 2008, pp. 1–10.

[65] M. Shao, W. Hu, S. Zhu, G. Cao, S. Krishnamurthy, and T. L. Porta, "Cross-layer enhanced source location privacy in sensor networks," in *Proceedings of the 6th Annual IEEE Communications Society Conference on Sensor, Mesh and Ad Hoc Communications and Networks*, Piscataway, NJ, USA, 2009, pp. 324–332.

[66] J. Hill, R. Szewczyk, A. Woo, S. Hollar, D. Culler, and K. Pister, "System architecture directions for networked sensors," *SIGARCH Comput. Archit. News*, vol. 28, no. 5, pp. 93–104, Nov 2000.

[67] J. Yao and G. Wen, "Preserving source-location privacy in energy-constrained wireless sensor networks," in *28th International Conference on Distributed Computing Systems Workshops, ICDCS '08*, June 2008, pp. 412–416.

[68] Y. Zhang, W. Liu, Y. Fang, and D. Wu, "Secure localization and authentication in ultra-wideband sensor networks," *Selected Areas in Communications, IEEE Journal on*, vol. 24, no. 4, pp. 829–835, April 2006.

[69] L. Hu and D. Evans, "Localization for mobile sensor network," in *the tenth ACM Annual International Conference on Mobile Computing and Networking (Mobicom)*, 2004, pp. 45–57.

[70] H. Chan and A. Perrig, "Pike: peer intermediaries for key establishment in sensor networks," in *INFOCOM 2005. 24th Annual Joint Conference of the IEEE Computer and Communications Societies. Proceedings IEEE*, vol. 1, March 2005, pp. 524–535.

[71] WikipediA, "Quartic function," $http://en.wikipedia.org/wiki/Quartic_function$.

[72] G. Bianchi, "Jamming sensor networks: attack and defense strategies," *IEEE Network*, vol. 20, no. 3, pp. 41–47, March 2006.

[73] H.-W. L. A. Pathan and C. seon Hong, "Security in wireless sensor networks: issues and challenges," in *the 8th International Conference on Advanced Communication Technology (ICACT)*, vol. 2, 2006, pp. 6–1048.

[74] G. Bianchi, "Performance analysis of the ieee 802.11 distributed coordination function," *IEEE Journal on Selected Areas in Communications*, vol. 18, no. 3, pp. 535–547, march 2000.

[75] J. Li, J. Jannotti, D. Couto, D. R. Karger, and R. Morris, "A scalable location service fo geographic ad hoc routing," in *MobiCom's 2000*, Seattle, WA, 2000, pp. 120–130.

[76] P.Rapitis, V. Vitsas, and K. Paparrizos, "Packet delay metrics for ieee 802.11 distributed coordination function," *Journal Mobile Networks and Applications*, vol. 14, no. 6, pp. 772–781, December 2009.

[77] J. Kim and S. Bohacek, "A survey-based mobility model of people for simulation of urban mesh networks," in *Proceeding of MeshNets*, 2005.

[78] B. Sun, F. Yu, K. Wu, Y. Xiao, and V. Leung, "Enhancing security using mobility-based anomaly detection in cellular mobile networks," *Vehicular Technology, IEEE Transactions on*, vol. 55, no. 4, pp. 1385–1396, July 2006.

[79] V. Vukadinovic, O. R. Helgason, and G. Karlsson, "An analytical model for pedestrian content distribution in a grid of streets," *Mathematical and Computer Modelling*, vol. 57(11-12), pp. 2933–2944, June 2013.

[80] F. Bai, N. Sadagopan, and A. Helmy, "Important: a framework to systematically analyze the impact of mobility on performance of routing protocols for adhoc networks," in *Proceeding of IEEE INFOCOM 2003*, vol. 2, March 2003, pp. 825–835.